



W 4 Z84b 2008
Zode, Gulab Shalikram.
Bone morphogenetic protein 4
inhibits TGF-[beta]2

UNTHSC - FW



M03K2E

LEWIS LIBRARY
UNT Health Science Center
3500 Camp Bowie Blvd.
Ft. Worth, Texas 76107-2699

Zode, Gulab Shalikram, **Bone Morphogenetic Protein 4 Inhibits TGF- β 2 Stimulation of Extracellular Matrix Proteins in Optic Nerve Head Cells: Role of Gremlin in ECM Modulation.** Doctor of Philosophy (Cell Biology and Genetics), May 2008; 177pp; 34 figures; bibliography, 192 titles.

The glaucomatous neuropathy is caused by irreversible loss of retinal ganglion axons in the optic nerve head (ONH). The extensive remodeling of the extracellular matrix (ECM) in the glaucomatous ONH including increased synthesis and deposition of ECM (increased collagens, basement proteins, and elastin) is associated with loss of axons. Transforming growth factor-beta2 (TGF- β 2) is increased in glaucomatous ONH and is thought to be responsible for increased synthesis and deposition of ECM proteins of the ONH. Bone morphogenetic proteins (BMPs) normally maintain the balance of ECM proteins via opposing TGF- β 2 stimulated ECM proteins in various cell types. BMP antagonist gremlin inhibits BMPs function, thus may play an important role in ECM modulation. We previously demonstrated that human ONH expresses BMP-4, BMP receptor and BMP antagonist gremlin. Therefore, we hypothesize that elevated TGF- β 2 in the glaucomatous ONH induces gremlin expression that blocks BMP-4 inhibition of TGF- β 2 signaling, leading to increased ECM synthesis and deposition.

First, we examined whether human ONH tissues and ONH cells express the canonical BMP signaling pathway. This study demonstrated that ONH tissues and ONH cells express BMP-4 and Smad signaling pathway. Treatment of ONH cells with BMP-4 increased phosphorylation of R-Smad1/5/8 phosphorylation and interaction with Co-

Smad4 indicating activation of the Smad signaling pathway. Therefore, cells within the human ONH can respond to locally released BMP via activation of Smad signaling.

Second, we examined the signaling pathways utilized by TGF- β 2 to stimulate ECM in ONH cells. This study demonstrated that TGF- β 2 is increased in glaucomatous ONH. Recombinant TGF- β 2 increased ECM deposition in ONH cells. TGF- β 2 activated phosphorylation of R-Smad2/3 but did not alter phosphorylation of ERK1/2, p38, and JNK1/2 in ONH cells. Inhibition of either TGF- β I receptor activity or phosphorylation of R-Smad3 or knockdown of R-Smad2/3 via siRNA reduced TGF- β 2 stimulated ECM in ONH cells. Thus, TGF- β 2 requires R-Smad2/3 to stimulate ECM proteins in ONH cells.

Lastly, we investigated the potential effects of BMP-4 and gremlin on TGF- β 2 stimulated ECM in ONH cells. BMP-4 significantly reduced TGF- β 2 stimulation of ECM proteins. Addition of gremlin blocked the BMP-4 effect, increasing ECM proteins in ONH cells. Gremlin levels were significantly increased in the human glaucomatous ONH tissues. Interestingly, recombinant gremlin also increased ECM proteins in ONH cells. Gremlin stimulation of ECM proteins required activation of the TGF- β receptor and R-Smad3. TGF- β 2 increased gremlin mRNA and protein in ONH cells. Thus, TGF- β 2 induced gremlin expression intensifies TGF- β 2 effects on ECM metabolism by inhibiting BMP-4 antagonism of TGF- β 2 signaling.

In conclusion, elevated TGF- β 2 and gremlin in the glaucomatous ONH are involved in the pathogenesis of glaucomatous ONH. Elevated TGF- β 2 directly increases ECM and also induces gremlin expression, which further aids TGF- β 2 to stimulate ECM via


inhibiting BMPs antagonism of TGF- β 2 signaling, leading to unopposed TGF- β 2 stimulated ECM proteins. Interestingly, R-smad3 is required for TGF- β 2 or gremlin induced ECM remodeling in ONH cells. Therefore, modulation of R-smad3 provides a novel therapeutic target for preventing ECM remodeling in glaucoma.

**BONE MORPHOGENETIC PROTEIN 4 INHIBITS TGF-B2 STIMULATION OF
EXTRACELLULAR MATRIX PROTEINS IN OPTIC NERVE HEAD CELLS:
ROLE OF GREMLIN IN ECM MODULATION**

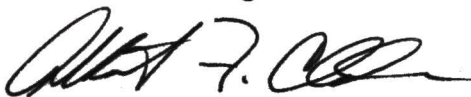
Gulab S. Zode, B. Pharm

APPROVED

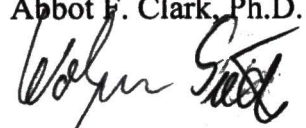
Major Professor:


Robert J. Wordinger, Ph.D.

Committee Member:


Abbot F. Clark, Ph.D.


Committee Member:


Wolfram Siede, Ph.D.

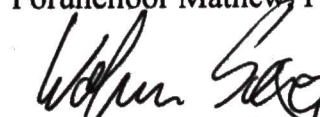
Committee Member:


Harold Sheedlo, Ph.D.

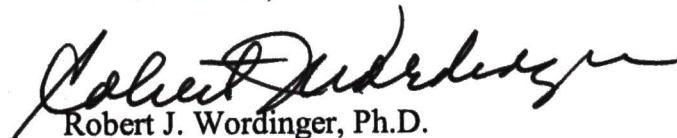
University Member:


Porunelloor Mathew, Ph.D.

Graduate Advisor:



Wolfram Siede, Ph.D.

Department Chair:


Robert J. Wordinger, Ph.D.

Accepted:

Graduate Dean:


Jamboor K. Vishwanatha, Ph.D.

Bone Morphogenetic Protein 4 Inhibits TGF- β 2 Stimulation of Extracellular Matrix
Proteins in Optic Nerve Head Cells: Role of Gremlin in ECM Modulation.

DISSERTATION

Presented to the Graduate Council of the

Graduate School of Biomedical Science

University of North Texas

Health Science Center at Fort Worth

In Partial Fulfillment of the Requirements

For the Degree of

Doctor of Philosophy

By

Zode Gulab Shalikram

Fort Worth, Texas

May 2008

ACKNOWLEDGEMENTS

This project was supported by grant from the National Institute of Health to Dr. Robert J. Wordinger (EY12783). Fellowship support to Gulab Shalikaram Zode was provided by the Graduate School of Biomedical Sciences and Department of Cell Biology and Genetics, at University of North Texas, Health Science Center at Fort Worth.

This investigation would not have been possible without the able guidance and mentorship of Dr. Robert J. Wordinger. I would like to acknowledge him for his enthusiasm, openness, constant encouragement, and freedom. I am very grateful to him. I am also thankful towards the Graduate School of Biomedical Science and the Department of Cell Biology and Genetics in giving me opportunity to do research. I would like to thank Dr. Abbot F. Clark for his constant help, encouragement, and support in conducting research. I am also grateful to staff and students in the laboratories of Dr. Robert J. Wordinger for their significant contribution in completing this project.

Finally, I would also like to thank Arti Sharma for her support. I extend my deepest gratitude towards my parents who have encouraged me unconditionally.

TABLE OF CONTENTS

Acknowledgements.....	VI
List of Figures.....	VIII
Chapters	
I. Introduction.....	1
II. Activation of the BMP Canonical Signaling Pathway in Human Optic Nerve Head Tissue and Isolated Optic Nerve Head Astrocytes and Lamina Cribrosa Cells.....	29
III. Transforming Growth Factor- β 2 Increases Extracellular Matrix Proteins via Activation of Smad Signaling Pathway in Optic Nerve Head Cells.....	72
IV. Bone Morphogenetic Protein 4 Inhibits TGF- β 2 Stimulation of Extracellular Matrix Proteins in Optic Nerve Head Cells: Role of Gremlin in ECM Modulation.....	121
V. CONCLUSIONS.....	172
VI. CHAPTER	176

LIST OF FIGURES

Chapter I

Figure1. The proposed mechanism for ECM changes in the glaucomatous ONH.....	5
Figure2. Elevated TGF- β 2 is associated with ECM remodeling in glaucomatous ONH...	7
Figure3. Regulation of BMP and TGF- β 2 signaling.....	11
Figure 4: Schematic Representation of Effect of BMP-4, Gremlin, and TGF- β 2 on ECM.....	15

Chapter II

Figure1. Chemiluminescence detection of BMP-4 secreted by human ONH astrocytes & lamina cribrosa.....	56
Figure2. Chemiluminescence detection of Smad proteins in ONH Astrocytes and LC...	57
Figure3. Colocalization of Smad4 and pSmad1 in ONH astrocytes and LC cells.....	58
Figure4. Chemiluminescence detection of Smad proteins in BMP-4-treated ONH astrocytes and LC cells.....	59
Figure5. Coimmunoprecipitation study of Co-Smad4 with phosphorylated R-Smad1/5/8 in ONH astrocytes and LC cells.....	60
Figure6. Localization of Smad6 and Smad7 in human ONH astrocytes and LC cells....	61

Figure7. Immunohistochemical localization of BMP-4 in human ONH tissue.....	62
Figure8. Western blot analysis of BMP-4 and Smad proteins by ONH tissues.....	63
Figure9. Colocalization of Smad4 with R-pSmad1 and Smad5 in ONH tissue.....	64
 Chapter III	
Figure1. Immunohistochemical Evaluation of TGF- β 2 and FN Localization in Normal and Glaucomatous ONH Tissues.....	101
Figure2. Western Blot Analysis of TGF- β 2 Protein in ONH Cells and tissues.....	103
Figure3. Recombinant TGF- β 2 Dose Dependently Increases FN and PAI-1 in ONH Astrocytes and LC Cells.....	104
Figure4. Recombinant TGF- β 2 Increases ECM Proteins in ONH Astrocytes and LC Cell.....	105
Figure5. Inhibition of Activity Type I TGF- β Receptor Blocks TGF- β 2-Driven ECM Stimulation.....	106
Figure6. Phosphorylation of ERK1/2, p38, or JNK1/2 Pathways in ONH Astrocytes and LC Cells.....	107
Figure7. R-Smads Phosphorylation by Recombinant TGF- β 2 in ONH Cells.....	108

Figure8. Colocalization of pSmad3 and Smad4 in LC Cells.....	109
Figure9. Inhibition of Phosphorylation of Smad3 Reduced TGF- β 2 Stimulation of FN in ONH Astrocytes and LC Cells.....	110
Figure10. Inhibition of Smad3 via siRNA Blocks TGF- β 2 Stimulation of FN and PAI-1 in ONH Astrocytes and LC Cells.....	111
Figure11. Inhibition of Smad2 via siRNA Blocks TGF- β 2 Stimulation of FN and PAI-1 in ONH Astrocytes and LC Cells.....	113
 Chapter IV	
Figure1. BMP-4 Dose Dependently Inhibits TGF- β 2 Stimulation of FN and PAI-1 Proteins in ONH Astrocytes and LC Cells.....	150
Figure2. BMP-4 Inhibits TGF- β 2 Mediated Stimulation of ECM Proteins in ONH Astrocytes and LC Cells.....	152
Figure3. Gremlin Blocks BMP-4 Inhibition of TGF- β 2-Induced FN and PAI-1 in Human ONH Astrocytes and LC Cells.....	154
Figure4. Gremlin Expression in Human ONH Tissues, ONH Astrocytes and LC.....	156
Figure5. Immunohistochemical Evaluation of Gremlin Expression in Normal	

and Glaucomatous ONH Tissues.....	157
Figure6. Effect of Gremlin on ECM Proteins in ONH astrocytes and LC cells.....	159
Figure7. Inhibition of Type I TGF- β Receptor or siRNA Knockdown of R-Smad3 Blocks Gremlin Stimulation of FN and PAI-1 in ONH Astrocytes.....	160
Figure8. Effect of TGF- β 2 on Gremlin mRNA and Protein in ONH Cells.....	162
Figure9. Interactions between gremlin, BMP-4, and TGF- β 2 that modulates ECM in the ONH.....	163
Chapter V	
Figure1. Gremlin Inhibition of BMP-4 Antagonism of TGF- β 2 Increases ECM Proteins in the Glaucomatous ONH.....	175

Chapter I

INTRODUCTION

Primary Open angle Glaucoma (POAG)

Glaucoma is the second leading cause of irreversible blindness in the world, affecting over 70 millions individuals¹. Primary open-angle glaucoma (POAG) is a progressive optic neuropathy, characterized by irreversible loss of axons of the retinal ganglion cells²⁻⁴. The pathogenic factors responsible for POAG are still unknown. However, elevated intraocular pressure (IOP) is major known treatable risk factor^{5, 6}. Elevated IOP is caused by impaired aqueous humor outflow and is associated with characteristic morphological and biochemical changes in trabecular meshwork (TM). Elevated IOP in the anterior chamber is thought to induce optic nerve head (ONH) changes that lead to death of retinal ganglion cells^{5, 7-9}.

Optic Nerve Head (ONH)

Optic nerve head is an intraocular portion of optic nerve. Human ONH is formed by gathering of retinal ganglion axons, which run superficially in the retina and bend at right angle at optic nerve head¹⁰. The microscopical examination of human ONH has been studied by many researchers¹⁰⁻¹⁹. Human ONH shows a characteristic structure referred as lamina cribrosa (LC). The LC region is divided into four different parts^{10, 11, 16, 20, 21}. Surface nerve fiber layer consists mainly of nerve fibers. The prelaminar region consists of nerve bundles that turn at right angle to enter in the pores of lamina cribrosa. Laminar

regions mainly consist of lamina cribrosa which forms pores for the passage of nerve bundles. In post-laminar region, neurons get myelinated.

Lamina Cribrosa (LC)

The LC region of the ONH is composed of characteristic sieve-like connective tissue cribriform plates through which RGC axons exit the eye.^{10, 11} Collagen fibrils in this region are arranged in characteristic sheath-like structure accommodating the nerve bundles. These collagen sheaths are in continuous with sclera giving the structural framework to the optic nerve head. These collagen structures appear to give protection from mechanical forces and also supporting the blood vessels in this region¹⁰. The elastic fibers are restricted to prelaminar and laminar region, indicating that laminar region is more elastic than post-laminar region¹⁰. Therefore, LC plates together with collagen sheath and elastic fibers form connective tissue network, which gives structural and elastic framework against mechanical force of IOP¹⁰.

These LC plates consist of ECM proteins such as elastin and collagens (type I, III, V, and VI). The correct organization and assembly of the collagen and elastic fibers gives a structural framework and elasticity to the ONH that protects it from mechanical stress^{12-14, 22}. There are two major cell types located in LC region; ONH astrocytes and LC cells make and secrete these ECM proteins.

ONH astrocytes and LC cells

ONH astrocytes and LC cells play an important role in maintaining normal homeostasis of ONH. ONH astrocytes support functions to the axons, form the interface between connective tissue surfaces and surround blood vessels²². In the prelaminar region, astrocytes form glial columns. In laminar region, astrocytes are present at the edge of collagen sheath and extend their processes to neighboring cells. GFAP-positive cells in post-laminar region show characteristics of fibrous astrocytes²².

Lamina cribrosa cells reside in the cribriform plates of the LC. LC cells can be distinguished from astrocytes because they do not express GFAP²³. LC cells also form contacts with astrocytes processes. Origin and cell type of these cells are still unknown. However, ONH cells (ONH astrocytes and LC cells) appear to make and secrete growth factors such as BMPs, TGF- β s, and neurotrophins^{24, 25}. Cultured LC cells also make and secrete collagen I, VI, IV, elastin, fibronectin, and laminins (Zode, unpublished).

It is interesting to note the presence of LC cells and unique structure and functions of astrocytes in pre-laminar and laminar region compared to post-laminar region. It has been suggested that cells located in ONH play an important role not only during development but also in disease such as glaucoma¹⁰. In support of this hypothesis, studies have demonstrated that ONH astrocytes in the ONH become activated and secrete higher amount of growth factors²⁶.

Extracellular Matrix (ECM) Remodeling Accompanies Axonal Damage in the Glaucomatous Optic Nerve Head (ONH)

In glaucoma, elevated IOP can damage the optic nerve head (ONH), which is detrimental to RGC axon viability^{7, 27}. Optic nerve head changes resulting from elevated IOP include compression of retinal ganglion axons at the lamina cribrosa (LC) region, blockage of axoplasmic flow, and inhibition of retrograde neurotrophin transport to RGCs^{9, 13, 16, 21, 28-30}. The glaucomatous ONH shows characteristic cupping and excavation of the optic disc, collapse and remodeling of the LC region and activation of ONH astrocytes^{12, 16, 20, 22, 26}. There is extensive remodeling of ECM in the LC including increased synthesis and deposition of ECM proteins. Increased area and density of the basement membrane including thickened collagen fibers (increased collagen I, and VI) and altered elastic fibers have been correlated to weakness of the LC^{14, 21}. Extracellular remodeling may lead to collapse of the LC and cupping of the optic nerve head (Figure 1).

Previous studies have shown a positive correlation between loss of axons and elevated IOP in a rat experimental glaucoma model^{5, 28, 31}. In a mouse model (DBA/2J), an early sign of axon damage was located to the region of the optic nerve analogous to the human lamina cribrosa³². In this region, astrocytes form an intricate network with RGC axons. Recently, RGC death has been linked to ECM-related changes in matrix metalloprotease-9 (MMP-9) and laminin expression in the retina³³. Valliant et al 2003 demonstrated that RGC death is associated with IOP induced abnormal extracellular matrix remodeling³⁴. This is further supported by the fact that in the central nervous system (CNS), neuronal

apoptosis is associated with increased MMP-9 activity³⁴. These studies indicate that abnormal ECM synthesis and degradation is most likely playing a pivotal role in axon loss and subsequent death of RGC (figure2).

Taken together, elevated IOP causes damage to the ONH, remodeling ECM in the LC (Figure 1). This leads to incorrect organization and assembly of collagens and elastic fibers, leading to cupping of the LC. It is proposed that ONH cells are involved in increasing ECM proteins by upregulating TGF- β 2 synthesis in the LC region (Figure 1)²⁶.

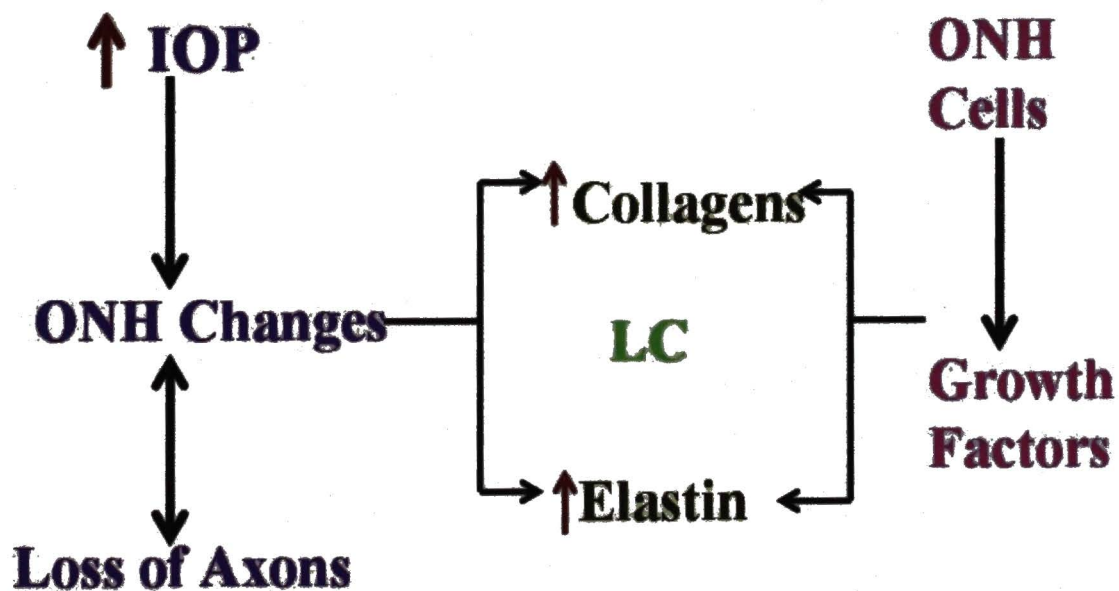


Figure1: The proposed mechanism for increased ECM in the glaucomatous ONH.

Elevated TGF- β 2 Levels in the Glaucomatous ONH are Associated with Increased ECM Proteins

Transforming growth factor- β 2 belongs to the TGF- β superfamily and plays a fundamental role in the biology of the ECM³⁵. In fibrotic diseases, elevated TGF- β 2 levels increase ECM proteins³⁶. Recent reports indicate that TGF- β 2 is involved in the pathogenesis of POAG. Patients with glaucoma have elevated levels of TGF- β 2 in their aqueous humor^{37, 38} and TGF- β 2 has been shown to increase ECM proteins in human TM cells³⁹⁻⁴¹. In cultured human perfused-anterior eye segments, TGF- β 2 has also been shown to increase IOP and ECM proteins in outflow tissues⁴². In human TM cells, TGF- β 2 increased the synthesis of ECM proteins and its cross-linking by tissue transglutaminase 2^{41, 43}.

Both TGF- β 1 and TGF- β 2 are expressed in ONH tissue. However, TGF- β 2 is the predominant type found in the ONH tissues⁴⁴. In glaucomatous ONH, TGF- β 2 levels are increased (Figure2)⁴⁴. TGF- β 2 treatment upregulates mRNA and protein expression of collagen I, collagen IV, fibronectin, connective tissues growth factor (CTGF), tissue transglutaminase (TGM2), and thrombospondin-1 (TSP-1) in ONH astrocytes (Figure2) and suggested that TGF β -2 could be an initiation factor of ECM modification in the glaucomatous ONH^{45, 46}. Kirwan et al (2005) demonstrated that TGF- β 1 induces expression of ECM proteins in LC cells^{47, 48}. Thus, LC cells may be playing a pivotal role in fibrosis of the glaucomatous ONH (Figure2). These observations suggest that in the glaucomatous ONH, elevated TGF- β 2 is associated with ECM remodeling.

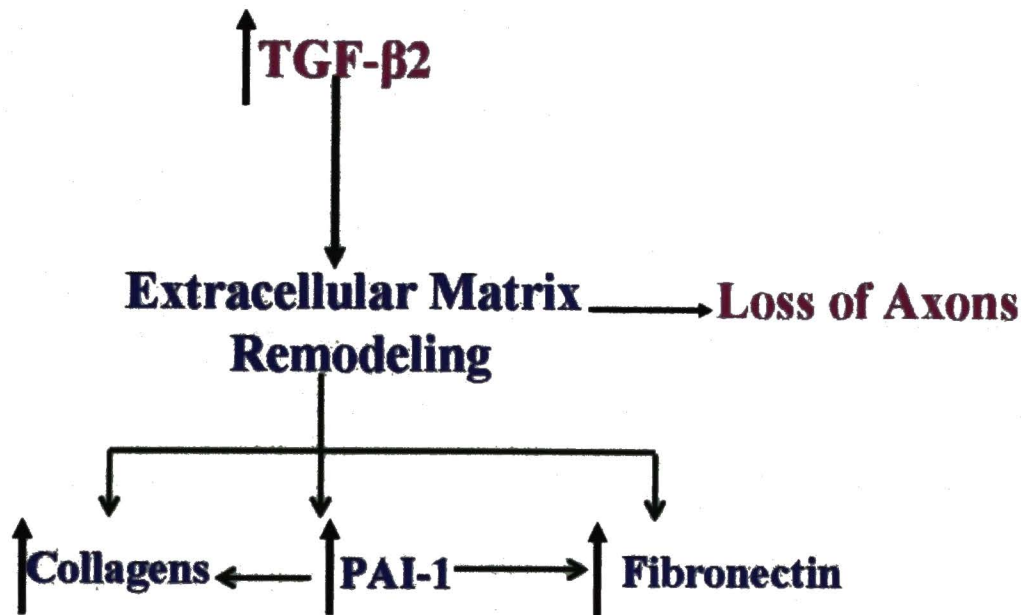


Figure 2: Elevated TGF-β2 is associated with ECM remodeling in the glaucomatous ONH

Bone Morphogenetic Proteins

Bone morphogenetic proteins (BMP) were originally identified as osteoinductive cytokines that promote bone and cartilage formation but are now known to control multiple functions in a variety of cells⁴⁹. Knockout studies in mice indicate that BMP-4 and BMP-7 are essential in the early morphogenesis of the eye⁵⁰. A heterozygous deficiency of BMP-4 results in anterior segment dysgenesis and elevated IOP⁵⁰. Previous work in our laboratory demonstrated that ONH astrocytes and LC cells express BMPs and BMP receptor²⁴. The exact role of BMPs in human ONH astrocytes and LC cells is unknown. However, recent reports indicate that BMPs may function as anti-fibrotic

agents primarily via inhibiting the profibrotic actions of TGF- β in various fibrotic diseases. BMPs have been shown to antagonize TGF- β signaling in fibrotic diseases in the kidney, lung, and liver⁵¹⁻⁵³. BMP-4 inhibited TGF- β 2 stimulated ECM synthesis and deposition in cultured TM cells³⁹. Zeisberg and colleagues, 2003 demonstrated that BMP-7 inhibits TGF- β induced epithelial-to-mesenchymal transition and reverses chronic renal injury⁵¹. Izumi et al., 2006 reported that BMP-7 opposes TGF- β 1 mediated collagen induction in mouse pulmonary myofibroblasts⁵³. Finally, in mesangial cells, BMP7 inhibits TGF β -driven fibrogenesis, primarily by reducing nuclear accumulation of R-Smad3⁵⁴.

TGF- β and BMPs Signaling Pathways

In most cell types, TGF- β isoforms and BMPs utilize the canonical Smad signaling pathway⁵⁵. However, in some cells, these cytokines also utilize non-canonical signaling pathways including p38^{MAPK}, ERK or JNK—cJUN in a condition dependant manner^{56, 57}. Bone morphogenetic protein and TGF β bind to distinct type II receptors which then form a complex with type I receptors. Type II receptors are constitutively active kinases that transphosphorylates the type I receptor upon ligand binding and subsequently leading to the activation of intracellular Smad signaling (Figure3)^{49, 55, 58}.

The intracellular Smads can be classified into three groups^{55, 59}. Receptor-Smads (R-Smads) transmit signals from receptors to the nucleus and activate gene transcription. R-

Smad1/5/8 mediates BMP signaling while R-Smad2/3 mediates TGF- β signaling (Figure 3). Inhibitory Smads (I-Smads) antagonize signaling by inhibiting R-Smads at two different levels. I-Smads can inhibit activation of R-Smad either by binding to R-Smad in the cytoplasm or by competing for Co-Smad4 (Figure 3). I-Smad6 and I-Smad7 are inhibitory Smad. The common-mediator Smad (Co-Smad 4) acts as adaptor molecule for R-Smads. Transiently associated R-Smads dissociate from the type I receptor and form a complex with Co-Smad4 and the heteromeric complex translocates to the nucleus to regulate target genes (Figure3).

In non-Smad signaling pathways, BMPs and TGF- β are known to activate p38^{MAPK}, ERK or JNK—cJUN pathway⁵⁷. There are three different mechanisms by which these non-Smad pathways transmit their signal. First, the activated receptor directly phosphorylates these non-Smad kinases and initiates parallel signaling pathways. Second, non-Smad signaling proteins directly phosphorylate Smad proteins and thus modify the activity of Smads. Third, activated Smads directly interact with non-Smad pathways and modulate the activity of kinases, thus transducing their signals to non-Smad pathways.

Co-Smad 4 is a common adaptor molecule for BMP and TGF- β related R-Smads⁵⁸. Therefore, the amount of Co-Smad4 binding to R-Smads (R-Smad2/3 or R-Smad1/5/8) determines the strength of the signal. In a BMP and TGF β activated cell, availability of Co-Smad4 determines the strength of the signal. Activation of both BMP and TGF β signaling simultaneously will result into competition for Co-Smad4 (Figure3). Exogenous administration of BMPs has been shown to decrease TGF- β mediated fibrosis. The exact

mechanism for BMPs inhibition of TGF- β 2 is not fully understood. However, exogenous treatment of BMP can compete for Co-Smad4, shifting Co-Smad4 from TGF- β signaling towards BMP signaling. Some studies have suggested that in normal cells, BMPs maintain an intricate balance with TGF- β by regulating R-Smad transport into the nucleus. For example, in mesangial cells BMP7 inhibits TGF β signaling by reducing nuclear accumulation of R-Smad3⁵⁴.

Intracellular, I-Smads (Smad6 and Smad7) can interact with R-Smads and inhibit BMP and TGF- β signaling⁶⁰. I-Smad6 has been shown to interact specifically with R-Smad1, but not with R-Smad2, to form an inactive R-Smad1/I-Smad6 complex. Thus, I-Smad6 competes with Smad4 for binding to R-Smad1 to block BMP signaling. Interestingly, I-Smad6 has recently been shown to directly bind to and inhibit TAK1 suggesting that I-Smads not only inhibit the canonical BMP-Smad pathway, but the TAK1-mediated BMP-MAPK pathway as well.

Extracellularly, BMP associated proteins can act as BMP antagonists⁵⁹. For example, noggin, chordin, follistatin, and members of the DAN (Differential screening-selected gene Aberrative in Neuroblastoma) family including Cerberus, caronte, gremlin (Drm), and Dan is thought to inhibit BMP signaling via binding directly to BMPs and prevent the ligand from interacting with the receptor complex⁶¹⁻⁶³.

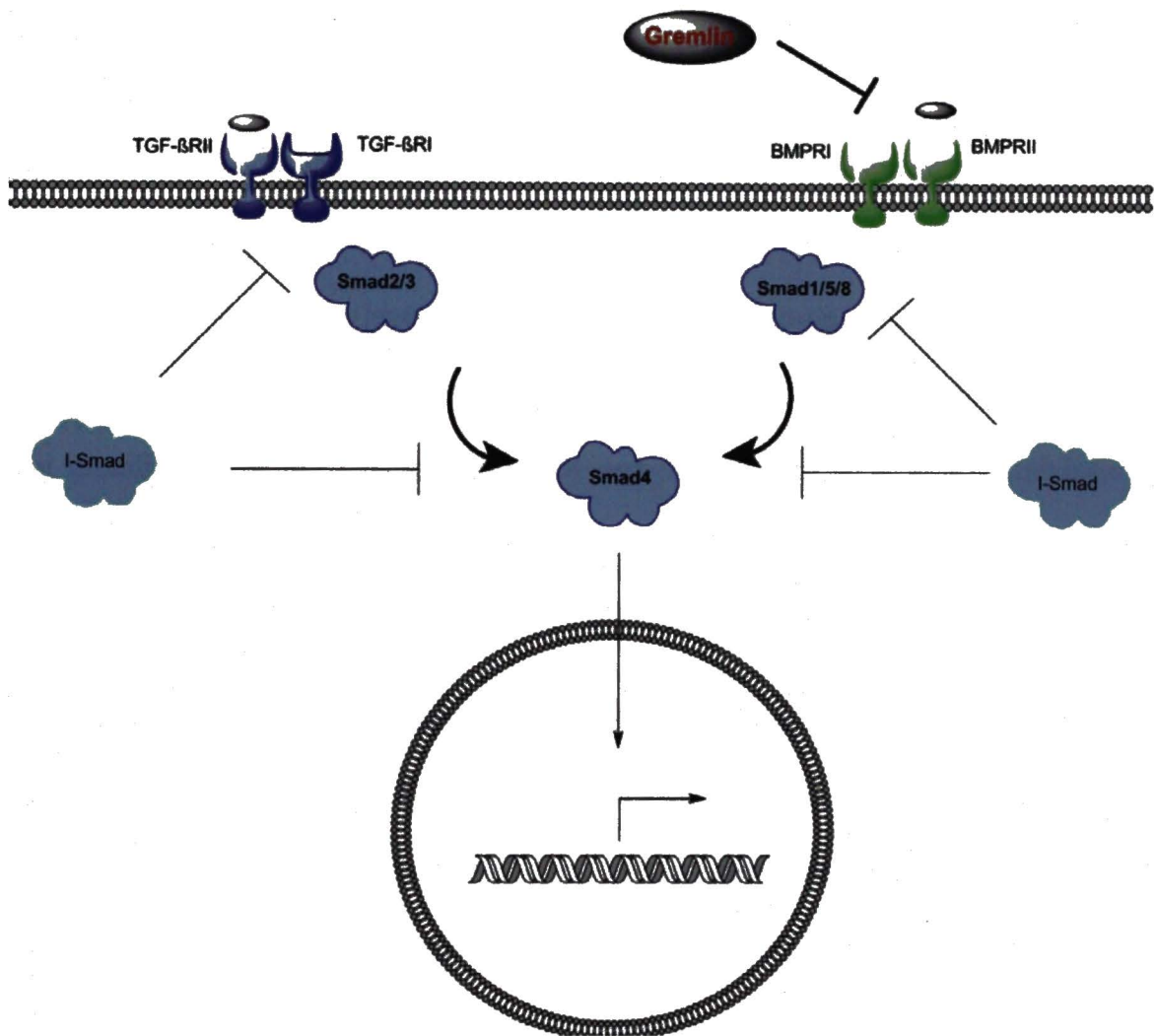


Figure3 : Regulation BMP and TGF- β Signaling

Gremlin Modulates ECM in Fibrosis

Intracellular and extracellular antagonists tightly regulate the biological activity of BMPs. Gremlin is an important extracellular BMP antagonist that acts by directly binding BMP-2, BMP-4 and BMP-7, thus preventing these BMPs from interacting with their high affinity receptor complex (Figure 3)⁶³. Previous reports suggest that BMP antagonists,

such as gremlin, are likely to play an important role in regulating multiple cell functions both during early development and in adult tissues. Gremlin is implicated in glomerulosclerosis, tubulointerstitial fibrosis and cellular hypertrophy^{62, 64-66}. The recapitulation of gremlin expression in fibrotic diseases appears to be associated with increased TGF- β protein levels. Kane et al., (2005) demonstrated that high glucose stimulated an increase in gremlin mRNA in bovine retinal pericytes⁶⁷. They also reported that gremlin expression was modulated by anti-TGF- β 1 antibody and by inhibition of MAPK activation. Using immunohistochemistry, gremlin was localized in the mouse retina to the nerve fiber layer, ganglion cell layer and inner plexiform layer.

Gremlin has been shown to affect endothelial cell functions, independent of BMP-inhibition. It has been suggested that gremlin may have receptor mechanism actions. Gremlin acts as a negative regulator of monocyte chemotaxis via interaction with slit proteins⁶³. It appears that exogenous gremlin may bind to and act directly on endothelial cells to modulate angiogenesis including endothelial cell migration⁶⁸.

Gremlin is involved in fibrosis of kidney, lung, liver and osteoarthritis^{62, 66, 69-71}. In the kidney of diabetic animals, TGF- β has been shown to increase gremlin and CTGF⁶⁴. Gremlin induction appears to modulate mesangial cell functions. In diabetic retinopathy, high glucose, mechanical strain, and TGF- β upregulates gremlin expression^{62, 65, 72}. Gremlin induction in TM appears to play an important role in modulation of ECM proteins. We reported that gremlin inhibits BMP-4 activity in cultured TM cells and increased outflow resistance in a perfusion cultured human eye anterior segment model³⁹.

⁶¹. Significantly, we noted that both gremlin mRNA and protein are increased in glaucomatous human TM cell lines. We have suggested that, in POAG, elevated gremlin expression by TM cells inhibits BMP-4 antagonism of TGF- β 2 leading to increased ECM deposition and elevated IOP.

A similar pathology is observed in the glaucomatous ONH, including increased ECM proteins and elevated TGF- β 2. Therefore, we hypothesize that in glaucoma, elevated TGF- β 2 levels in the optic nerve head induce gremlin expression that inhibits BMP-4 antagonism of TGF- β 2 stimulation of ECM proteins, thus leading to increased ECM synthesis and deposition.

Specific Aims

The cupping, compression and excavation of the glaucomatous ONH are associated with increased ECM synthesis and deposition. Characteristic ECM remodeling accompanies axonal damage in the glaucomatous ONH. TGF- β 2 is involved in the pathogenesis of POAG (Figure4). Elevated TGF- β 2 levels in the glaucomatous ONH are associated with increased ECM proteins synthesis and degradation. Bone morphogenetic proteins, a member of TGF- β superfamily, maintain normal homeostasis by modifying actions of other growth factors (Figure 4). ONH tissues and ONH cells express and make BMP-4, BMP receptors and BMP antagonist gremlin. However, the exact role of BMPs in the ONH is not known. Previously, we demonstrated that BMP-4 selectively counteracts the action of TGF- β 2 on ECM synthesis and deposition in human TM cells. In addition, elevated levels BMP antagonist inhibited BMP-4 antagonism of TGF- β 2 signaling leading to increased ECM deposition and elevated IOP (figure 4).

Therefore, we hypothesize that in glaucoma, elevated TGF- β 2 levels in the ONH induce gremlin expression that inhibits BMP-4 antagonism of TGF- β 2 signaling, thus leading to increased ECM synthesis and deposition.

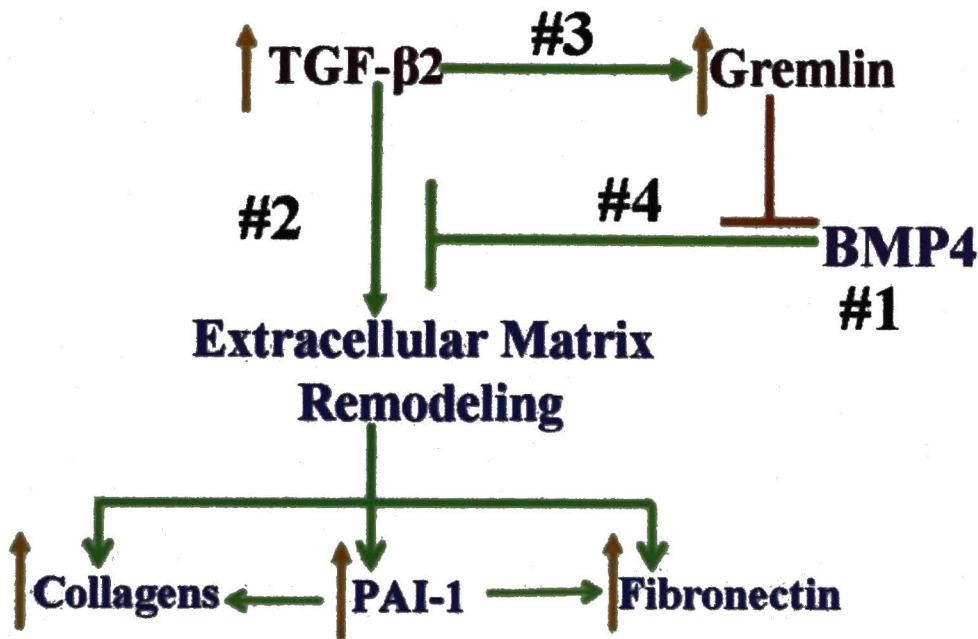


Figure 4: Schematic Representation of Effect of BMP-4, Gremlin, and TGF- β 2 on ECM

To test this hypothesis, the following specific aims are proposed.

Specific Aim #1: To demonstrate human ONH tissues and ONH cells express the canonical BMP signaling pathway

Confluent human ONH astrocytes and LC cells will be cultured in serumfree medium and conditioned medium will be subjected to western blot analysis of BMP-4. Human ONH astrocytes and LC cells were incubated with 10ng/ml BMP-4. Phosphorylation of R-Smad1/5/8 and co-localization and interaction of R-pSmad1 with Co-Smad4 will be analyzed using western blot, co-immunoprecipitation and immunostaining. Human ONH

tissues will be analyzed for Smad signaling pathway via western blot and immunostaining.

Specific Aim # 2: To demonstrate that TGF- β 2 increases ECM proteins via activation of Smad signaling pathway in ONH Astrocytes and LC Cells

ONH astrocytes and LC cells will be incubated with various concentrations of TGF- β 2 (1.25, 2.5, 5, 10, and 20ng/ml) for 24 hrs. Cell lysates and culture medium will be collected and subjected to western blot and ELISA for analysis of ECM proteins.

For Phosphorylation of R-Smads, ERK1/2, p38, or JNK1/2, confluent ONH astrocytes and LC cells will be incubated with recombinant TGF- β 2 (5ng/ml) for 30 minutes, 60 minutes, and 120 minutes. Cell lysates will be collected and analyzed with phospho-specific antibodies using immunoblotting

To examine the effect of inhibiting the type I TGF- β receptor (Alk5) or inhibiting phosphorylation of R-Smad3 (SIS3), cells will be preincubated with SB431542 or SIS3 respectively for 1 hour prior to treatment. ECM proteins and R-Smad2/3 will be analyzed using western blot.

Specific Aim #3: To demonstrate that human ONH astrocytes and lamina cribrosa (LC) cells express and secrete gremlin and that TGF- β 2 treatment upregulates gremlin expression in ONH astrocytes and LC cells.

Human ONH astrocytes and LC cells will be preincubated with TGF- β receptor inhibitor 1 hour prior to treatment with recombinant TGF- β 2. Gremlin protein in conditioned medium and cell lysates will be assessed by western blot analysis. Gremlin mRNA expression will be determined by QPCR.

Specific Aim# 4: To demonstrate that gremlin inhibition of BMP-4 increases TGF- β 2 stimulated ECM proteins in human ONH astrocytes and LC cells.

ONH astrocytes and LC cells will be treated with either TGF- β 2 (5ng/ml) alone, BMP-4 (10ng/ml) alone, TGF- β 2 (5 ng/ml) and BMP-4 (10ng/ml), or TGF- β 2 (5 ng/ml), BMP-4 (10ng/ml), and gremlin (1ug/ml). Total cell lysate and culture medium will be subjected to western immunoblotting and ELISA immunoassay for analysis of ECM proteins.

References

1. Quigley HA. Number of people with glaucoma worldwide. *Br J Ophthalmology* 1996;80:389-393.
2. Grierson I, Calthorpe CM. Characteristics of meshwork cells and age changes in the outflow system of the eye: Their relevance to primary open angle glaucoma. Mills KB. *In Glaucoma. Proceedings of the Fourth International Symposium of the Northern Eye Institute*. New York: Pergamon; 1989. 12-31 pp.
3. Rohen JW, Lutjen-Drecoll E, Flugel C, Meyer M, Grierson I. Ultrastructure of the trabecular meshwork in untreated cases of primary open-angle glaucoma (POAG). *Exp Eye Res* 1993;56:683-92.
4. Lutjen-Drecoll E, Rohen JW. Morphology of aqueous outflow pathways in normal and glaucomatous eyes. Ritch R, Shields MB, Krupin T. *In The glaucomas*. Mosby: St. Louis; 1996. 89-123 pp.
5. Chauhan BC, Pan J, Archibald ML, LeVatte TL, Kelly ME, Tremblay F. Effect of intraocular pressure on optic disc topography, electroretinography, and axonal loss in a chronic pressure-induced rat model of optic nerve damage. *Invest Ophthalmol Vis Sci* 2002;43:2969-76.

6. Rohen JW. Why is intraocular pressure elevated in chronic simple glaucoma? anatomical considerations. *Ophthalmology* 1983;90:758-65.
7. Guo L, Moss SE, Alexander RA, Ali RR, Fitzke FW, Cordeiro MF. Retinal ganglion cell apoptosis in glaucoma is related to intraocular pressure and IOP-induced effects on extracellular matrix. *Invest Ophthalmol Vis Sci* 2005;46:175-82.
8. Johnson EC, Morrison JC, Farrell S, Deppmeier L, Moore CG, McGinty MR. The effect of chronically elevated intraocular pressure on the rat optic nerve head extracellular matrix. *Exp Eye Res* 1996;62:663-74.
9. Quigley HA, Addicks EM. Chronic experimental glaucoma in primates. II. effect of extended intraocular pressure elevation on optic nerve head and axonal transport. *Invest Ophthalmol Vis Sci* 1980;19:137-52.
10. Oyama T, Abe H, Ushiki T. The connective tissue and glial framework in the optic nerve head of the normal human eye: Light and scanning electron microscopic studies. *Arch. Histol. Cytol.* 2006;69:341-356.
11. Birch M, Brotchie D, Roberts N, Grierson I. The three-dimensional structure of the connective tissue in the lamina cribrosa of the human optic nerve head. *Ophthalmologica* 1997;211:183-191.
12. Hernandez MR, Pena JD. The optic nerve head in glaucomatous optic neuropathy. *Arch Ophthalmol* 1997;115:389-95.

13. Hernandez M GH. *Extracellular matrix of the trabecular meshwork and optic nerve head*. St. Louis: Mosby; 1996. 213-49 pp.
14. Hernandez MR, Andrzejewska WM, Neufeld AH. Changes in the extracellular matrix of the human optic nerve head in primary open-angle glaucoma. *Am J Ophthalmol* 1990;109:180-8.
15. Morrison JC, Dorman-Pease ME, Dunkelberger GR, Quigley HA. Optic nerve head extracellular matrix in primary optic atrophy and experimental glaucoma. *Arch Ophthalmol* 1990;108:1020-4.
16. Quigley HA, Addicks EM. Regional differences in the structure of the lamina cribrosa and their relation to glaucomatous optic nerve damage. *Arch Ophthalmol* 1981;99:137-43.
17. Hayreh SS. Anatomy and physiology of the optic nerve head. *Trans.Am.Acad.Ophthalmol.Otolaryngol.* 1974;78:OP240-54.
18. Anderson DR. Ultrastructure of human and monkey lamina cribrosa and optic nerve head. *Arch Ophthalmol* 1969;82:800-14.
19. Varma R, Minckler D. Anatomy and pathophysiology of the retina and optic nerve. Ritch R, Shields MB, Krupin T., Mosby: St. Louis; 1996. 139-175 pp.

20. Emery JM, Landis D, Paton D, Boniuk M, Craig JM. The lamina cribrosa in normal and glaucomatous human eyes. *Trans.Am.Acad.Ophthalmol.Otolaryngol.* 1974;78:OP290-7.
21. Quigley HA, Hohman RM, Addicks EM, Massof RW, Green WR. Morphologic changes in the lamina cribrosa correlated with neural loss in open-angle glaucoma. *Am J Ophthalmol* 1983;95:673-91.
22. Hernandez MR. The optic nerve head in glaucoma: Role of astrocytes in tissue remodeling. *Prog Retin Eye Res* 2000;19:297-321.
23. Hernandez MR, Igoe F, Neufeld AH. Cell culture of the human lamina cribrosa. *Invest Ophthalmol Vis Sci* 1988;29:78-89.
24. Zode GS, Clark AF, Wordinger RJ. Activation of the BMP canonical signaling pathway in human optic nerve head tissue and isolated optic nerve head astrocytes and lamina cribrosa cells. *Invest.Ophthalmol.Vis.Sci.* 2007;48:5058-5067.
25. Wordinger RJ, Agarwal R, Talati M, Fuller J, Lambert W, Clark AF. Expression of bone morphogenetic proteins (BMP), BMP receptors, and BMP associated proteins in human trabecular meshwork and optic nerve head cells and tissues. *Mol Vis* 2002;8:241-50.
26. Yuan L, Neufeld AH. Activated microglia in the human glaucomatous optic nerve head. *J.Neurosci.Res.* 2001;64:523-532.

27. Li Guo, Stephen E. Moss, Robert A. Alexander, Robin R. Ali, Frederick W. Fitzke, and M. Francesca Cordeiro. Retinal ganglion cell apoptosis in glaucoma is related to intraocular pressure and IOP-induced effects on extracellular matrix. *DOI: 10.1167/iovs.04-0832* 2005;46:175-182.
28. Quigley HA, McKinnon SJ, Zack DJ, et al. Retrograde axonal transport of BDNF in retinal ganglion cells is blocked by acute IOP elevation in rats. *Invest Ophthalmol Vis Sci* 2000;41:3460-6.
29. Quigley HA. Neuronal death in glaucoma. *Prog Retin Eye Res* 1999;18:39-57.
30. Quigley HA, Nickells RW, Kerrigan LA, Pease ME, Thibault DJ, Zack DJ. Retinal ganglion cell death in experimental glaucoma and after axotomy occurs by apoptosis. *Invest Ophthalmol Vis Sci* 1995;36:774-86.
31. Morrison JC, Moore CG, Deppmeier LM, Gold BG, Meshul CK, Johnson EC. A rat model of chronic pressure-induced optic nerve damage. *Exp Eye Res* 1997;64:85-96.
32. Howell GR, Libby RT, Jakobs TC, et al. Axons of retinal ganglion cells are insulted in the optic nerve early in DBA/2J glaucoma. *J Cell Biol*. 2007;179:1523-1537.
33. Chintala SK, Zhang X, Austin JS, Fini ME. Deficiency in matrix metalloproteinase gelatinase B (MMP-9) protects against retinal ganglion cell death after optic nerve ligation. *J Biol Chem* 2002;277:47461-8.

34. Vaillant C, Meissirel C, Mutin M, Belin MF, Lund LR, Thomasset N. MMP-9 deficiency affects axonal outgrowth, migration, and apoptosis in the developing cerebellum. *Mol Cell Neurosci* 2003;24:395-408.
35. Verrecchia F, Mauviel A. Transforming growth factor-beta and fibrosis. *World J.Gastroenterol.* 2007;13:3056-3062.
36. Schnaper HW, Hayashida T, Hubchak SC, Poncelet AC. TGF-beta signal transduction and mesangial cell fibrogenesis. *Am.J.Physiol.Renal Physiol.* 2003;284:F243-52.
37. Tripathi RC, Li J, Chan WF, Tripathi BJ. Aqueous humor in glaucomatous eyes contains an increased level of TGF-beta 2. *Exp Eye Res* 1994;59:723-7.
38. Picht G, Welge-Luessen U, Grehn F, Lutjen-Drecoll E. Transforming growth factor beta 2 levels in the aqueous humor in different types of glaucoma and the relation to filtering bleb development. *Graefes Arch Clin Exp Ophthalmol* 2001;239:199-207.
39. Wordinger RJ, Fleenor DL, Hellberg PE, et al. Effects of TGF-beta2, BMP-4, and gremlin in the trabecular meshwork: Implications for glaucoma. *Invest.Ophthalmol.Vis.Sci.* 2007;48:1191-1200.
40. Gottanka J, Chan D, Eichhorn M, Lutjen-Drecoll E, Ethier CR. Effects of TGF-beta2 in perfused human eyes. *Invest.Ophthalmol.Vis.Sci.* 2004;45:153-158.

41. Welge-Lussen U, May CA, Lutjen-Drecoll E. Induction of tissue transglutaminase in the trabecular meshwork by TGF-beta1 and TGF-beta2. *Invest Ophthalmol Vis Sci* 2000;41:2229-38.
42. Fleenor DL, Shepard AR, Hellberg PE, Jacobson N, Pang IH, Clark AF. TGFbeta2-induced changes in human trabecular meshwork: Implications for intraocular pressure. *Invest Ophthalmol Vis Sci* 2006;47:226-34.
43. Tovar-Vidales T, Roque R, Clark AF, Wordinger RJ. Tissue transglutaminase expression and activity in normal and glaucomatous human trabecular meshwork cells and tissues. *Invest. Ophthalmol. Vis. Sci.* 2008;49:622-628.
44. Pena JD, Taylor AW, Ricard CS, Vidal I, Hernandez MR. Transforming growth factor beta isoforms in human optic nerve heads. *Br J Ophthalmol* 1999;83:209-18.
45. Neumann C, Yu A, Welge-Lussen U, Lutjen-Drecoll E, Birke M. The effect of TGF- β 2 on elastin, type VI collagen, and components of the proteolytic degradation system in human optic nerve astrocytes. *Invest. Ophthalmol. Vis. Sci.* 2008;49:1464-1472.
46. Fuchshofer R, Birke M, Welge-Lussen U, Kook D, Lutjen-Drecoll E. Transforming growth factor-beta 2 modulated extracellular matrix component expression in cultured human optic nerve head astrocytes. *Invest. Ophthalmol. Vis. Sci.* 2005;46:568-578.

47. Kirwan RP, Fenerty CH, Crean J, Wordinger RJ, Clark AF, O'Brien CJ. Influence of cyclical mechanical strain on extracellular matrix gene expression in human lamina cribrosa cells in vitro. *Mol. Vis.* 2005;11:798-810.
48. Kirwan RP, Leonard MO, Murphy M, Clark AF, O'Brien CJ. Transforming growth factor-beta-regulated gene transcription and protein expression in human GFAP-negative lamina cribrosa cells. *Glia* 2005;52:309-324.
49. Balemans W, Van Hul W. Extracellular regulation of BMP signaling in vertebrates: A cocktail of modulators. *Dev Biol* 2002;250:231-50.
50. Chang B, Smith RS, Peters M, et al. Haploinsufficient Bmp4 ocular phenotypes include anterior segment dysgenesis with elevated intraocular pressure. *BMC Genet* 2001;2:18.
51. Zeisberg M, Hanai J, Sugimoto H, et al. BMP-7 counteracts TGF-beta1-induced epithelial-to-mesenchymal transition and reverses chronic renal injury. *Nat. Med.* 2003;9:964-968.
52. Kinoshita K, Iimuro Y, Otogawa K, et al. Adenovirus-mediated expression of BMP-7 suppresses the development of liver fibrosis in rats. *Gut* 2007;56:706-714.
53. Izumi N, Mizuguchi S, Inagaki Y, et al. BMP-7 opposes TGF-beta1-mediated collagen induction in mouse pulmonary myofibroblasts through Id2. *Am.J.Physiol.Lung Cell.Mol.Physiol.* 2006;290:L120-6.

54. Wang S, Hirschberg R. Bone morphogenetic protein-7 signals opposing transforming growth factor beta in mesangial cells. *J Biol Chem* 2004;279:23200-6.
55. von Bubnoff A, Cho KW. Intracellular BMP signaling regulation in vertebrates: Pathway or network? *Dev Biol* 2001;239:1-14.
56. Zhang M, Fraser D, Phillips A. ERK, p38, and smad signaling pathways differentially regulate transforming growth factor-beta1 autoinduction in proximal tubular epithelial cells. *Am.J.Pathol.* 2006;169:1282-1293.
57. Rahimi RA, Leof EB. TGF-beta signaling: A tale of two responses. *J.Cell.Biochem.* 2007;102:593-608.
58. Nohe A, Keating E, Knaus P, Petersen NO. Signal transduction of bone morphogenetic protein receptors. *Cell.Signal.* 2004;16:291-299.
59. Wordinger RJ, Clark AF. Bone morphogenetic proteins and their receptors in the eye. *Exp.Biol.Med.(Maywood)* 2007;232:979-992.
60. Attisano L, Tuen Lee-Hoeflich S. The smads. *Genome Biol* 2001;2:REVIEWS3010.
61. Wordinger RJ, Zode G, Clark AF. Focus on molecules: Gremlin. *Exp.Eye Res.* 2007.
62. Dolan V, Murphy M, Alarcon P, Brady HR, Hensey C. Gremlin - a putative pathogenic player in progressive renal disease. *Expert Opin.Ther.Targets* 2003;7:523-526.

63. Topol LZ, Bardot B, Zhang Q, et al. Biosynthesis, post-translation modification, and functional characterization of Drm/Gremlin. *J.Biol.Chem.* 2000;275:8785-8793.
64. Murphy M, McMahon R, Lappin DW, Brady HR. Gremlins: Is this what renal fibrogenesis has come to? *Exp.Nephrol.* 2002;10:241-244.
65. Lappin DW, Hensey C, McMahon R, Godson C, Brady HR. Gremlins, glomeruli and diabetic nephropathy. *Curr Opin Nephrol Hypertens* 2000;9:469-72.
66. Boers W, Aarrass S, Linthorst C, Pinzani M, Elferink RO, Bosma P. Transcriptional profiling reveals novel markers of liver fibrogenesis: Gremlin and insulin-like growth factor-binding proteins. *J.Biol.Chem.* 2006;281:16289-16295.
67. Kane R, Stevenson L, Godson C, Stitt AW, O'Brien C. Gremlin gene expression in bovine retinal pericytes exposed to elevated glucose. *Br.J.Ophthalmol.* 2005;89:1638-1642.
68. Chen B, Blair DG, Plisov S, et al. Cutting edge: Bone morphogenetic protein antagonists Drm/Gremlin and dan interact with slits and act as negative regulators of monocyte chemotaxis. *J.Immunol.* 2004;173:5914-5917.
69. Myllarniemi M, Lindholm P, Ryynanen MJ, et al. Gremlin-mediated decrease in bone morphogenetic protein signaling promotes pulmonary fibrosis. *Am.J.Respir.Crit.Care Med.* 2008;177:321-329.

70. Koli K, Myllarniemi M, Vuorinen K, et al. Bone morphogenetic protein-4 inhibitor gremlin is overexpressed in idiopathic pulmonary fibrosis. *Am.J.Pathol.* 2006;169:61-71.
71. Dolan V, Murphy M, Sadler D, et al. Expression of gremlin, a bone morphogenetic protein antagonist, in human diabetic nephropathy. *Am.J.Kidney Dis.* 2005;45:1034-1039.
72. McMahon R, Murphy M, Clarkson M, et al. IHG-2, a mesangial cell gene induced by high glucose, is human gremlin. regulation by extracellular glucose concentration, cyclic mechanical strain, and transforming growth factor-beta1. *J Biol Chem* 2000;275:9901-4.

Chapter II

ACTIVATION OF THE BMP CANONICAL SIGNALING PATHWAY IN HUMAN OPTIC NERVE HEAD TISSUE AND ISOLATED OPTIC NERVE HEAD ASTROCYTES AND LAMINA CRIBROSA CELLS

Gulab S. Zode, Abbot F. Clark, and Robert J. Wordinger

Abstract

Bone morphogenetic proteins (BMPs) are members of the transforming growth factor (TGF)- β superfamily that controls multiple functions in a variety of cells. We have previously shown that human optic nerve head (ONH) astrocytes and lamina cribrosa (LC) cells express BMP and BMP receptor mRNA and proteins. The purpose of the present study was to determine whether human ONH tissues express the canonical BMP signaling pathway and whether ONH cells secrete BMP-4 and respond to exogenous BMP-4 through this pathway. Well-characterized human ONH astrocytes ($N = 2$) and LC cells ($N = 3$) were treated with exogenous BMP-4 (20 ng/mL) for various times. Western immunoblot analysis was used to detect secreted BMP-4 in serum-free conditioned media of ONH cells and in human ONH tissues ($N = 4$) and Smad proteins in total cell lysate of ONH cells and tissues. Intracellular colocalization of p-R-Smad1 with Co-Smad4 and localization of inhibitory Smads (e.g., I-Smad6 and I-Smad7) were studied through immunocytochemistry. In addition, coimmunoprecipitation was used to verify the interaction of p-R-Smad1 with Co-Smad4. ONH astrocytes and LC cells secrete BMP-4 and synthesize R-Smad1, R-Smad5, I-Smad6, I-Smad7, and Co-Smad4 proteins. Exposure to BMP-4 for either 10 or 60 minutes resulted in increased p-R-Smad1 and p-R-Smad1/5/8 protein levels that declined after 12 hours of treatment. Immunocytochemistry and coimmunoprecipitation studies revealed that p-R-Smad1/5/8 and Co-Smad4 interact and colocalize in the nucleus. BMP-4 treatment resulted in increased coprecipitation of p-R-Smad1/5/8 and Co-Smad4. I-Smad6 and I-Smad7 are localized in the nucleus and

cytoplasm of ONH astrocytes and LC cells. Proteins for BMP-4, p-R-Smad1/5/8, R-Smad1, R-Smad5, R-Smad8, and Co-Smad4 are present in human ONH tissues. In addition, phosphorylated Smad1 and Smad5 colocalize with Smad4 in the nuclei of ONH tissues. These results indicate that BMP-4 and Smad signaling proteins are present in human ONH tissues, isolated ONH astrocytes, and LC cells. In addition, exogenous BMP-4 treatment of ONH astrocytes and LC cells results in downstream signaling through the canonical Smad pathway. Thus, cells within the human ONH may respond to locally released BMP through paracrine or autocrine mechanisms

Introduction

Glaucoma is a heterogeneous group of optic neuropathies affecting more than 67 million individuals worldwide and is a major cause of visual impairment and irreversible blindness.¹ Elevated intraocular pressure (IOP) is the major risk factor in the development of glaucomatous optic neuropathy.^{2 3 4} Elevated IOP has been shown to affect the optic nerve head (ONH) by causing cupping and excavation that is associated with collapse and remodeling of the lamina cribrosa (LC).^{5 6 7 8} Optic nerve head changes are also associated with inhibited retrograde transport of neurotrophic factors in retinal ganglion cells (RGCs)^{9 10} and death of RGCs through apoptosis.^{11 12}

The LC region is the main structural component of the ONH through which RGC axons exit the eye.^{11 13} ONH astrocytes and LC cells are two major cell types that can be isolated from this region.^{8 14} Glaucomatous ONH changes are associated with activation of astrocytes, altered growth factor synthesis, and changes in extracellular matrix (ECM) synthesis or degradation.^{6 7 11 15 16} Growth factors play an important role in maintaining normal homeostasis in ocular tissues, including the ONH. Maintenance of an intricate balance between growth factors is essential for normal functioning.¹⁷ Thus, alterations in growth factor secretion or signaling may play a role in the pathogenesis of glaucoma.

Bone morphogenetic proteins (BMPs) were originally identified as osteoinductive cytokines that promote bone and cartilage formation, but they are now known to control multiple functions in a variety of cells.^{18 19} BMPs initiate signaling by binding to cell

surface type I and type II serine/threonine kinase receptors.^{19 20 21 22} On ligand binding, the type II BMP receptor transphosphorylates the type I BMP receptor. Downstream BMP signaling involves Smad signaling proteins. Receptor-regulated Smads (R-Smad1, R-Smad5, and R-Smad8) transiently associate with the type I BMP receptor and undergo direct phosphorylation. Subsequently, the phosphorylated R-Smad associates with common Smad4 (Co-Smad4), and the heteromeric complex translocates to the nucleus to regulate target genes.^{18 19 20 21 22 23 24 25}

Mice with a heterozygous deficiency of Bmp-4 result in developmental abnormalities of the optic nerve and anterior segment dysgenesis and elevated intraocular pressure,²⁶ indicating an important role of BMP-4 in the eye. In addition, recent reports have indicated that BMPs can inhibit TGF- β signaling. For example, in mesangial cells of the kidney, BMP-7 inhibits TGF- β signaling by reducing nuclear accumulation of R-Smad3.²⁷ Interestingly, we have demonstrated that BMP-4 can counteract the action of TGF- β 2-induced fibronectin synthesis in human trabecular meshwork (TM) cells.²⁸

We have previously reported that isolated ONH astrocytes and LC cells express mRNA and proteins for various BMPs and BMP receptors.¹⁷ However, for BMPs to be able to signal through autocrine or paracrine mechanisms in the human ONH, it is important to determine whether the canonical BMP/Smad signaling pathway is active. Thus, the objectives of this present study were to determine whether (1) BMP-4 and Smad proteins are present in human ONH cells and tissue, (2) cultured human ONH astrocytes and LC cells secrete BMP-4 and respond to exogenous BMP-4 treatment through the canonical

Smad signaling pathway, and (3) human ONH tissues express the canonical BMP/Smad canonical signaling pathway.

Materials and Methods

Optic Nerve Head Dissection and Cell Culture.

Human ONH cells were generated from dissected ONHs and characterized according to previous reports.^{29 30} Briefly, human donor eyes from regional eye banks were obtained within 24 hours of death, and the LC region of the ONH was dissected from the remaining ocular tissue. Lamina cribrosa tissues were cut into three to four explants and placed in culture plates containing Dulbecco modified Eagle medium (DMEM; Hyclone Laboratories, Logan, UT) containing L-glutamine (0.292 mg/mL; Gibco BRL Life Technologies, Grand Island, NY), penicillin (100 U/mL)/streptomycin (0.1 mg/mL; Gibco BRL Life Technologies), and amphotericin B (4 µg/mL; Gibco BRL Life Technologies). Cells that did not express glial fibrillary acidic protein (GFAP) were characterized as LC cells. Cells that expressed neural cell adhesion molecule [NCAM] and GFAP were characterized as ONH astrocytes. Confluent cells were passaged using 0.25% trypsin (Sigma-Aldrich, St. Louis, MO) and were maintained in 5%/CO₂/95% O₂ at 37°C.

Treatment with Exogenous BMP-4

ONH astrocytes and LC cells were grown in DMEM plus 10% FBS until they were 70% to 80% confluent. The cells were washed twice with PBS, cultured in serum-free DMEM for 24 hours, and treated with 20 ng/mL recombinant BMP-4 protein (R&D Systems, Minneapolis, MN) for 10 minutes, 30 minutes, 60 minutes, 12 hours, or 24 hours.

Protein Extraction and Western Blot Analysis

Cell Lysate. Total cellular protein was extracted from cultured ONH astrocytes and LC cells (Mammalian Protein Extraction Buffer; 78501; Pierce Biotech, Rockford, IL) with protease inhibitor cocktail (78415; Pierce Biotech). Protein concentration was determined using a protein assay system (Bio-Rad Dc; Bio-Rad Laboratories, Richmond, CA). Cellular protein was separated on denaturing polyacrylamide gels and then transferred to polyvinylidene difluoride (PVDF) membranes by electrophoresis.²⁹ The blots were blocked (SuperBlock Blocking Buffer, Prod 37537; Pierce Biotech) for 2 hours. The blots were then incubated overnight with the following primary antibodies: R-Smad1 (9512; Cell Signaling, Beverly, MA), R-Smad 5 (51-3700; Zymed, San Francisco, CA), p-R-Smad1 (566411; Calbiochem, La Jolla, CA), p-R-Smad1/5/8 (AB3848; Chemicon International, Temecula, CA), I-Smad6 (Zymed), I-Smad7 (Santa Cruz Biotechnology, Santa Cruz, CA), and Co-Smad4 (MAB 1132; Chemicon International). The membranes were washed with Tris-buffered saline Tween buffer (TBST) and processed with corresponding horseradish peroxidase-conjugated secondary antibody (donkey anti-rabbit

[SC-2077] or goat anti-mouse [SC-2005]; Santa Cruz Biotechnology). The proteins were then visualized in an imager (Fluor Chem 8900; Alpha Innotech, San Leandro, CA) using enhanced chemiluminescence detection reagents (SuperSignal West Femto Maximum Sensitivity Substrate; Pierce Biotechnology). To ensure equal protein loading, the same blot—developed with a horseradish peroxidase-conjugated secondary antibody (goat anti-mouse [SC-2005]; Santa Cruz Biotechnology)—was incubated again with a β -actin monoclonal antibody (Chemicon International).

Secreted BMP-4. To detect secreted BMP in conditioned medium, cells were maintained in serum-free DMEM for either 24 hours or 48 hours, and conditioned medium was concentrated 50-fold using a resin (StrataClean Resin, catalog no. 400714–61; Stratagene, La Jolla, CA). To ensure equal loading of protein, equal volumes of conditioned medium were loaded. Western blot analysis was conducted as described, and the blots were incubated overnight with a BMP-4 antibody (mAb757; R&D Systems). The secondary antibody consisted of goat anti-mouse (SC-2005; Santa Cruz Biotechnology).

Tissue Lysate. Four normal human eyes (donor age, 53–90 years) were obtained from regional eye banks within 6 hours of death. ONH was isolated and collected in buffer (Mammalian Protein Extraction Buffer, 78501; Pierce Biotech, Rockford, IL) with protease inhibitor cocktail (78415; Pierce Biotech). Samples were sonicated three times for 5 seconds each and kept on ice for 15 minutes. Solubilized proteins were centrifuged, and supernatants were used for Western blot analysis of BMP-4 and Smad signaling proteins.

Immunostaining

ONH astrocytes and LC cells were grown on glass coverslips, fixed with 3.5% (vol/vol) formaldehyde in PBS, and treated with 0.02% (vol/vol) Triton X-100 in PBS (Fisher Scientific, Pittsburgh, PA). Nonspecific binding was blocked by 2-hour incubation with 10% (vol/vol) normal serum in PBS (Gibco BRL Life Technologies). For localization of I-Smad6 and I-Smad7, coverslips were incubated overnight with I-Smad6 antibody (Zymed) and I-Smad7 antibody (Santa Cruz Biotechnology). For colocalization of p-R-Smad1 with Co-Smad4, coverslips were incubated overnight with p-R-Smad1 antibody (566411; Calbiochem) and co-Smad4 antibody (mAb 1132; Chemicon International) diluted in 1.5% (vol/vol) normal serum, followed by a 2-hour incubation in appropriate Alexa Fluor 488 donkey anti-rabbit and 633-labeled donkey anti-mouse secondary antibodies (1:200 in 1.5% [vol/vol] normal serum; Molecular Probes, Inc., Eugene, OR). The IgG controls used rabbit and mouse IgG in place of the primary antibody. Coverslips incubated in 1.5% (vol/vol) normal serum in place of primary antibody served as negative controls. To visualize nuclei, sections were treated with 4',6'-diamino-2-phenylindole (DAPI) nuclear stain for 30 minutes. Coverslips were then mounted on clean glass slides using mountant (Aquamount; Lerner Laboratories Inc., Pittsburgh, PA). Images were captured using a confocal imaging system (Zeiss 410; Carl Zeiss, Thornwood, NY).

For immunostaining of BMP-4 in ONH tissues, three normal human donor eyes were obtained from regional eye banks within 6 hours of death and fixed in 10% formalin. Fixed tissues were dehydrated and embedded in paraffin, and 8- μ m sections were

obtained. Sections were deparaffinized, rehydrated, and placed in 0.02% Triton X-100, followed by 20 mM glycine for 15 minutes each. Sections were blocked in 10% normal serum and incubated with anti-BMP-4 antibody (mAb1049; Chemicon International). After three washes, sections were incubated with appropriate secondary antibody (Alexa Fluor donkey anti-mouse, 1:200 in 1.5% [vol/vol] normal serum; Molecular Probes, Inc.) for 45 minutes. Sections were treated with DAPI for 30 minutes, washed, and mounted. Images were captured using a confocal imaging system (Zeiss 410; Carl Zeiss, Thornwood, NY).

For colocalization of p-R-Smad1 with Co-Smad4 in ONH tissues, coverslips were incubated overnight with p-R-Smad1 antibody and Co-Smad4 antibody diluted 1:100 in 1.5% (vol/vol) normal serum, followed by 2-hour incubation in appropriate Alexa Fluor488 donkey anti-rabbit and 633-labeled donkey anti-mouse secondary antibodies. Sections were treated with DAPI for 30 minutes, washed, and mounted. Images were captured using a confocal imaging system (Zeiss 410; Carl Zeiss).

Coimmunoprecipitation

ONH astrocyte and LC cell lysates were solubilized in immunoprecipitation buffer (M-PER Mammalian Protein Extraction Buffer; Pierce Biotechnology) with an excess amount of immunoprecipitating p-R-Smad1/5/8 antibody (3 μ g). The total volume was adjusted to 0.5 mL with immunoprecipitation buffer. Samples were then incubated overnight at 4°C. An appropriate amount of immobilized protein G (Sigma-Aldrich) was added, and samples were incubated overnight with gentle mixing at 4°C. The samples

were then washed six times with the immunoprecipitating buffer and were eluted using SDS-PAGE electrophoresis buffer, which was subsequently immunoblotted for interacting Co-Smad-4 protein.

Results

ONH Astrocytes and LC Cells Secrete BMP-4

We have previously shown that cells isolated from human ONH express mRNA and proteins for BMPs and BMP receptors.¹⁷ In this study, we first sought to determine whether cells isolated from the human ONH secrete BMPs. As demonstrated in [Figure 1](#), ONH astrocytes and LC cells secrete BMP-4. A recombinant protein for BMP-4 was used as a positive control for antibody specificity. Two bands at 22 kDa and 25 kDa, corresponding to the glycosylated and nonglycosylated forms of BMP-4, were detected. Secretion of BMP-4 appeared to increase in most cell lines from 24 to 48 hours. There was no apparent difference in secretion of BMP-4 between ONH astrocytes and LC cells. Although we previously demonstrated that ONH astrocytes and LC cells make proteins for BMP-4, BMP-5, and BMP-2, in Western blot analysis of conditioned medium, we found that ONH astrocytes and LC cells secrete higher amounts of BMP-4 ([Fig. 1](#)) than BMP-5 (data not shown). BMP-2 secretion was not detected in ONH cells.

Presence of Smad Signaling Proteins in ONH Astrocytes and LC Cells

The canonical downstream signaling pathway for BMPs uses intracellular Smad proteins.^{18 20 21 25} Thus, we sought to determine whether R-Smads (p-R-Smad1, R-Smad1, and R-Smad5) and Co-Smad4 were present in ONH astrocytes and LC cells. [Figure 2](#) demonstrates Western blot analysis for several Smad signaling proteins in each of two ONH astrocyte and LC cell lines. Proteins for R-Smad1, R-Smad5, and Co-Smad4

were detected in the cell lysates of ONH astrocytes and LC cells. In addition, Western blot analysis detected phosphorylated R-Smad1 (p-R-Smad1) protein in cell lysates of ONH astrocytes and LC cells in the absence of exogenous BMP, indicating autocrine/paracrine BMP signaling was occurring. Antibodies specific for phosphorylated R-Smad5 were unavailable. There were no apparent differences in protein levels of p-R-Smad1, R-Smad1, R-Smad5, and Co-Smad4 between ONH astrocytes and LC cells.

Coimmunolocalization of Phosphorylated R-Smad1 (p-R-Smad1) and Co-Smad4 in ONH Astrocytes and LC Cells

BMP ligands bind to cell-surface BMP receptors and activate downstream signaling through phosphorylation of R-Smads.^{20 21 22} Phosphorylated R-Smads form complexes with Co-Smad4 in the cytoplasm and then together translocate to the nucleus. We therefore examined colocalization of p-R-Smad1 and Co-Smad4 in ONH astrocytes and LC cells. Representative images of colocalization of Co-Smad4 and p-R-Smad1 in ONH astrocytes and LC cells are shown in Figure 3. Nuclear and cytoplasmic colocalization of p-R-Smad1 with Co-Smad4 were observed in untreated ONH astrocytes and LC cells, again indicating endogenous autocrine/paracrine Smad signaling was occurring. No staining was observed with nonimmune serum (data not shown) or when primary antibody was omitted.

Exogenous BMP-4 Increases Phosphorylated Smad Proteins in ONH Astrocytes and LC Cells

Having shown that ONH astrocytes and LC cells secrete BMP-4 and synthesize R-Smad and Co-Smad4 signaling proteins, we next sought to determine whether exogenous BMP-4 causes activation of downstream R-Smad signaling proteins. As shown in [Figure 4](#), we examined protein levels of p-R-Smad1, p-R-Smad1/5/8, R-Smad1, R-Smad5, and Co-Smad4 in BMP-4-treated ONH astrocytes ([Fig. 4A](#)) and LC cells ([Fig. 4C](#)). Increased protein levels of phosphorylated R-Smad1 and R-Smad1/5/8 were detected in ONH astrocytes and LC cells when treated with exogenous BMP-4. Densitometry analysis demonstrated that phosphorylation of R-Smad1 and R-Smad1/5/8 increased after 10 minutes of BMP-4 treatment and was highest at 60 minutes of BMP-4 treatment ([Figs. 4B](#) [4D](#)). There was a fourfold increase in the phosphorylation of R-Smad1/5/8 over R-Smad1 in ONH astrocytes and LC cells when treated with BMP-4 for 60 minutes. Phosphorylation appeared to decrease after 12 hours. Levels of nonphosphorylated R-Smad1 and R-Smad5 did not change in ONH astrocytes and LC cells when treated with exogenous BMP-4. Thus, our data indicate that ONH astrocytes and LC cells are capable of responding to exogenous BMP-4 through the canonical Smad signaling proteins (e.g., R-Smads and Co-Smad4).

BMP-4 Treatment Increases Coimmunoprecipitation of Co-Smad4 with p-R-Smad1/5/8 in ONH Astrocytes and LC Cells

To verify our coimmunolocalization study, we coimmunoprecipitated p-R-Smad1/5/8 with Co-Smad4 to determine whether BMP-4 treatment would increase the interaction between Co-Smad4 and p-R-Smad1. Co-Smad4 was detected in the Western blot when the p-R-Smad1/5/8 antibody was used to immunoprecipitate the cell lysate, followed by immunoblotting for Co-Smad4 (Fig. 5) . The coimmunoprecipitation appeared to increase after 60 minutes of BMP-4 treatment and declined after 2 hours of BMP-4 treatment.

Presence of Inhibitory Smads (I-Smad6 and I-Smad7) in ONH Astrocytes and LC Cells
BMP and TGF- β signaling are regulated by a variety of extracellular and intracellular mechanisms.^{18 31 32 33} Intracellular control of BMP and TGF- β signaling is mediated by the inhibitory Smads (e.g., I-Smad6 and I-Smad7). I-Smads are located predominantly in the nucleus but can be transported rapidly into the cytoplasm after ligand stimulation. In the cytoplasm, they bind to R-Smads and prevent interaction with Co-Smad4 and subsequent translocation to the nucleus.^{18 20 21 32 34} We used immunostaining and Western blot analysis to determine whether ONH astrocytes and LC cells express I-Smads. Positive immunostaining for I-Smad6 and I-Smad7 was observed in LC (Figs. 6A 6B) and ONH astrocyte (Figs. 6C 6D) cell lines. Nuclear and cytoplasmic localization of I-Smad6 and I-Smad7 were observed. No staining was observed with nonimmune serum or when primary antibody was omitted. To support the immunolocalization data, we performed Western blot analysis for I-Smad6 and I-Smad7 in total cell lysate of ONH astrocytes and LC cell lines. I-Smad6 and I-Smad-7 were present in astrocytes and LC cells (Fig. 6E) .

With respect to the Western blot analysis, I-Smad7 protein appeared to be present in greater amounts in ONH astrocyte and LC cell lines, suggesting that intracellular control of BMP and TGF- β signaling in ONH astrocytes and LC cells may occur via I-Smads.

BMP-4 Is Localized in Human ONH Tissues

Having shown secretion of BMP-4 and the presence of endogenous Smad signaling in cultured ONH astrocytes and LC cells, we sought to determine whether BMP-4 is localized to ONH tissues obtained from postmortem human donors. We performed immunostaining on paraffin-embedded human ONH sections. H&E staining revealed the orientation of retina and lamina cribrosa region (Fig. 7A) . Immunostaining of ONH tissues demonstrated that BMP-4 is localized in ONH (Fig. 7B) and is more prominent in the LC region (Fig. 7C) .

Presence of BMP-4 and Smad Signaling Proteins in Human Optic Nerve Head Tissues

We performed Western blot analysis of human ONH tissues to determine whether BMP-4 and Smad signaling proteins are present in vivo. BMP-4 was present in ONH tissues (Fig. 8) . Western blot analysis also demonstrated the presence of phosphorylated R-Smad1, total R-Smad1, R-Smad5, and Co-Smad4 at their expected relative sizes. The presence of BMP-4 and phosphorylated Smads in human ONH tissues indicates that Smad signaling can occur in the human ONH.

Coimmunolocalization of R-Smad5, Phosphorylated R-Smad1 (p-R-Smad1) with Co-Smad4 in Human ONH Tissue

Having shown the presence of BMP-4 and Smad signaling proteins in human ONH tissues, we next sought to determine whether phosphorylated R-Smads colocalize in the nucleus in situ. We performed colocalization of p-R-Smad1 and R-Smad5 with Smad4 in ONH tissues (Fig. 9). Nuclear and cytoplasmic colocalization of p-R-Smad1 and Smad5 with Co-Smad4 was observed in ONH tissues, indicating the presence of endogenous Smad signaling in the human ONH. No staining was observed with IgG treatment or when primary antibody was omitted. Interestingly, increased colocalization of R-Smad5 with Smad4 was observed compared with R-Smad1, indicating that R-Smad5 may play a major role in endogenous Smad signaling in the human ONH.

Discussion

Glaucomatous damage to the ONH consists of cupping and excavation of the optic disc, collapse and remodeling of the LC, and activation of optic nerve head astrocytes.^{7 8 11 15 35 36} Many of these changes are induced by elevated IOP because similar ONH changes are seen in animal models of ocular hypertension-induced glaucoma.^{13 16 37} However, glaucomatous damage to the ONH also occurs at low IOP in some glaucoma patients. Growth factors appear to play an important role in maintaining normal homeostasis in the ONH, and alterations in growth factors or growth factor receptors may be involved in glaucoma pathogenesis of the ONH.²⁸ We have reported that cells isolated from the human ONH express growth factors, including neurotrophins and their receptors.^{29 30} Members of the TGF- β superfamily of growth factors have been implicated in glaucomatous changes in the ONH.^{35 38 39} Elevated levels of TGF- β 2 in the ONH are associated with glaucomatous changes in the ECM, and TGF- β 2 and connective tissue growth factor alter ECM metabolism in cultured ONH cells.³⁸ TGF- β 1 expression is increased in stretched human LC cells, simulating the backward bowing of the LC tissue in glaucoma.^{40 41}

Other members of the TGF- β family of growth factors include the BMPs.¹⁹ We have previously demonstrated that human ONH astrocytes and LC cells express mRNA for BMPs and BMP receptors and synthesize proteins for BMP-2, BMP-5, BMP-4, BMP-7, and BMP receptors BMPRIA, BMPRIB and BMPRII.¹⁷ Although BMPs were initially

identified as osteoinductive factors that promote bone and cartilage formation, they also regulate a number of cellular functions in other tissues, including development, morphogenesis, cell proliferation, and apoptosis.¹⁹ A good example of the role of BMPs in the eye is the finding that mice with a heterozygous deficiency of Bmp-4 have developmental abnormalities of the optic nerve, anterior segment dysgenesis, and elevated intraocular pressure.²⁶

BMPs also appear to modulate TGF- β 2 signaling and fibrosis. BMP-7 inhibits TGF β -induced kidney fibrosis,²⁷ and we recently showed that BMP-4 inhibits TGF- β 2 induction of fibronectin in cultured human trabecular meshwork cells.³⁰ It is interesting to speculate that BMPs may act similarly in the ONH given the apparent involvement of TGF- β in damage and remodeling of the glaucomatous ONH and the finding that ONH cells and tissue express BMPs. As a first step to evaluate the potential role of BMPs in the ONH, we determined whether isolated ONH astrocytes and LC cells secrete BMP-4, express Smad proteins of the canonical BMP signaling pathway, and respond to exogenous BMP-4. We also sought to determine whether BMP-4 and proteins for the canonical BMP signaling pathway were present in human ONH tissues.

Our data demonstrate that ONH astrocytes and LC cells constitutively secrete BMP-4 and express R-Smad1, R-Smad5, and Co-Smad4 proteins. Phosphorylated R-Smad1 was present in both cell types, and p-R-Smad1 and Co-Smad4 were found within cell nuclei. Co-Smad4 requires association with activated R-Smads to enter the nucleus.²⁵ The presence of Co-Smad4 in the nuclei of ONH astrocytes and LC cells in conjunction with

p-R-Smad1 indicates that translocation of the signaling complex occurs in the absence of exogenous BMP-4. Together these data indicate that autocrine BMP signaling occurs in cultured ONH astrocytes and LC cells. We previously reported that BMP protein and BMP receptor proteins are present in ONH tissues,¹⁷ suggesting in vivo BMP autocrine signaling.

In addition to Smad signaling in ONH cells, we demonstrate that BMP-4 is localized in the ONH and is more prominent in the LC region. The presence of BMP-4, R-Smad1, R-Smad5, Co-Smad4, and phosphorylated R-Smad1/5/8 in the human ONH and the finding that pSmad1 and Smad5 colocalize with Smad4 in the nucleus indicates activation of the canonical Smad signaling pathway in the ONH tissues. To our knowledge, this is the first study to demonstrate that Smad signaling occurs in human ONH cells and tissues.

In addition to our evidence for BMP autocrine signaling, human ONH astrocytes and LC cells also respond to exogenous BMP-4 with increased activation of the Smad signaling pathway. The addition of exogenous BMP-4 increased the phosphorylation of p-R-Smad1 and p-R-Smad1, p-R-Smad5, and p-R-Smad8 (specific antibodies to the phosphorylated forms of R-Smad5 and R-Smad8 are unavailable). We also found increased coprecipitation of Smad4 with pSmad1/5/8. The increased protein levels recognized by the p-R-Smad1/5/8 antibody was fivefold greater than the increase in protein levels of p-R-Smad1, indicating that R-Smad5 or R-Smad8 may be activated to a greater degree by BMP-4 in ONH astrocytes and LC cells. The inhibitory effect of BMP on TGF- β 2 signaling in mesangial cells is mediated mainly through R-Smad5,²⁷

supporting the preferential involvement of select R-Smads in some BMP signaling pathways. Taken together, these results indicate that ONH astrocytes and LC cells respond to exogenous BMP-4 through the phosphorylation of R-Smads and increased interaction with Smad4, and they suggest that R-Smad5 and R-Smad8 are the major R-Smads used by ONH astrocytes and LC cells in BMP signaling.

The BMP signaling pathway is tightly controlled in virtually all cells.¹⁸ Extracellular and intracellular control mechanisms have been reported.²⁵ The most widely studied intracellular control mechanism involves inhibitory Smads (I-Smads).^{20 32 34} I-Smad6 and I-Smad7 compete with the receptor Smads (e.g., R-Smad1, R-Smad5, R-Smad8) for binding to the activated BMPRI receptor. Inhibitory Smads function to block transmission of signals from the membrane to the nucleus and are located predominantly in the nucleus but are transported rapidly to the cytoplasm after ligand stimulation.^{20 21} Inhibitory Smad6 can inhibit BMP signaling by competing with Co-Smad4 for complex formation with R-Smads. Inhibitory Smad6 is induced by various signals such as mechanical stress, TGF- β 1, and BMPs. Smad6 preferentially inhibits BMP signaling, whereas Smad7 inhibits TGF- β and BMP signaling.^{19 20 21 31} In our study, we also focused on the presence of I-Smad proteins in cells isolated from the human ONH. Our results indicate that I-Smad6 and I-Smad7 were present in the nucleus and cytoplasm of the ONH astrocytes and LC cells in the absence of BMP, suggesting that both I-Smads are constitutively expressed in these cell lines. The presence of both I-Smads indicates that the inhibition of BMP signaling may be occurring.

The function of BMP secretion and signaling within the human ONH may be multifaceted. BMP proteins could use unique autocrine/paracrine signaling mechanisms to regulate homeostasis and the microenvironment of the normal ONH. BMP signaling within the human ONH may regulate the local cellular activity of TGF- β 2. Within a given tissue, the action of most growth factors is often counterbalanced by the action of other growth factors.²⁸ This results in only small changes in tissue structure and function. TGF- β 2 is capable of inducing the expression of ECM and basement membrane components in cultured ONH astrocytes.³⁸ Thus autocrine/paracrine BMP signaling may be involved in the regulation of TGF- β 2 effects on ECM components in the ONH. Elevated levels of TGF- β 2 in glaucoma may disrupt the intricate balance between BMP and TGF- β 2, leading to increased deposition of ECM proteins within the ONH.

In conclusion, we show that ONH astrocytes and LC cells secrete BMP-4. ONH astrocytes and LC cells make Smad signaling proteins that undergo phosphorylation, suggesting BMP endogenous signaling. Exposure to exogenous BMP-4 caused increased phosphorylation of R-Smad and increased interaction R-Smad with Smad4, suggesting that ONH astrocytes and LC cells respond to exogenous BMP. Our results demonstrate that autocrine/paracrine BMP signaling occurs in ONH astrocytes and LC cells. Cytoplasmic localization of inhibitory Smads in ONH astrocytes and LC cells suggest that these factors play roles in regulating autocrine/paracrine BMP signaling. We also show that BMP-4 is localized in human ONH tissues. The presence of phosphorylated Smad1, total Smad5, and Smad4 and their colocalization in the nucleus indicates the

presence of autocrine/paracrine Smad signaling in ONH tissues. These studies demonstrate that ONH astrocytes and LC cells are capable of responding to exogenous BMP-4 through receptor Smads. Thus, cells of the ONH may be targets for and may respond to locally released BMP.

Acknowledgements

The authors thank Paula Billman (Alcon Research, Ltd.) and the Central Florida Lions Eye and Tissue Bank for ocular tissue and Anne-Marie Brun for her technical assistance.

Figure Legends

Figure1. *Chemiluminescence detection of BMP-4 secreted by human ONH astrocytes and lamina cribrosa.* Two ONH astrocyte and two LC cell lines were grown in serum-free DMEM for 24 to 48 hours. Conditioned medium was collected and concentrated 50 times before it was loaded onto a gel. A recombinant protein for BMP-4 (50 ng/lane) was loaded as a positive control.

Figure 2. *Chemiluminescence detection of Smad proteins in ONH astrocytes and LC cells.* Total cellular protein was collected from two ONH astrocyte and two LC cell lines and electrophoresed in SDS-PAGE gels; this was followed by Western immunoblotting. Both cell types expressed intermediate Smad signaling proteins, including R-Smad1, R-Smad5, and Co-Smad4 and phosphorylated R-Smad1. β -actin was used as internal loading control.

Figure 3. *Colocalization of Smad4 and pSmad1 in ONH astrocytes and LC cells.* ONH astrocytes and LC cells were kept in serum-free medium for 24 hours. Cells were then fixed and stained with antibodies for Co-Smad4 (monoclonal antibody) and p-R-Smad1 (rabbit antibody), followed by incubation with two secondary antibodies, donkey anti-mouse Alexa Fluor 633 (*red*) and donkey anti-rabbit Alexa Fluor 488 (*green*). (A, C) Colocalization of Smad4 (*red*) with pSmad1 (*green*) in cultured LC cells and ONH astrocytes, respectively. DAPI stain was used to counterstain the nucleus *blue*. (B, D) Cells incubated without primary antibody or with IgG (not shown) were used as negative

controls. Colocalization of Co-Smad4 and p-R-Smad1 in the nucleus in untreated cells indicates the presence of endogenous BMP signaling.

Figure 4. Chemiluminescence detection of Smad proteins in BMP-4-treated ONH astrocytes and LC cells. Human ONH astrocytes and LC cells were treated with exogenous BMP-4 (20 ng/mL) for various times (10 minutes, 30 minutes, 60 minutes, 12 hours, 24 hours) and compared with vehicle control (0 minutes). Phosphorylated R-Smad1, phosphorylated R-Smad1/5/8, R-Smad5, R-Smad1, and co-Smad4 were measured by Western blot and analyzed by densitometry. β -actin was used as loading control. (A, B) Western immunoblot and corresponding densitometric analysis of relative R-pSmad1 and R-pSmad1/5/8 protein levels normalized to β -actin in LC cells. (C, D) Western immunoblot and corresponding densitometric analysis of relative R-pSmad1 and R-pSmad1/5/8 protein levels normalized to β -actin in ONH astrocytes.

Figure 5. Coimmunoprecipitation study of Co-Smad4 with phosphorylated R-Smad1/5/8 in ONH astrocytes and LC cells. ONH astrocytes and LC cells were treated with exogenous BMP-4 for various times (0 minutes, 20 minutes, 60 minutes, 2 hours). Equal amount of cell lysate was incubated with immunoprecipitating antibody p-R-Smad1/5/8 and immunoblotted for co-Smad4. Co-Smad4 immunoprecipitated with p-R-Smad1/5/8 in ONH astrocytes and LC cells.

Figure 6. Localization of Smad6 and Smad7 in human ONH astrocytes and LC cells. Human ONH astrocytes and LC cells were fixed and stained with antibodies for I-Smad6

and I-Smad7. (A, B) Immunostaining for I-Smad6, I-Smad7, IgG, and no primary antibody control in ONH astrocytes. (C, D) Immunostaining for I-Smad6, I-Smad7, IgG, no primary antibody control in LC cells. Positive staining of these inhibitory Smads in the nucleus and cytoplasm indicates an active role of inhibitory I-Smad6 and I-Smad7 in ONH astrocytes and LC cells. Cells incubated without primary antibody or with IgG were used as negative control. (E) Western immunoblot analysis of I-Smad6 and I-Smad7 in two ONH astrocytes and two LC cell lines. Western blot demonstrated the presence of Smad6 and Smad7 proteins of 66 kDa and 60 kDa, respectively.

Figure 7. Immunohistochemical localization of BMP-4 in human ONH tissue.

Representative immunohistochemical localization of BMP-4 in human ONH tissue shown in Figure 7. Four normal human eyes were fixed, sectioned, and stained with anti BMP-4 antibody. Slides were incubated in 1.5% PBS-BSA without primary antibody and with IgG as negative control. (A) H&E staining of ONH tissue (100x) and (B) BMP-4 localization (100x) were used for orientation of staining in the LC region. (C) BMP-4 localization in the human ONH at higher magnification (400x). (D) No primary control in the human ONH (400x).

Figure 8. Western blot analysis of BMP-4 and Smad signaling proteins by human

ONH tissues. Western blot analysis of BMP-4 (58 kDa), p-R-Smad1/5/8 (66 kDa), R-Smad1 (60 kDa), R-Smad5 (60 kDa), and co-Smad4 (66 kDa) in four human ONH tissues. Approximately 15 µg total protein lysate was obtained from four human eye donors (ages 53, 80, 85, 88 years) and loaded on SDS-PAGE gel. β-actin was used as

loading control. The Western blot demonstrates the presence of BMP-4 and Smad signaling proteins in human ONH tissues.

Figure 9. Colocalization of Smad4 with R-pSmad1 and Smad5 in ONH tissue. (A) Colocalization of pSmad1 (*green*) with Smad4 (*red*) in human ONH tissue (1200x). (B) Colocalization of Smad5 (*green*) with Smad4 (*red*) in human ONH tissue (1200x). (C) Colocalization of Smad5 with Smad4 at higher magnification (2800x) of the sections used in (B). (D) IgG and no primary antibody control with a DAPI (400x). Colocalization of pSmad1 and Smad5 with smad4 in the nucleus and cytoplasm indicates the presence of endogenous Smad signaling in human ONH tissues.

Figures

Figure 1

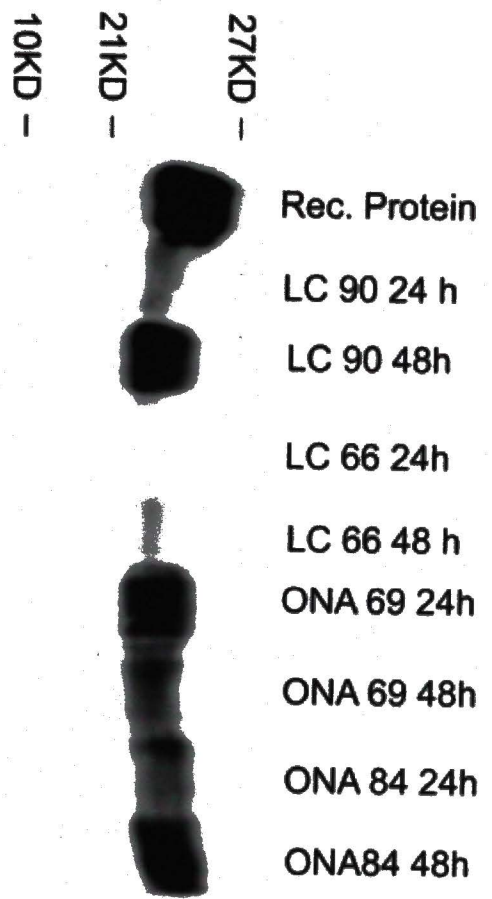


Figure 2

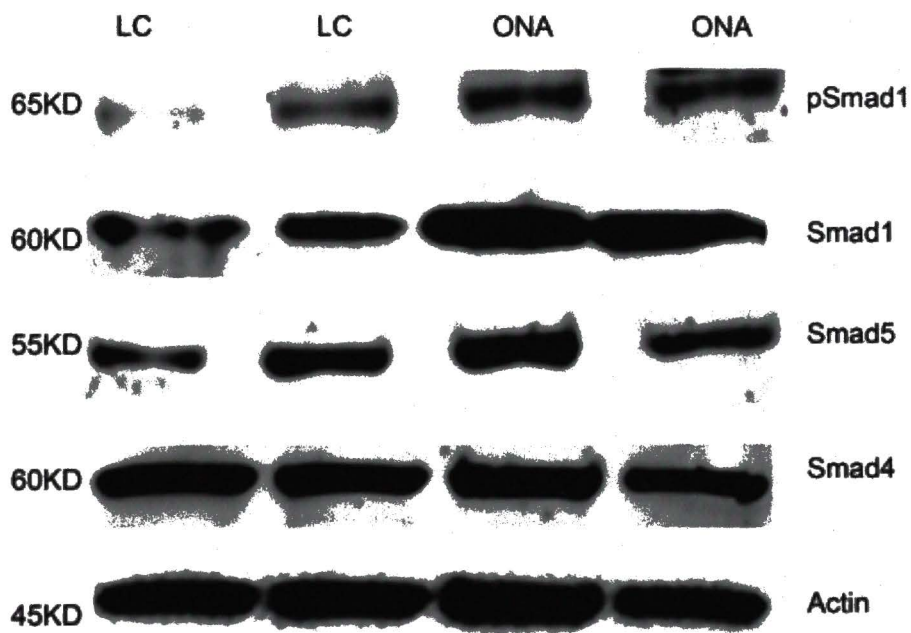


Figure3

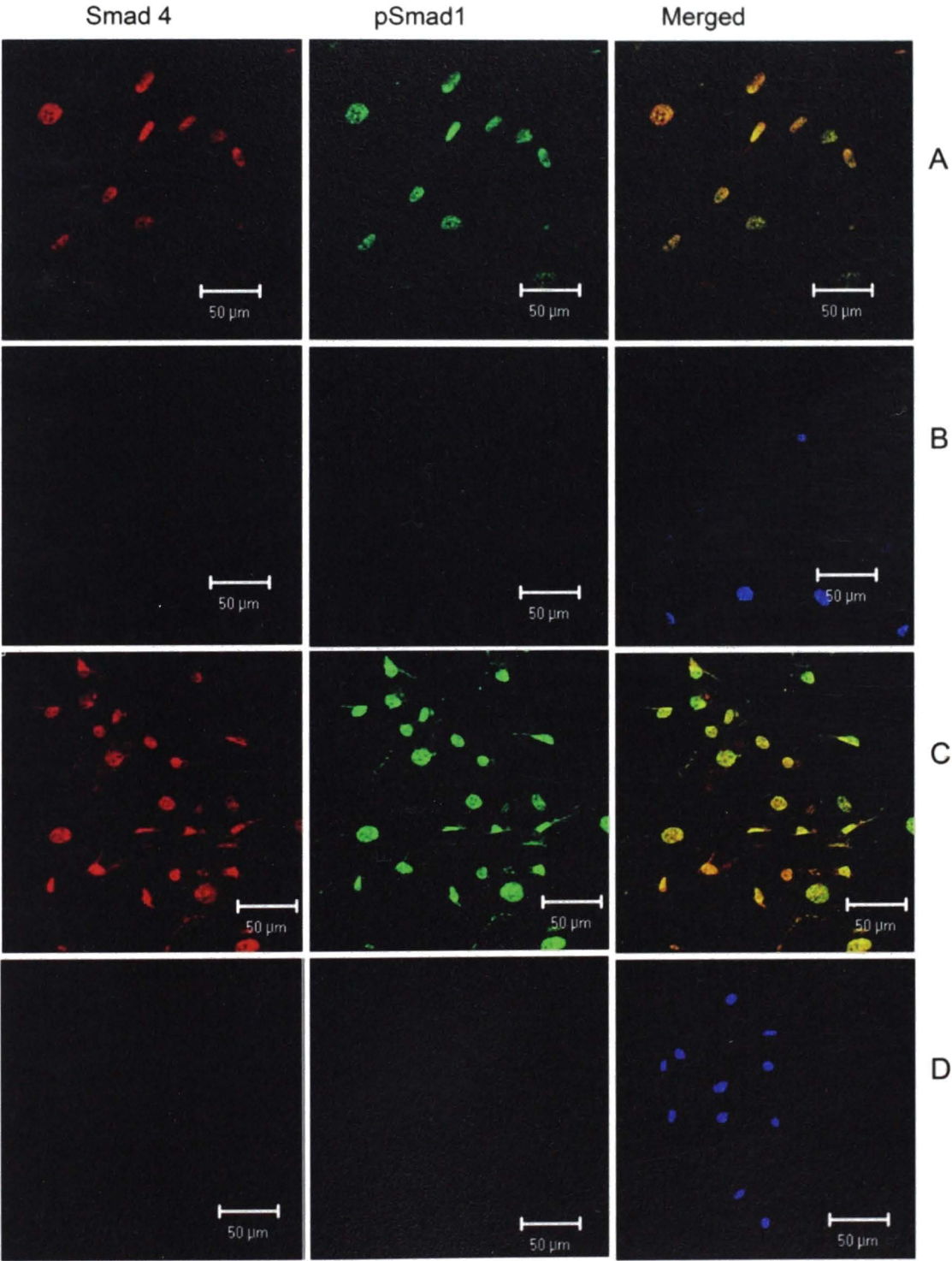


Figure 4

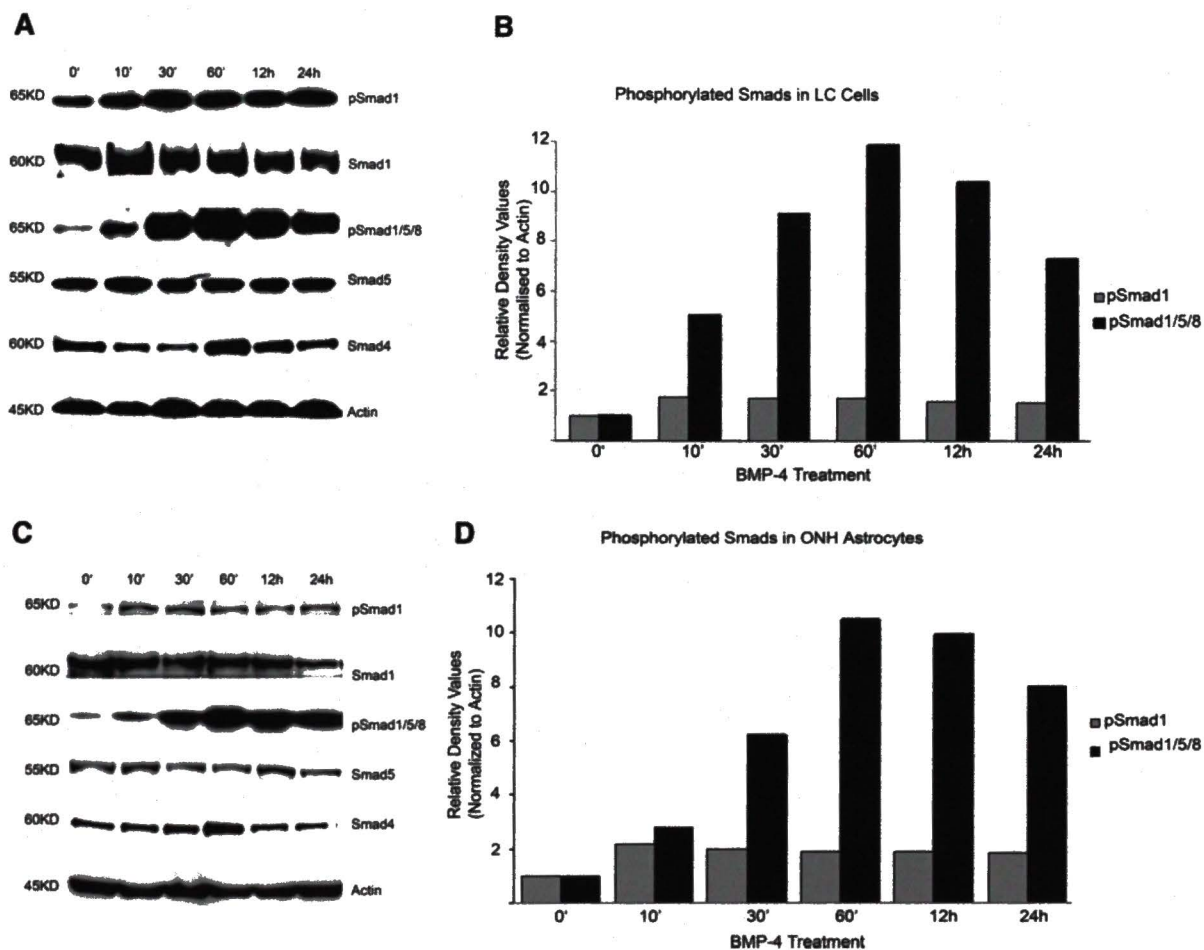


Figure 5

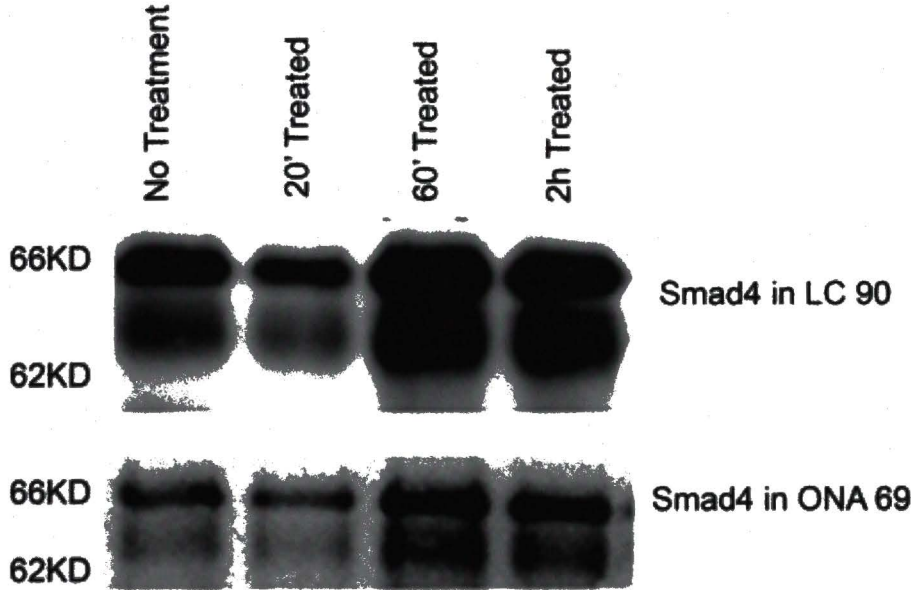


Figure 6

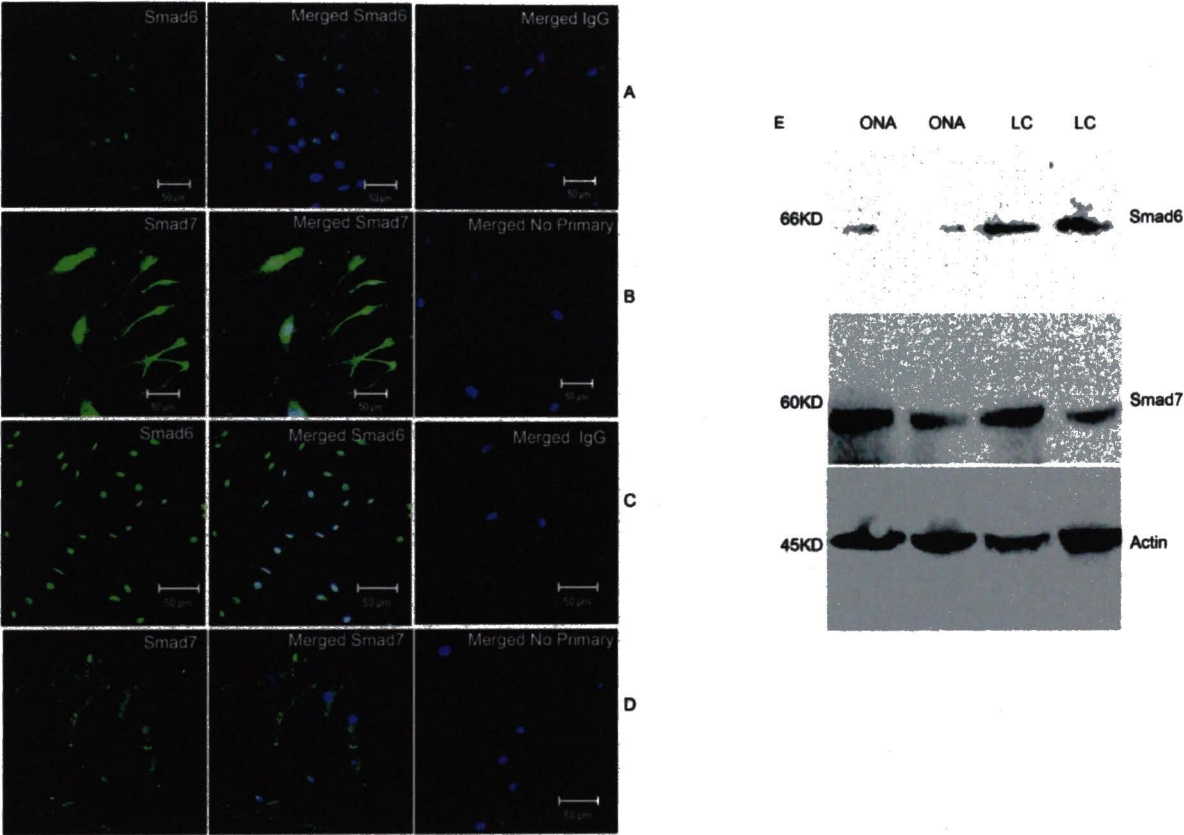


Figure 7

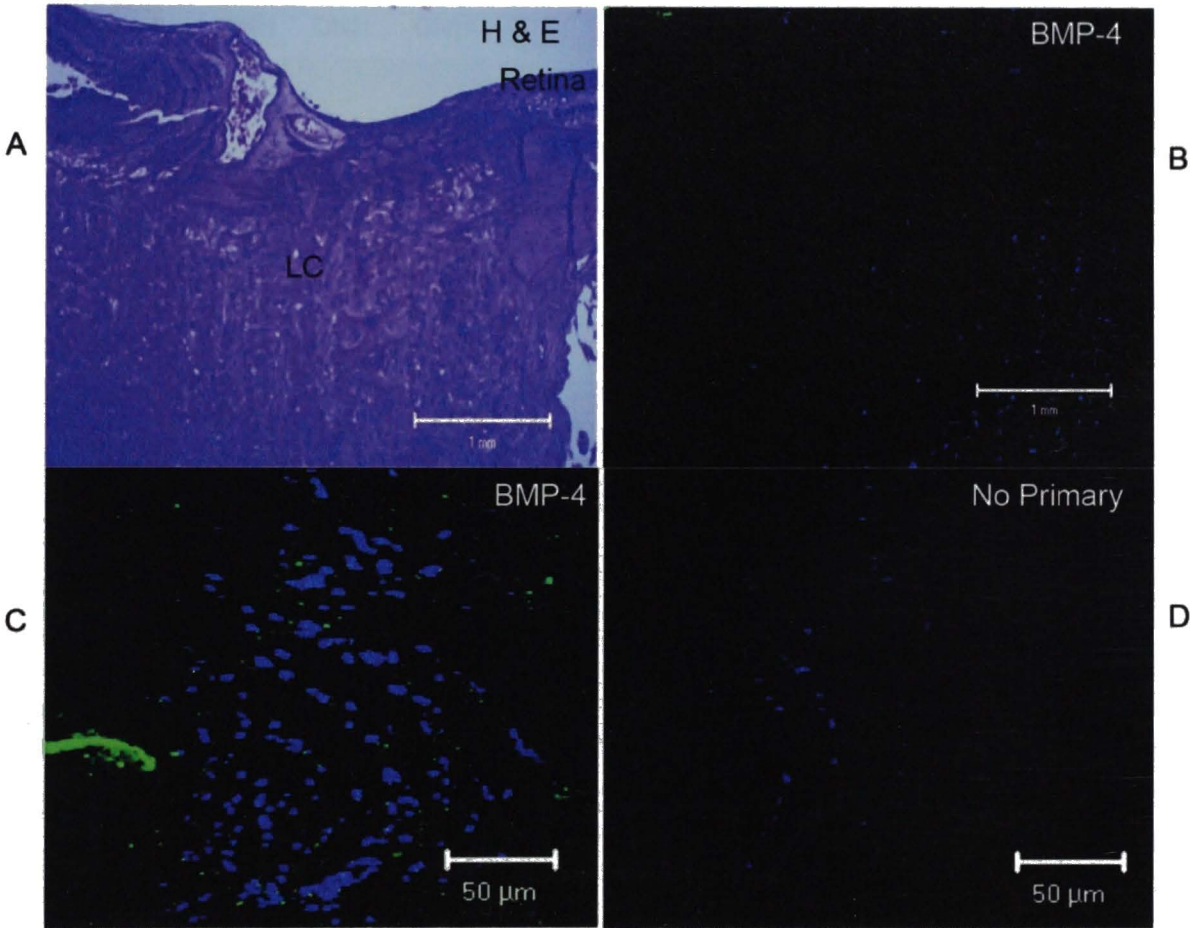


Figure 8

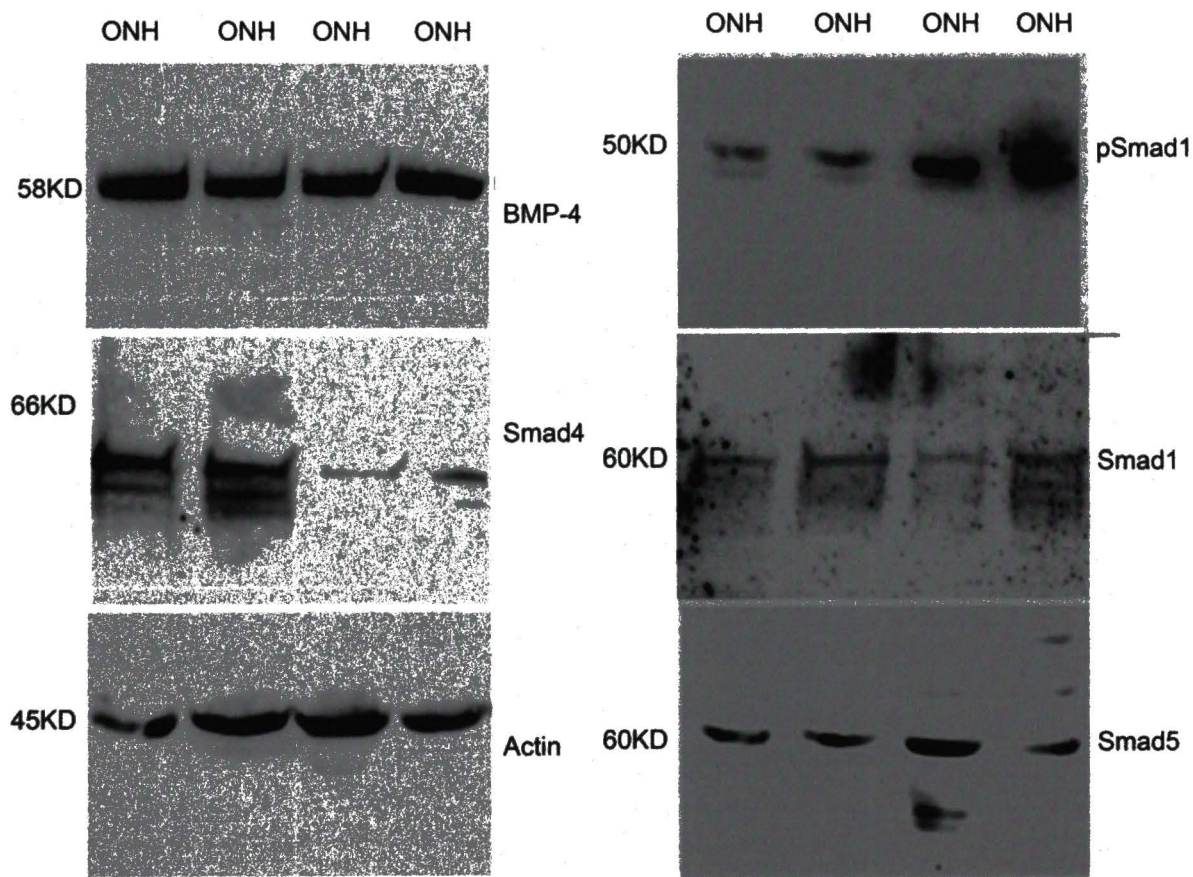
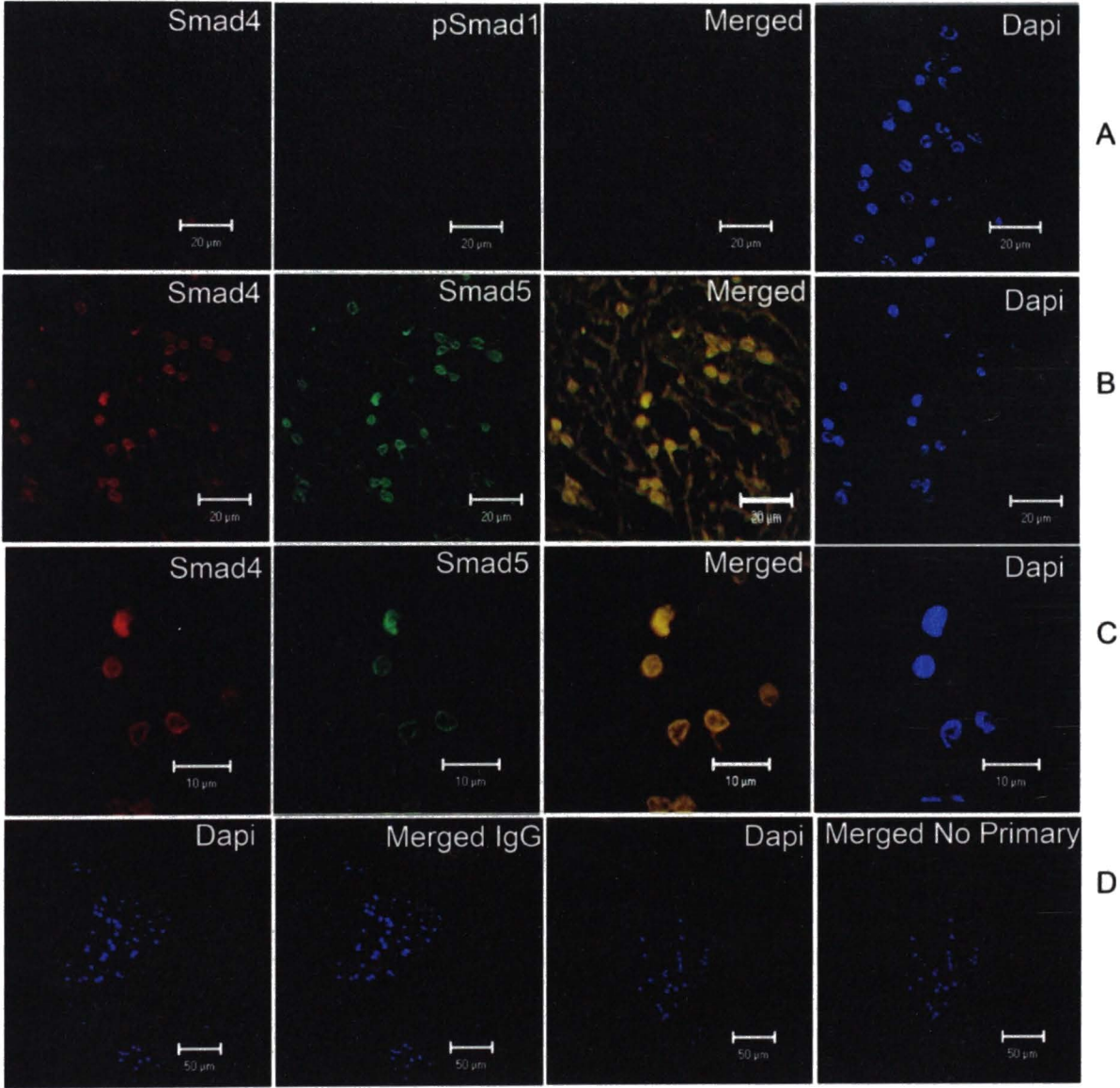


Figure 9



References

1. Quigley HA. Number of people with glaucoma worldwide. *Br J Ophthalmology*. 1996;80:389–393
2. Rohen JW. Why is intraocular pressure elevated in chronic simple glaucoma? anatomical considerations. *Ophthalmology*. 1983;90:758–765.
3. Rohen JW, Lutjen-Drecoll E, Flugel C, Meyer M, Grierson I. Ultrastructure of the trabecular meshwork in untreated cases of primary open-angle glaucoma (POAG). *Exp Eye Res*. 1993;56:683–692.
4. Grierson I, Calthorpe CM. Characteristics of meshwork cells and age changes in the outflow system of the eye: their relevance to primary open angle glaucoma. Mills KB eds. *Glaucoma: Proceedings of the Fourth International Symposium of the Northern Eye Institute*. 1989;12–31. Pergamon New York.
5. Anderson DR. Ultrastructure of human and monkey lamina cribrosa and optic nerve head. *Arch Ophthalmol*. 1969;82:800–814.
6. Hernandez M, Gong H. Extracellular matrix of the trabecular meshwork and optic nerve head. Ritch R Shields MB Krupin T eds. *The Glaucomas*. 1996;213–249. St. Louis Mosby.

7. Hernandez MR, Andrzejewska WM, Neufeld AH. Changes in the extracellular matrix of the human optic nerve head in primary open-angle glaucoma. *Am J Ophthalmol.* 1990;109:180–188.
8. Hernandez MR, Pena JD. The optic nerve head in glaucomatous optic neuropathy. *Arch Ophthalmol.* 1997;115:389–395.
9. Guo L, Moss SE, Alexander RA, Ali RR, Fitzke FW, Cordeiro MF. Retinal ganglion cell apoptosis in glaucoma is related to intraocular pressure and IOP-induced effects on extracellular matrix. *Invest Ophthalmol Vis Sci.* 2005;46:175–182.
10. Quigley HA. Neuronal death in glaucoma. *Prog Retin Eye Res.* 1999;18:39–57.
11. Quigley HA, Hohman RM, Addicks EM, Massof RW, Green WR. Morphologic changes in the lamina cribrosa correlated with neural loss in open-angle glaucoma. *Am J Ophthalmol.* 1983;95:673–691.
12. Quigley HA, Nickells RW, Kerrigan LA, Pease ME, Thibault DJ, Zack DJ. Retinal ganglion cell death in experimental glaucoma and after axotomy occurs by apoptosis. *Invest Ophthalmol Vis Sci.* 1995;36:774–786.
13. Morrison JC, Dorman-Pease ME, Dunkelberger GR, Quigley HA. Optic nerve head extracellular matrix in primary optic atrophy and experimental glaucoma. *Arch Ophthalmol.* 1990;108:1020–1024.

14. Hernandez MR, Igoe F, Neufeld AH. Cell culture of the human lamina cribrosa. *Invest Ophthalmol Vis Sci.* 1988;29:78–89.
15. Hernandez MR. The optic nerve head in glaucoma: role of astrocytes in tissue remodeling. *Prog Retin Eye Res.* 2000;19:297–321.
16. Johnson EC, Morrison JC, Farrell S, Deppmeier L, Moore CG, McGinty MR. The effect of chronically elevated intraocular pressure on the rat optic nerve head extracellular matrix. *Exp Eye Res.* 1996;62:663–674.
17. Wordinger RJ, Agarwal R, Talati M, Fuller J, Lambert W, Clark AF. Expression of bone morphogenetic proteins (BMP), BMP receptors, and BMP associated proteins in human trabecular meshwork and optic nerve head cells and tissues. *Mol Vis.* 2002;8:241–250.
18. von Bubnoff A, Cho KW. Intracellular BMP signaling regulation in vertebrates: pathway or network?. *Dev Biol.* 2001;239:1–14.
19. Hogan BL. Bone morphogenetic proteins: multifunctional regulators of vertebrate development. *Genes Dev.* 1996;10:1580–1594.
20. Attisano L, Tuen Lee-Hoeflich S. The Smads. *Genome Biol.* 2001;2:REVIEWS3010.

21. Balemans W, Van Hul W. Extracellular regulation of BMP signaling in vertebrates: a cocktail of modulators. *Dev Biol.* 2002;250:231–250.
22. Yamashita H, Ten Dijke P, Heldin CH, Miyazono K. Bone morphogenetic protein receptors. *Bone.* 1996;19:569–574.
23. Wozney JM, Rosen V, Celeste AJ, et al. Novel regulators of bone formation: molecular clones and activities. *Science.* 1988;242:1528–1534.
24. Roberts AB, Heine UI, Flanders KC, Sporn MB. Transforming growth factor-beta: major role in regulation of extracellular matrix. *Ann NY Acad Sci.* 1990;580:225–232.
25. Nohe A, Keating E, Knaus P, Petersen NO. Signal transduction of bone morphogenetic protein receptors. *Cell Signal.* 2004;16:291–299.
26. Chang B, Smith RS, Peters M, et al. Haploinsufficient Bmp4 ocular phenotypes include anterior segment dysgenesis with elevated intraocular pressure. *BMC Genet.* 2001;2:18.
27. Wang S, Hirschberg R. Bone morphogenetic protein-7 signals opposing transforming growth factor beta in mesangial cells. *J Biol Chem.* 2004;279:23200–23206.

28. Wordinger RJ, Fleenor DL, Hellberg PE, et al. Effects of TGF- β 2, BMP-4, and gremlin in the trabecular meshwork: implications for glaucoma. *Invest Ophthalmol Vis Sci.* 2007;48:1191–1200.
29. Lambert W, Agarwal R, Howe W, Clark AF, Wordinger RJ. Neurotrophin and neurotrophin receptor expression by cells of the human lamina cribrosa. *Invest Ophthalmol Vis Sci.* 2001;42:2315–2323.
30. Lambert WS, Clark AF, Wordinger RJ. Neurotrophin and trk expression by cells of the human lamina cribrosa following oxygen-glucose deprivation. *BMC Neurosci.* 2004;5:51.
31. Souchelnytskyi S, Nakayama T, Nakao A, et al. Physical and functional interaction of murine and xenopus Smad7 with bone morphogenetic protein receptors and transforming growth factor-beta receptors. *J Biol Chem.* 1998;273:25364–25370.
32. Zhao J, Crowe DL, Castillo C, Wuenschell C, Chai Y, Warburton D. Smad7 is a TGF-beta-inducible attenuator of Smad2/3-mediated inhibition of embryonic lung morphogenesis. *Mech Dev.* 2000;93:71–81.
33. Nakao A, Afrakhte M, Moren A, et al. Identification of Smad7, a TGF β -inducible antagonist of TGF- β signalling. *Nature.* 1997;389:631–635.

34. Imamura T, Takase M, Nishihara A, et al. Smad6 inhibits signalling by the TGF-beta superfamily. *Nature*. 1997;389:622–626.
35. Cordeiro MF, Khaw PT. The healing optic nerve in glaucoma: transforming growth factor beta and optic nerve head remodeling. *Br J Ophthalmol*. 1999;83:132–133.
36. Quigley HA, Addicks EM. Regional differences in the structure of the lamina cribrosa and their relation to glaucomatous optic nerve damage. *Arch Ophthalmol*. 1981;99:137–143.
37. Fukuchi T, Ueda J, Hanyu T, Abe H, Sawaguchi S. Changes in transforming growth factor-beta and platelet-derived growth factor in the optic nerve head in monkey experimental glaucoma. *Nippon Ganka Gakkai Zasshi*. 1999;103:193–200.
38. Fuchshofer R, Birke M, Welge-Lussen U, Kook D, Lutjen-Drecoll E. Transforming growth factor-beta 2 modulated extracellular matrix component expression in cultured human optic nerve head astrocytes. *Invest Ophthalmol Vis Sci*. 2005;46:568–578
39. Gottanka J, Chan D, Eichhorn M, Lutjen-Drecoll E, Ethier CR. Effects of TGF- β 2 in perfused human eyes. *Invest Ophthalmol Vis Sci*. 2004;45:153–158.

40. Kirwan RP, Crean JK, Fenerty CH, Clark AF, O'Brien CJ. Effect of cyclical mechanical stretch and exogenous transforming growth factor-beta1 on matrix metalloproteinase-2 activity in lamina cribrosa cells from the human optic nerve head. *J Glaucoma*. 2004;13:327–334.
41. Kirwan RP, Fenerty CH, Crean J, Wordinger RJ, Clark AF, O'Brien CJ. Influence of cyclical mechanical strain on extracellular matrix gene expression in human lamina cribrosa cells in vitro. *Mol Vis*. 2005;11:798–810.

Chapter III

TRANSFORMING GROWTH FACTOR-B2 INCREASES EXTRACELLULAR MATRIX PROTEINS VIA ACTIVATION OF SMAD SIGNALING PATHWAY IN OPTIC NERVE HEAD CELLS

Gulab S. Zode, Anirudh Sethi, Abbot F. Clark, and Robert J. Wordinger

Abstract

Elevated levels of transforming growth factor- β 2 (TGF- β 2) are associated with glaucomatous neuropathy primarily via increasing the extracellular matrix (ECM) proteins and remodeling the optic nerve head (ONH). Here, we demonstrate that TGF- β 2 and fibronectin (FN) are significantly increased in the human glaucomatous ONH. Optic nerve head astrocytes and lamina cribrosa (LC) cells make and secrete TGF- β 2. Recombinant TGF- β 2 increased ECM protein synthesis and secretion in ONH astrocytes and LC cells. However, the signaling pathway utilized by TGF- β 2 to stimulate ECM synthesis and secretion by ONH cells is not clearly established. Recombinant TGF- β 2 phosphorylated R-Smad2/3 but did not alter ERK1/2, p38, and JNK1/2 phosphorylation in ONH astrocytes and LC cells. TGF- β 2 also increased pSmad3 co-localization with Co-Smad4 in the nucleus of ONH astrocytes and LC cells indicating activation of Smad signaling pathway. Inhibition of activity of TGF- β I receptor by SB431542 or Smad3 phosphorylation by SIS3 reduced TGF- β 2 stimulated ECM proteins. Moreover, inhibition of R-Smad3 via siRNA knockdown of Smad3 reduced TGF- β 2 stimulated ECM proteins. Smad2 knockdown also decreased TGF- β 2 stimulated ECM in ONH astrocytes. These studies indicate that Smad2/3 is required for TGF- β 2 stimulation of ECM proteins in human ONH astrocytes and LC cells.

Introduction

Primary open angle glaucoma (POAG) is a progressive optic neuropathy, characterized by irreversible loss of retinal ganglion cell (RGC) axons¹. The exact pathogenic factor(s) responsible for POAG are still unknown. However, elevated intraocular pressure (IOP) is major treatable risk factor². The chronic elevation of IOP induces optic nerve head (ONH) changes, including compression of retinal ganglion cell (RGC) axons at the level of the lamina cribrosa (LC), blockage of axoplasmic flow, and inhibition of retrograde neurotrophin transport to RGCs¹⁻⁶. The glaucomatous ONH shows characteristic cupping and excavation of the optic disc, collapse and remodeling of the LC, and activation of ONH astrocytes⁷⁻¹¹.

The LC consists of a characteristic sieve-like structure through which RGC axons exit the eye. These laminar plates consist of extracellular matrix proteins such as elastin and collagens (I, III, V, and VI). The correct organization and assembly of the collagen fibers and elastin gives a supportive framework and elasticity to the ONH that protects RGC axons from mechanical stress^{7, 9, 12, 13}. Major cell types present in the human ONH include ONH astrocytes and LC cells^{8, 14}. These cells support RGC axons by synthesizing growth factors (e.g. neurotrophins) and ECM proteins¹⁵.

Remodeling of the ECM, including changes in fibrillar collagens, basement membrane components, and elastin composition is characteristic of the glaucomatous ONH. The ECM changes include backward bowing of the laminar plates with increased amounts of collagen I, IV, and VI. Altered elastin deposition in LC is thought to alter elastic

properties of the ONH. Increased synthesis and deposition of ECM proteins in the LC region may disrupt nutritional and mechanical support to RGC axons, resulting in RGC atrophy^{2, 4-7}. Many studies suggest that ONH astrocytes and LC cells response to elevated IOP by increasing TGF- β 2 synthesis in the LC region, which in turn causes increased synthesis and deposition of ECM proteins.

Transforming growth factor- β 2 belongs to the TGF- β superfamily and plays a fundamental role in the biology of the ECM¹⁶⁻¹⁸. In fibrotic diseases, elevated TGF- β 2 modulates ECM synthesis and deposition¹⁶. TGF- β 2 appears to be involved in the pathogenesis of POAG. Patients with glaucoma have higher levels of TGF- β 2 in their aqueous humor (AH),¹⁹ and TGF- β 2 has been shown to increase ECM protein in human trabecular meshwork (TM) cells. In cultured human perfused-anterior segments, TGF- β 2 increased IOP^{20, 21}.

A similar pathophysiology is observed in glaucomatous ONH including elevated TGF- β 2 and increased deposition of ECM proteins. In the glaucomatous ONH, elevated TGF- β 2 is associated with ECM remodeling²². Fuchshofer et al 2005 demonstrated that TGF- β treatment upregulates mRNA and protein expression of collagen I, collagen IV, fibronectin, connective tissues growth factor (CTGF), tissue transglutaminase (TGM2), and thrombospondin-1 (TSP-1) in ONH astrocytes²³. These observations suggest that TGF- β 2 could be an initiation factor in ECM remodeling in the glaucomatous ONH.

TGF- β 2 signaling involves activation of TGF- β receptors and activation of downstream Smad or non-Smad signaling pathways. In the canonical Smad signaling pathway, TGF-

$\beta 2$ dimers bind to the type II receptor which transphosphorylates the type I receptor. Activated type I receptor then phosphorylates R-Smads (R-Smad2/3), which triggers heterodimerization with Co-Smad4 and translocation of the complex to the nucleus to activate specific gene targets²⁴⁻²⁶. In non-Smad signaling pathways, activated TGF- β receptors utilize ERK, p38^{MAPK}, or JNK signaling proteins to activate gene targets. Although TGF- β may utilize ERK, p38^{MAPK}, or JNK signaling pathways^{27, 28}, Smad 2 and especially Smad3 are thought to be primary TGF- $\beta 2$ -driven fibrogenesis signals in many cell types including mesangial cells, retinal pigment epithelial cells, and skin fibroblasts^{17, 18, 29-32}.

Although elevated TGF- $\beta 2$ levels are associated with increased synthesis and deposition of ECM proteins in the glaucomatous ONH, little is known about the underlying signaling mechanisms. Here, we examine the signaling mechanism for TGF- $\beta 2$ stimulation of ECM synthesis and deposition in human ONH astrocytes and LC cells.

Methods and Materials

Optic Nerve Head Dissection and Cell culture

Human ONH cells were generated from dissected ONHs and characterized according to previous reports^{14,15, 33}. Briefly, human donor eyes from regional eye banks were obtained within 24 hours of death, and the LC region of the ONH was dissected from the remaining ocular tissue. Lamina cribrosa tissues were cut into three to four explants and placed in culture plates containing Dulbecco's modified Eagle's medium (DMEM, Hyclone Laboratories, Logan, Utah) containing L-glutamine (0.292 mg/ml, Gibco BRL Life Technologies, Grand Island, NY), penicillin (100 units/ml)/streptomycin (0.1 mg/ml, Gibco BRL Life Technologies), amphotericin B (4 µg/ml, Gibco BRL Life Technologies), and 10% fetal bovine serum (Gibco BRL Life Technologies). Optic nerve head astrocytes and LC cells were isolated and characterized as previously reported³³.

Treatment of ONH Astrocytes and LC Cells

ONH astrocytes and LC cells were grown in 12 well plates. Confluent cells were washed twice with sterile PBS, and kept in serum free medium for 24 hours. Fresh serum free medium was added to ONH astrocytes and LC cells, and incubated with recombinant TGF-β2 (5ng/ml). For the TGF-β2 dose response study, ONH astrocytes and LC cells were incubated with various concentrations of TGF-β2 (1.25, 2.5, 5, 10, and 20ng/ml) for 24 hrs. Cell lysate and culture medium were collected for further studies.

To examine the effect of inhibiting the type I TGF- β receptor (Alk5) or inhibiting phosphorylation of Smad3, cells were preincubated with SB431542 (10uM, Pro. # S4317; Sigma-Aldrich, St. Louis, MO) or SIS3 (25um and 50uM, EMD Chemicals, Inc, San Diego, CA) respectively, for 1 hr prior to treatment.

For Phosphorylation of R-Smads, ERK1/2, p38, or JNK1/2, confluent ONH astrocytes and LC cells were washed twice with PBS and kept in serum-free medium for 24 hours. Next day, fresh serum-free medium was added and incubated with recombinant TGF- β 2 (5ng/ml) for 30 minutes, 60 minutes, and 120 minutes. Cell lysates were collected and analyzed with phospho-specific antibodies using immunoblotting.

Immunostaining

Six human donor eyes (3 age-matched normal and glaucomatous eyes) were obtained from regional eye banks within 6 hours of death and fixed in 10% formalin. Fixed tissues were dehydrated, embedded in paraffin, and 8-um sections were obtained. Sections were deparaffinized, rehydrated and placed in 0.1% triton, followed by 20 mM glycine for 15 minutes each. Sections were blocked in 10% normal serum. Slides were incubated overnight with primary antibody (Table 1) diluted 1:100 in 1.5% (v/v) normal serum, washed 3 times with PBS followed by 2 hour incubation with appropriate Alexa Fluor™ conjugated secondary antibodies (1:200, Invitrogen Corporation ,CA). Sections were incubated with DAPI for 30 minutes to stain nuclei, washed and then mounted. Images were captured using a Zeiss 410 confocal imaging system (Carl Zeiss, Thornwood, NY).

Images were captured from the lamina cribrosa region, and the relative intensity of TGF- β 2 and FN was analyzed using Image J software (NIH). Confocal images were opened in Image J software and relative intensity was measured. Statistical analysis of staining intensity was performed with an unpaired Student's t test using GraphPadPrism 5.

Colocalization of pR-Smad3 and Smad4

LC cells were grown in glass coverslips. Confluent cells were kept in serum-free medium for 24 hrs and incubated with recombinant TGF- β 2 (5ng/ml) in serum-free medium for 60 minutes. The cells were then fixed with 3.5% formaldehyde (in PBS) for 10 minutes. The coverslips were washed with PBS and treated with 0.02% Triton for 10 minutes. The coverslips were washed twice with PBS and blocked with 10% normal donkey serum for 1 hr. The coverslips were incubated overnight with primary antibodies for pR-Smad3 and Smad4, washed 4 times with PBS and incubated with secondary antibodies for 2 hrs. Sections were incubated with DAPI for 30 minutes to stain nuclei, washed and then mounted. Images were captured using a Zeiss 410 confocal imaging system (Carl Zeiss, Thornwood, NY).

Protein Extraction and Western Blot Analysis

Cell Lysate: Total cellular protein was extracted from cultured ONH astrocytes and LC cells using Mammalian Protein Extraction Buffer (#78501, Pierce Biotech, Rockford, IL.) with Protease Inhibitor Cocktail (#78415, Pierce Biotech, Rockford, IL). Protein concentration was determined using the Bio-Rad Dc protein assay system (Bio-Rad

Laboratories, Richmond, CA). Cellular proteins were separated on denaturing polyacrylamide gels and then transferred to PVDF membranes by electrophoresis. Blots were blocked with Super Block Blocking Buffer (Prod# 37537 Pierce Biotech, Rockford, IL) for 1hrs. The blots were then incubated overnight with specific primary antibodies (Table 1). The membranes were washed with tris-buffered saline tween buffer (TBST) and processed with corresponding horseradish peroxidase-conjugated secondary antibody (Table 1). The proteins were then visualized in a Fluor ChemTM 8900 imager (Alpha Innotech corporation, San Leandro, CA 94577) using ECL detection reagents (SuperSignal West Femto Maximum Sensitivity Substrate, Pierce Biotechnology). To ensure equal protein loading, the same blot was incubated again with a β -actin monoclonal antibody and the blot was developed using a horseradish peroxidase-conjugated secondary antibody.

Conditioned Medium: To detect secreted TGF- β 2 proteins in conditioned medium, confluent ONH astrocytes and LC cells were grown in serum-free medium for 24 hrs. Culture medium was concentrated 20 times and equal volumes of conditioned medium were analyzed in western blots and processed as described above.

ONH Tissue Lysate: Two normal human eyes (donor age, 55 and 76 year) were obtained from regional eye banks within 6 hours of death. ONH was isolated and collected in buffer (Mammalian Protein Extraction Buffer, cat # 78501, Pierce Biotech, Rockford, IL) with protease inhibitor cocktail (# 78415; Pierce Biotech, Rockford, IL).

Samples were then sonicated and centrifuged. Supernatants were used for western blot analysis of TGF- β 2.

ELISA Immunoassay for Fibronectin

Conditioned medium was obtained from ONH astrocytes and LC cells and centrifuged at 2000/rpm to remove cellular debris. A total 50 μ l of conditioned medium was diluted to 150 μ l with dilution buffer, and soluble fibronectin was quantified using a commercially available ELISA kit (cat # ECM 300; Chemicon International, Temecula, CA). Soluble fibronectin (μ g/ml) was plotted for each treatment using GraphPadPrism 5.

Small interfering RNA and transfection

siRNA for Smad2/3 and non-targeting siRNA controls were purchased from Dharmacon (SMARTpool). Transfection of siRNA was performed as described previously³¹. Briefly, ONH astrocytes and LC cells were plated in 12-well plates containing DMEM with 10% fetal bovine serum. At 30-40% confluence, transfection of siRNA was performed. In one tube, 4 μ l of DharmaFECT 1 Transfection Reagent (T-2001-01 Dharmacon, Inc. IL) was mixed gently with 200 μ l of Opti-MEM medium (Invitrogen Corporation, CA) and incubated 5 min at room temperature. In separate tubes, various concentrations of siRNA were mixed gently with 200 μ l of Opti-MEM medium. These two tubes were combined, gently mixed, and incubated for 20 min at room temperature. After incubation, Opti-MEM medium was added to obtain a final volume of 2 ml for each well (25nM and 50nM of Smad3 siRNA and 50nM of non-specific siRNA controls). Cells were washed

with sterile PBS twice and incubated with siRNA transfection solution for 48 h at 37 °C. After that, ONH cells were washed with serum-free DMEM medium and treated with TGF- β 2 (5ng/ml) in serum-free DMEM medium for 24 hrs. The culture medium and cell lysates were analyzed for Smad3, FN, PAI-1, and actin levels.

Table #1: List of Antibodies

Antibody (cat #)	Dilution	Source
Fibronectin (sc-18827)	1:1000	Santa Cruz Biotechnology, Inc. Santa Cruz, CA.
PAI-1 (sc-5297)	1:1000	Santa Cruz Biotechnology, Inc. Santa Cruz, CA.
TGF- β 2 (PAB-10580)	1:500	Santa Cruz Biotechnology, Inc. Santa Cruz, CA.
Collagen I (sc-8783)	1:500	Santa Cruz Biotechnology, Inc. Santa Cruz, CA.
Collagen VI (AB-7821)	1:2000	Millipore Corporate, Billerica, MA
Elastin (MAB-2503)	1:1000	Millipore Corporate, Billerica, MA
β -actin (MAB-1501)	1:2000	Millipore Corporate, Billerica, MA

Goat Anti Mouse(sc-2055)	1:2000 0	Santa Cruz Biotechnology, Inc. Santa Cruz, CA.
Goat Anti Rabbit	1: 20000	Millipore Corporate, Billerica, MA
pSmad3	1:500	Cell Signaling Technology, Inc., Danvers, MA
Smad3	1:500	Cell Signaling Technology, Inc., Danvers, MA
Pp38MAPK	1:500	Cell Signaling Technology, Inc., Danvers, MA
P38MAPK	1:500	Cell Signaling Technology, Inc., Danvers, MA
pJNK1/2	1:500	Cell Signaling Technology, Inc., Danvers, MA
JNK1/2	1:500	Cell Signaling Technology, Inc., Danvers, MA
pERK1/2	1:500	Santa Cruz Biotechnology, Inc. Santa Cruz, CA.

Results

Increased TGF- β 2 and Fibronectin (FN) Protein levels in the Glaucomatous Human ONH Tissues

To determine whether TGF- β 2 and fibronectin (FN) are increased in the glaucomatous ONH, we first examined three aged matched normal and glaucomatous ONH tissues. Figure 1A is a low power magnification photomicrograph (100X) of H & E stained sections of the human ONH for orientation purposes. The optic nerve, retina, and the lamina cribrosa region of the ONH are labeled. Figure 1B is a higher magnification photomicrograph (400X) of a H & E section of the human ONH showing the LC region. Figures 1C and 1D are representative examples of TGF- β immunolocalization merged with DAPI nuclear stain in normal and glaucomatous ONH that demonstrates TGF- β 2 is present in normal human ONH tissue sections and its level is increased in glaucomatous ONH tissues. Figures 1E and 1F are representative examples of FN merged with DAPI nuclear stain in normal and glaucomatous ONH that demonstrates FN is also present in normal human ONH tissue sections and its level is also increased in glaucomatous ONH tissues. No staining was observed with IgG treatment or when primary antibody was omitted (Figure 1G and H). In addition, we examined the relative intensity of staining using Image J software. Figures I and J demonstrate the relative intensity of TGF- β 2 and FN respectively as measured by Image J software (NIH). These results indicated that both TGF- β 2 and FN were significantly increased ($N=3$, $p<0.05$) in aged matched glaucomatous ONH tissues compared to age-matched controls. Interestingly,

immunostaining for TGF- β 2 and FN appeared to be more prominent along axon bundles in glaucomatous ONH tissues.

Presence of TGF- β 2 in ONH Cells and Tissues

To examine the role TGF- β 2 in ECM modulation *in the ONH*, we next sought to determine whether ONH astrocytes and LC cells synthesize and secrete endogenous TGF- β 2. Confluent ONH astrocytes and LC cells were kept in serum-free medium for 24 hours. Cell lysates and conditioned medium (20X) were analyzed for TGF- β 2. Western blot analysis demonstrated that ONH astrocytes and LC cells make and secrete endogenous TGF- β 2. In addition, lysates from human ONH tissues demonstrated the presence of endogenous TGF- β 2, confirming our results from immunostaining for TGF- β 2. Recombinant TGF- β 2 was used as a positive control for the antibody and demonstrated a band at 25 KD corresponding to the samples from ONH astrocytes and LC cells (Fig. 2). These results indicate the presence of TGF- β 2 both in human ONH tissues and isolated ONH astrocytes and LC cells.

TGF- β 2 Increases FN and PAI-1 in ONH Astrocytes and LC Cells in a Dose Dependent Manner

To understand the effect of increased TGF- β 2 on ECM proteins *in vitro*, we examined whether incubation of ONH astrocytes and LC cells with exogenous TGF- β 2 increase protein levels of FN and PAI-1. We first performed a dose response curve for TGF- β 2 effects on FN and PAI-1. Optic nerve head astrocytes and LC cells (N=3, each)

were treated with various concentrations of recombinant TGF- β 2 (1.25, 2.5, 5, 10, and 20ng/ml) for 48 hours. The effect of TGF- β 2 on FN and PAI-1 was examined using western blot analysis (Figure 3A-B) and ELISA for FN (Figure 3C). The western blot data indicated that TGF- β 2 increased both cellular (figure 3A) and secreted FN (figure 3B) and PAI-1 in a dose dependent manner in LC cells. The ELISA analysis indicated that TGF- β 2 significantly increased soluble FN levels at 5, 10, and 20 ng/ml in ONH astrocytes (n=3, $P<0.001$). Since a concentration of 5ng/ml significantly increased soluble FN, we choose to utilize this concentration in future studies.

Recombinant TGF- β 2 Increases ECM Proteins in ONH Astrocytes and LC Cells.

In these experiments, we sought to examine whether exogenous TGF- β 2 increases secretion of other ECM proteins that have been reported previously to be altered in the glaucomatous ONH. The proteins that were examined included type I collagen, type VI collagen, and elastin. ONH astrocytes and LC cells were treated with 5ng/ml recombinant TGF- β 2 for 24 hrs and culture medium (5X concentrated) was subjected to western blot analysis. Recombinant TGF- β 2 increased the secretion of type I collagen, type VI collagen, and elastin in ONH astrocytes and LC cells (Fig. 4)

Inhibition of the Type I TGF- β Receptor Reduces TGF- β 2 Stimulation of ECM Proteins.

In the TGF- β signaling pathway, activation of the type I TGF- β receptor (TGF- β RI) by the type II receptor (TGF- β RII) upon binding of TGF- β 2 dimers activates downstream

signaling²⁴. We examined whether TGF- β 2 effects on ECM are mediated via activation of type I TGF- β receptor by using SB431542, a selective and potent inhibitor of activity of TGF- β 1 activin receptor-like kinases (ALK5). Addition of SB431542 (5ug/ml) blocked TGF- β 2 stimulation of cellular FN and PAI-1 in ONH astrocytes and LC cells (Figure 5A). Densitometric analysis indicated that inhibition of TGF- β RI blocked TGF- β 2 stimulation of ECM proteins in ONH astrocytes and LC cells (figure 5B & 5C, $n=3$ *, $P < 0.05$ verses control; †, $P < 0.05$ verses TGF- β 2). These findings demonstrate that inhibition of TGF- β RI reduces TGF- β 2 up-regulation of ECM proteins in ONH astrocytes and LC cells.

TGF- β 2 Does Not Activate ERK1/2, p38, or JNK1/2 Pathways in ONH Astrocytes and LC Cells

To elucidate whether TGF- β 2 differentially activates non-Smad signaling pathways such as ERK1/2, p38, or JNK1/2 in ONH astrocytes and LC cells, we examined the phosphorylation of these signal kinases using immunoblotting with phospho-specific antibodies (Fig 6). In ONH astrocytes and LC cells, treatment with recombinant TGF- β 2 for 30 minutes, 60 minutes, or 120 minutes did not increase ERK1/2 phosphorylation compared to baseline control. Similarly, recombinant TGF- β 2 did not alter phosphorylation of p38 or JNK1/2 in ONH astrocytes and LC cells. Thus, TGF- β 2-driven stimulation of ECM proteins may not involve activation of ERK1/2, p38, or JNK1/2 in ONH astrocytes and LC cells (Fig 6).

Recombinant TGF- β 2 Increases Phosphorylation of R-Smads in ONH Astrocytes and LC Cells.

The canonical TGF- β signaling involves activation of R-Smads (Smad2/3). Thus, we examined whether recombinant TGF- β 2 increases the phosphorylation of R-Smad2/3 in ONH astrocytes and LC cells. ONH astrocytes and LC cells were incubated with TGF- β 2 (5ng/ml) and phosphorylation of Smad2 and Smad3 was analyzed using immunoblotting. Recombinant TGF- β 2 increased the phosphorylation of Smad2 and Smad3 compared to baseline control (Fig7). This finding suggests that activation of Smad signaling is involved in TGF- β 2-driven stimulation of ECM proteins in ONH astrocytes and LC cells.

TGF- β 2 Increases Co-localization of Phosphorylated R-Smad3 and Co-Smad4 in LC Cells

Activated R-Smads form a complex with Co-Smad4, which facilitates nuclear import and interaction with target genes. We examined whether TGF- β 2 increases the co-localization of p-Smad3 and Co-Smad4 in LC cells (Fig 8). Even in serum deprived, untreated LC cells, there is some co-localization of p-Smad3 and Smad4 in the nucleus, indicating the presence of an endogenous autocrine TGF- β signaling pathway. However, in TGF- β 2 stimulated LC cells, the colocalization of phosphorylated R-Smad3 and Co-Smad4 is increased in the cytoplasm as well as in nucleus. In addition, p-Smad3 and Co-Smad4 levels are increased in TGF- β 2 stimulated LC cells. This finding supports our previous immunoblotting results indicating that TGF- β 2 phosphorylates of R-smad3 which then translocates to nucleus to activate target genes for ECM proteins.

Inhibition of Phosphorylation of R-Smad3 Reduced TGF- β 2-Driven Stimulation of FN in ONH Astrocytes and LC Cells

To elucidate whether TGF- β 2-driven stimulation of ECM proteins is mediated via activation R-Smad3, we inhibited phosphorylation of Smad3 with SIS3 (a specific inhibitor of Smad3). ONH astrocytes and LC cells were preincubated with SIS3 (25 μ M and 50 μ M) 1 hour prior to treatment with TGF- β 2. TGF- β 2 stimulation of FN secretion was reduced to baseline control level upon addition of SIS3 in ONH astrocytes and LC cells (Fig 9). This finding suggests that TGF- β 2-driven stimulation of ECM proteins requires activation of R-Smad3.

Reduction of R-Smad3 via siRNA Blocks TGF- β 2-Driven Stimulation of FN and PAI-1 in ONH Astrocytes and LC Cells

TGF- β 2-driven fibrogenesis is thought to be mediated primarily via R-Smad2/3. We conducted siRNA knockdown of R-Smad3 along with control siRNAs (RISC-Free siRNAs and non-targeting siRNAs) for 48 hrs in ONH astrocytes and LC cells. Smad3 and actin protein levels were assessed using western blot (Figure 10A) and measured by densitometric analysis (Figure 10B). Transfection with Smad3-siRNA (25nM and 50nM) resulted in significant ($P<0.001$) reduction of R-Smad3 protein levels compared to control siRNAs (50nM) in ONH astrocytes and LC cells (Figure 10A and B). Control siRNAs did not significantly alter R-Smad3 proteins levels compared to vehicle control

indicating sequence-specific silencing of our target siRNAs (Figure 10A and B). ONH astrocytes were treated with TGF- β 2 with and without siRNAs for R-Smad3. Western blot and densitometric analysis demonstrated that reduction of R-Smad3 via siRNA (25nM and 50nM) significantly blocked the stimulatory effects of TGF- β 2 on FN and PAI-1 proteins (Figure 10A, B, and C). These results indicate that R-Smad3 is required for TGF- β 2 stimulation of ECM proteins in ONH astrocytes and LC cells.

Reduction of R-Smad2/3 via siRNA Reduces TGF- β 2-Driven Stimulation of FN and PAI-1 in ONH Astrocytes and LC Cells

TGF- β 2-driven fibrogenesis is thought to be mediated primarily via R-Smad2/3. We conducted siRNA knockdown of R-Smad2 or R-Smad3 along with control siRNAs (RISC-Free siRNAs and non-targeting siRNAs) for 48 hrs in ONH astrocytes and LC cells. Smad2, Smad3 and actin protein levels were assessed using western blot (Figure 10A and 11A) and measured by densitometric analysis (Figure 10B and 11B). Transfection with Smad3-siRNA (25nM and 50nM) resulted in significant ($P<0.001$) reduction of R-Smad3 protein levels compared to control siRNAs (50nM) in ONH astrocytes and LC cells (Figure 10A and B). Transfection with Smad2 siRNA (50nM) resulted in significant reduction in Smad2 levels (Figure 11A and 11B). Control siRNAs did not significantly alter R-Smad2 or R-smad3 proteins levels compared to vehicle control indicating sequence-specific silencing of our target siRNAs (Figure 10A,B and figure 11A,B)). ONH astrocytes were treated with TGF- β 2 with and without siRNAs for R-Smad3 or R-smad2. Western blot and densitometric analysis demonstrated that

reduction of R-Smad3 or R-smad2 via siRNA significantly reduced the stimulatory effects of TGF- β 2 on FN and PAI-1 proteins (Figure 10A, B, and C). These results indicate that R-Smad2 and R-Smad3 are required for TGF- β 2 stimulation of ECM proteins in ONH astrocytes and LC cells.

Discussion

In the present study, we show that TGF- β 2 and FN is significantly increased in glaucomatous ONH tissues and that treatment of ONH astrocytes and LC cells with exogenous TGF- β 2 increases ECM proteins. These findings support that elevated levels of TGF- β 2 are responsible for ECM remodeling of the glaucomatous ONH. The presence of TGF- β 2, pSmad3, and co-localization of pSmad3 with Co-Smad4 in ONH astrocytes and LC cells indicate the existence of an autocrine TGF- β 2 signaling pathway. Exogenous TGF- β 2 increased the phosphorylation of R-Smad2 and R-Smad3 but did not alter ERK1/2, P38 MAPK, or JNK1/2 phosphorylation. Increased phosphorylation and co-localization of pSmad3 with Co-Smad 4 in the nucleus of TGF- β 2 treated ONH astrocytes and LC cells indicates that TGF- β 2 activates R-Smad3. In addition, (1) inhibition of TGF- β RI activity via SB432542, (2) inhibition of Smad3 phosphorylation via SIS3, or (3) reducing the level of R-Smad3 or R-Smad2 via siRNA reduces the synthesis and secretion of various ECM proteins by ONH astrocytes and LC cells. These findings indicate that TGF- β 2 requires R-Smad2/3 to increase synthesis and deposition of ECM proteins by ONH astrocytes and LC cells.

It is now well established that in glaucoma, damage to the LC is associated with loss of RGC axons. The LC is the weakest part of the ONH, thus more vulnerable to elevated IOP¹³. The exact mechanism is unclear, however increased synthesis and deposition of ECM proteins in the LC region of glaucomatous ONH is thought to be detrimental for RGC axons. Altered ECM proteins in the glaucomatous ONH include increased collagen

deposition and degradation of elastin fibers^{6,7}. Another feature of the glaucomatous ONH is increased levels of TGF- β 2 that is known to modulate fibrosis. Pena et al found that production of TGF- β 2 is considerably increased in glaucomatous ONH²². Previous studies suggested that elevated TGF- β 2 is associated with ECM changes in LC region of glaucomatous ONH²³. Consistent with previous studies, we show that TGF- β 2 is significantly increased in LC region of the glaucomatous ONH. Interestingly, fibronectin, a basement membrane protein is also significantly increased in LC region of the same glaucomatous ONH tissue samples. Western blot analysis of TGF- β 2 in normal human ONH tissues confirms our immunostaining findings that TGF- β 2 is present in human ONH tissues.

Cells isolated from human ONH synthesize and secrete endogenous TGF- β 2 suggesting that ONH astrocytes and LC cells are most likely responsible for making TGF- β 2 *in vivo*. These findings also support the hypothesis that cells in the LC region of glaucomatous ONH respond to damage by synthesizing increased amounts of TGF- β 2 and ECM proteins. Treatment of ONH astrocytes and LC cells with recombinant TGF- β 2 increased soluble FN and PAI-1 in dose dependant manner. PAI-1 is involved in fibrosis by regulating the activity of matrix metalloprotease (MMPs). MMPs have been shown to be involved in ECM remodeling of glaucomatous ONH³⁴⁻³⁶. Increased type I and VI collagen and elastin is thought to alter the mechanical and elastic properties of LC in glaucomatous ONH. We show that TGF- β 2 increases type I and VI collagen and elastin

secretion in ONH astrocytes and LC cells. These *in vivo and in vitro* observations support the hypothesis that TGF- β 2 is involved in ECM changes in LC of glaucomatous ONH.

Binding of TGF- β 2 to the type II TGF- β receptor (TGF- β RII) phosphorylates type I TGF- β receptor (TGF- β RII). The activated TGF- β RII recruits, phosphorylates and activates the type I receptor (TGF- β RI). The activation of TGF- β RI is an essential event in TGF- β 2 signaling³⁷. Therefore, we examined whether inhibition of the TGF- β receptor would block TGF- β stimulation of FN and PAI-1. SB431532 is a potent and specific inhibitor of TGF- β RI activity. Mori et al., 2004 demonstrated that SB431542 inhibits pro-fibrotic actions of TGF- β 2 in skin fibroblasts. Our findings demonstrate that inhibition of TGF- β RI blocks pro-fibrotic actions of TGF- β 2 in ONH astrocytes and LC cells. These results indicate that inhibition of TGF- β RI blocks TGF- β 2 induced fibrogenesis in the ONH astrocytes and LC cells.

Downstream effectors of TGF- β 2 signaling involve the canonical Smad signaling pathways and non-Smad signaling pathways^{17, 18, 27, 28, 31, 38-40}. TGF- β 2 induced signals to stimulate fibrogenesis include Smad2 and Smad3.^{17, 30} In most cell types, Smad3 are preferred in TGF- β 2-induced ECM stimulation. In some cells, non-Smad pathways including ERK, p38MAPK, and JNK are activated by TGF- β 2^{28, 39, 41}. These pathways appear to facilitate or antagonize Smad signals depending on cell types. In ONH astrocytes and LC cells, TGF- β 2 did not activate phosphorylation of ERK, p38MAPK, or JNK indicating that TGF- β 2 may not utilize non-canonical signaling pathways to induce ECM changes in the ONH.

Interestingly, TGF- β 2 phosphorylated both Smad2 and Smad3 in ONH astrocytes and LC cells. Since Smad3 has been reported to be involved in TGF- β mediated fibrosis, we choose to investigate whether Smad3 is required for TGF- β 2 stimulation of various ECM proteins by ONH astrocytes and LC cells. Several findings from the present experiments support the involvement of R-smad2/3 in TGF- β 2 stimulation of ECM proteins. First, treatment of ONH astrocytes and LC cells with TGF- β 2 increased phosphorylation of Smad3. Second, TGF- β 2 treatment caused increased co-localization of Co-Smad4 and pSmad3 in LC cells, indicating the translocation of this active complex into the nucleus. Interestingly, there was some co-localization of Co-Smad4 and pSmad3 in untreated cells suggesting the presence of autocrine TGF- β 2 signaling. The finding that ONH astrocytes and LC cells make and secrete TGF- β protein supports the presence of an endogenous TGF- β 2 autocrine signaling mechanism. Third, inhibition of TGF- β RI by SB431542 blocked TGF- β 2 stimulation of FN and PAI-1. Fourth, SIS3, a specific inhibitor of Smad3 phosphorylation decreased TGF- β 2 stimulation of FN and PAI-1 in ONH astrocytes and LC cells. Fifth, knockdown of Smad3 or Smad2 via siRNA inhibited TGF- β 2 stimulation of FN and PAI-1 in ONH astrocytes and LC cells.

In summary, the present study provides *in vivo and in vitro* evidence to support the hypothesis that TGF- β 2 is involved in ECM remodeling of in glaucomatous ONH. In addition, TGF- β 2-driven ECM stimulation requires activation canonical Smad signaling pathway via the TGF- β RI receptor and phosphorylation R-Smad2/3 in ONH astrocytes and LC cells.

Figure Legends

Figure1. Immunohistochemical Evaluation of TGF- β 2 and FN Localization in Normal and Glaucomatous ONH Tissues

Representative immunostaining for TGF- β 2 and FN localization in three aged matched normal verses glaucomatous human ONH tissues. H & E stained ONH samples at lower magnification (A) and at higher magnification (B) showing optic nerve, LC = lamina cribrosa, ONH = optic nerve head, and retinal layer. TGF- β 2 merged with DAPI in normal ONH (C) and in glaucomatous ONH (D); FN merged with DAPI in normal ONH (E) and in glaucomatous ONH (F); Control IgG merged with DAPI (G) and control (no primary antibody) merged with DAPI (H) in normal ONH. (I, J) Relative intensity measurements of TGF- β 2 and FN in three aged matched normal and glaucomatous ONH tissues. There was statistically significant higher staining for TGF- β 2 and FN in glaucomatous ONH tissues compared to normal human ONH tissues, indicating TGF- β 2 and FN is increased in glaucomatous ONH tissues (student t test). [$P < 0.05$; * verses normal human ONH tissues; $n=3$].

Figure 2: Western Blot Analysis of TGF- β 2 Protein in ONH Cells and Tissues. Two ONH astrocytes and LC cells were grown in serum-free medium for 24 hrs. Culture medium (20X concentrated) and cell lysates were subjected to western blot analysis for secreted and cellular TGF- β 2. Optic nerve head was dissected from two human donor eye (age 55 and 76 years) and tissues lysate were utilized for western blot analysis of TGF- β 2. Recombinant TGF- β 2 (2ng) was used as positive control.

Figure 3: Recombinant TGF- β 2 Dose Dependently Increases Fibronectin and PAI-1 in ONH Astrocytes and LC Cells

ONH astrocytes and LC cells (N=3) were treated with various concentrations of recombinant TGF- β 2 (1.25, 2.5, 5, 10, and 20ng/ml). The effect of TGF- β 2 was examined using A) western blot analysis for cellular fibronectin, PAI-1, and β -actin in LC cells; B) secreted fibronectin and PAI-1 in LC cells; C) ELISA for soluble FN in ONH astrocytes. Recombinant TGF- β 2 significantly increased secreted FN in ONH astrocytes at concentration of 5ng/ml. ($n=3$ *, $P < 0.001$ verses control).

Figure 4: Recombinant TGF- β 2 Increases ECM Proteins in ONH Astrocytes and LC Cells. ONH astrocytes and LC cells were treated with 5ng/ml recombinant TGF- β 2 for 24 hrs and culture medium (5X concentrated) was subjected to western blot analysis of collagen I, collagen VI, and elastin. Recombinant TGF- β 2 increased secretion collagen I, collagen VI, and elastin in ONH astrocytes and LC cells.

Figure 5: Inhibition of Activity Type I TGF- β Receptor Blocks TGF- β 2-Driven ECM Stimulation. ONH astrocytes and LC cells were preincubated with SB431542 (Type I TGF- β receptor inhibitor) 1 hr prior to treatment with recombinant TGF- β 2 (5ng/ml). (A) Total cellular FN and PAI-1 were assessed by western blot in ONH astrocytes and LC cells. Cellular FN was measured by densitometry, normalized to actin, and analyzed using one way ANOVA in ONH astrocytes (B) and LC cells (C). Type I TGF- β receptor inhibitor reduced TGF- β 2-induced stimulation of fibronectin ($n=3$ *, $P < 0.05$ verses control; †, $P < 0.05$ verses TGF- β 2).

Figure 6: Phosphorylation of ERK1/2, p38, or JNK1/2 Pathways in ONH Astrocytes and LC Cells: ONH astrocytes and LC cells were incubated with recombinant TGF- β 2 (5ng/ml) for 30 minutes, 60 minutes, and 120 minutes and cell lysate was subjected to western blot analysis for phosphorylated ERK1/2, total ERK1/2, phosphorylated p38, total p38, phosphorylated JNK1/2, total JNK1/2, and actin. Recombinant TGF- β 2 treatment of ONH astrocytes and LC cells did not alter phosphorylation ERK, p38, and JNK1/2 at 30 minutes, 60 minutes and 120 minutes.

Figure 7: R-Smads Phosphorylation by Recombinant TGF- β 2 in ONH Astrocytes and LC Cells. ONH astrocytes and LC cells were incubated with recombinant TGF- β 2 (5ng/ml) for 30 minutes, 60 minutes, and 120 minutes. Cell lysate was analyzed for phosphorylated R-Smad3, total R-Smad3, phosphorylated R-Smad2, R-Smad2, and actin. Recombinant TGF- β 2 increased phosphorylation of R-Smad3 and R-Smad2 in ONH astrocytes and LC cells.

Figure 8: Colocalization of pSmad3 and Smad4 in LC Cells. LC cells were incubated with recombinant TGF- β 2 (5ng/ml) for 60 minutes. Cells were fixed and stained with antibodies for pSmad3 and Smad4. (A) Colocalization of pSmad3 and Smad4 in untreated LC cells. (B) Colocalization of pSmad3 and Smad4 in TGF- β 2 treated LC cells. (C) Rabbit and mouse IgG in LC cells. Treatment of LC cells with recombinant TGF- β 2 increased colocalization of Smad3 and Smad4.

Figure 9: Inhibition of Phosphorylation of Smad3 Reduced TGF- β 2 Stimulation of FN in ONH Astrocytes and LC Cells. ONH astrocytes and LC cells were preincubated with

SIS3 (Specific Inhibitor of Smad3) 1 hr prior to treatment with TGF- β 2. Conditioned medium was subjected to western blot analysis for FN. Preincubation of ONH astrocytes and LC cells with SIS3 (25uM and 50uM) reduced TGF- β 2 stimulation of secretion of FN.

Figure 10: Inhibition of Smad3 via siRNA Blocks TGF- β 2 Stimulation of FN and PAI-1 in ONH Astrocytes and LC Cells

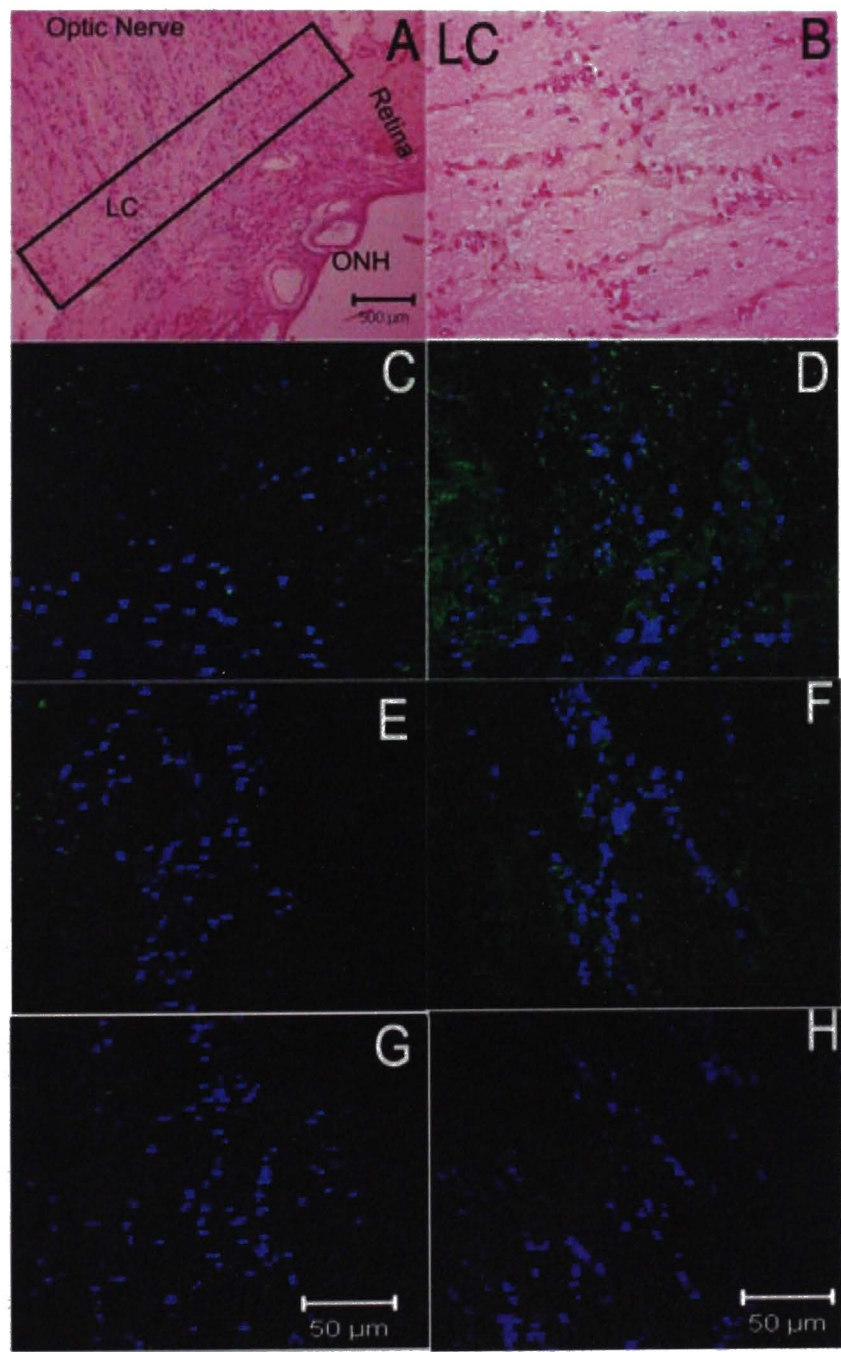
(A) siRNA knockdown of R-Smad3 blocked TGF- β 2 induced stimulation of FN and PAI-1 in ONH astrocytes and LC cells. ONH astrocytes and LC cells were treated with siRNA for Smad3 (25nM and 50nM) and siRNA controls (lane 1= Non-targeting siRNA; lane 2 = RISC-Free siRNA) for 48 hrs and then treated with recombinant TGF- β 2 (5ng/ml) for 24 hrs. Cellular FN, PAI-1, total Smad3, and actin were assessed by western blot. (B) Specific silencing of R-Smad3. Relative density of R-Smad3 and actin was measured using densitometric analysis of above western blot. R-Smad3 was normalized to actin and fold change in R-Smad over vehicle control was plotted using graph pad prism ($n=3$, $P<0.001$). (C, D) R-Smad3 knockdown reduced TGF- β 2-induced stimulation of FN and PAI-1. Relative densities of FN, PAI-1, and actin were measured using densitometric analysis of above western blot. Relative FN or PAI-1 was normalized to actin and fold change in FN (C) or PAI-1 (D) over vehicle control was plotted using graph pad prism ($n=3$, $P<0.001$).

Figure 11. Inhibition of Smad2 via siRNA Reduced TGF- β 2 Stimulation of FN and PAI-1 in ONH Astrocytes and LC Cells

(A) siRNA knockdown of R-Smad2 reduced TGF- β 2 induced stimulation of FN in ONH astrocytes and LC cells. ONH astrocytes and LC cells were treated with siRNA for Smad2 (50nM in duplicate) and siRNA controls (Non-targeting siRNA) for 48 hrs and then treated with recombinant TGF- β 2 (5ng/ml) for 24 hrs. Cellular FN, total Smad2, and actin were assessed by western blot. (B) Relative density of R-Smad2 and actin was measured using densitometric analysis of above western blot. R-Smad2 was normalized to actin and fold change in R-Smad2 over vehicle control was plotted using graph pad prism ($n=2$, $P<0.05$). (C, D) Relative densities of FN, PAI-1, and actin were measured using densitometric analysis of above western blot. Relative FN or PAI-1 was normalized to actin and fold change in FN (C) or PAI-1 (D) over vehicle control was plotted using graph pad prism ($n=2$, $P<0.05$).

Figures

Figure 1



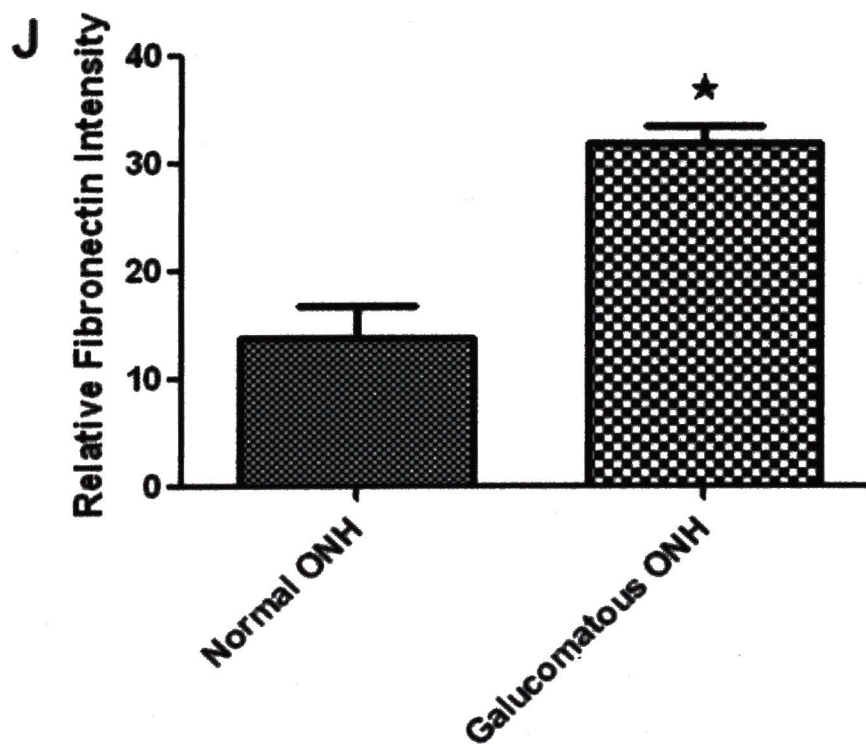
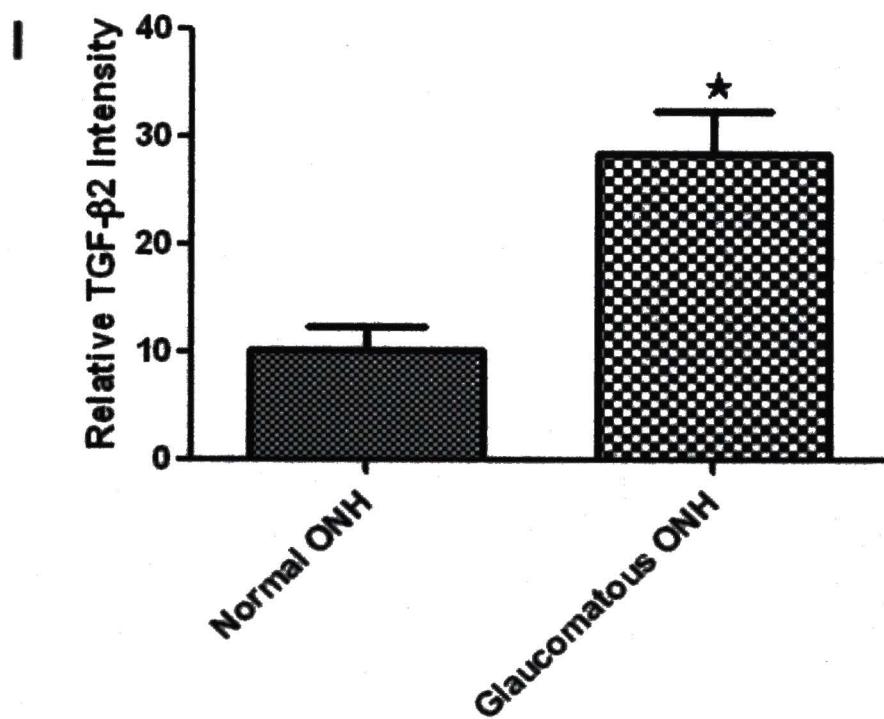


Figure 2

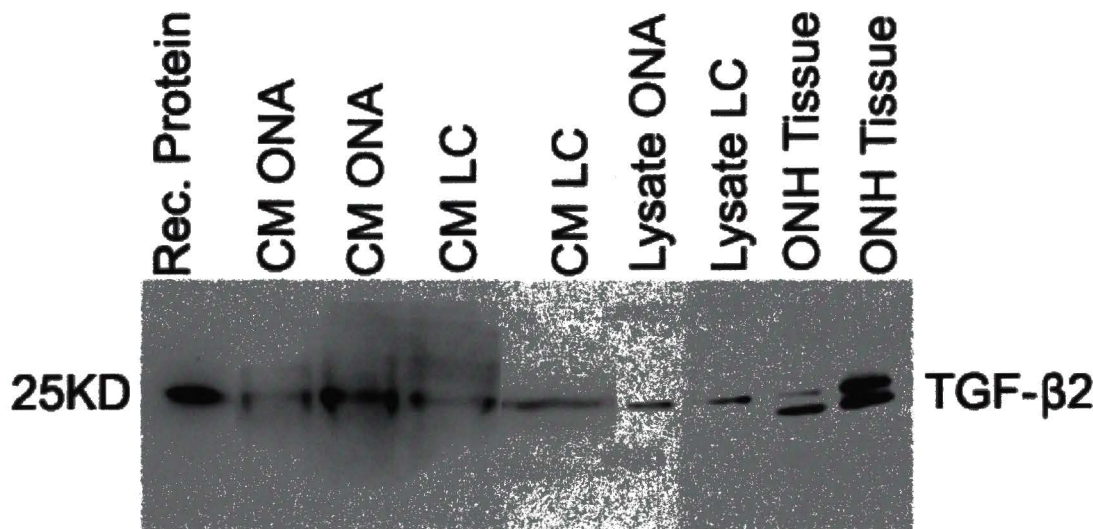


Figure 3

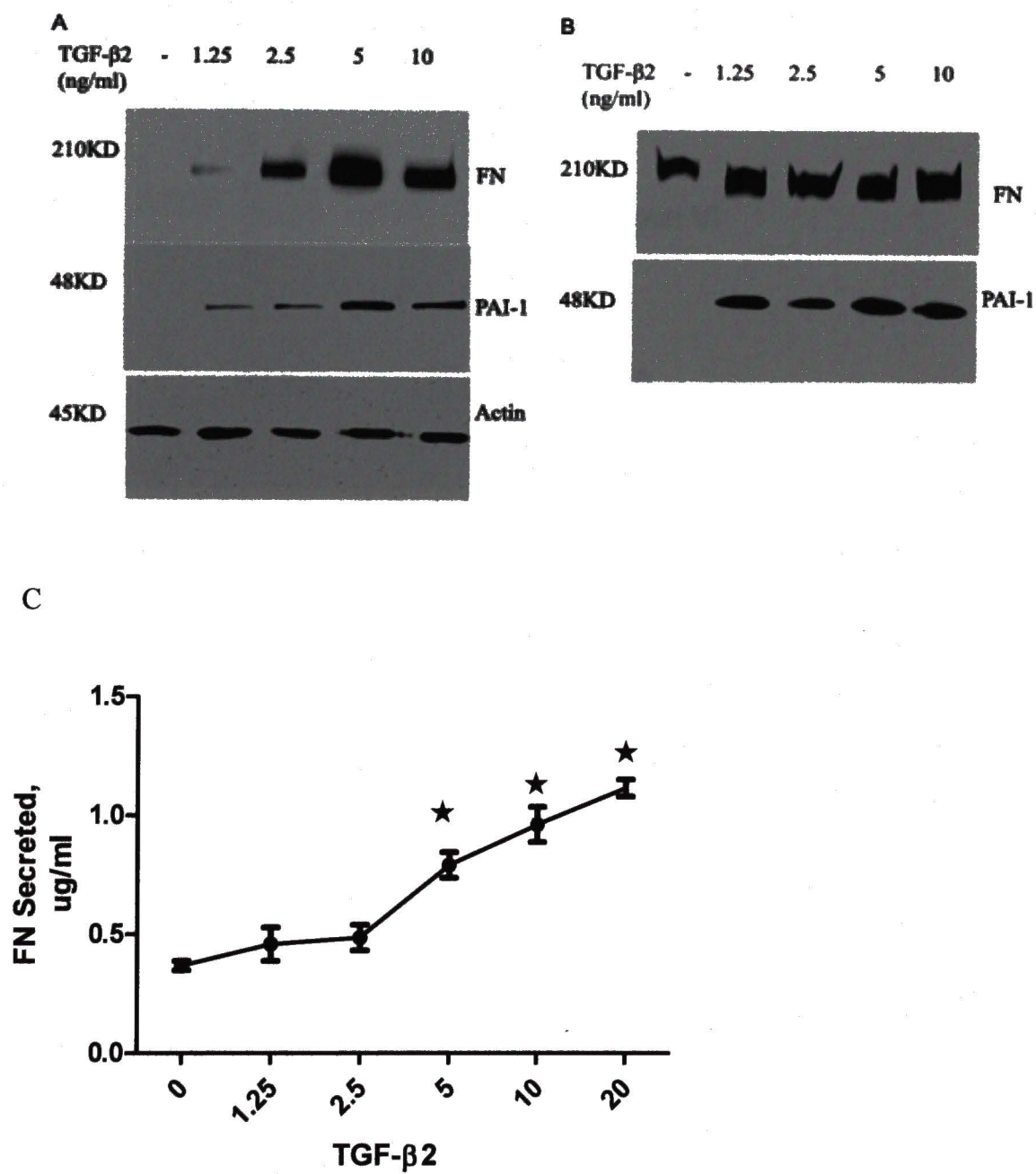


Figure 4

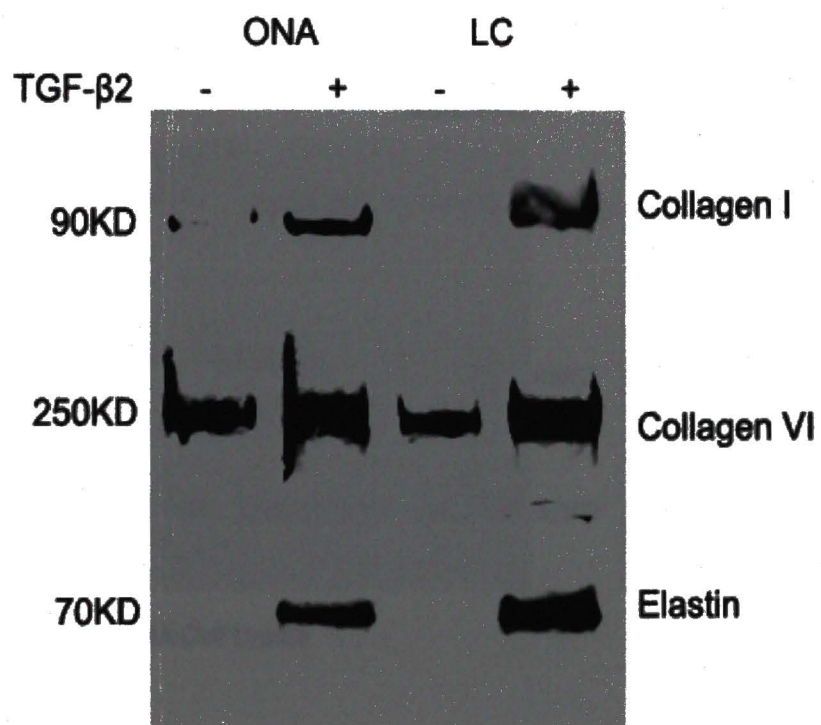


Figure 5

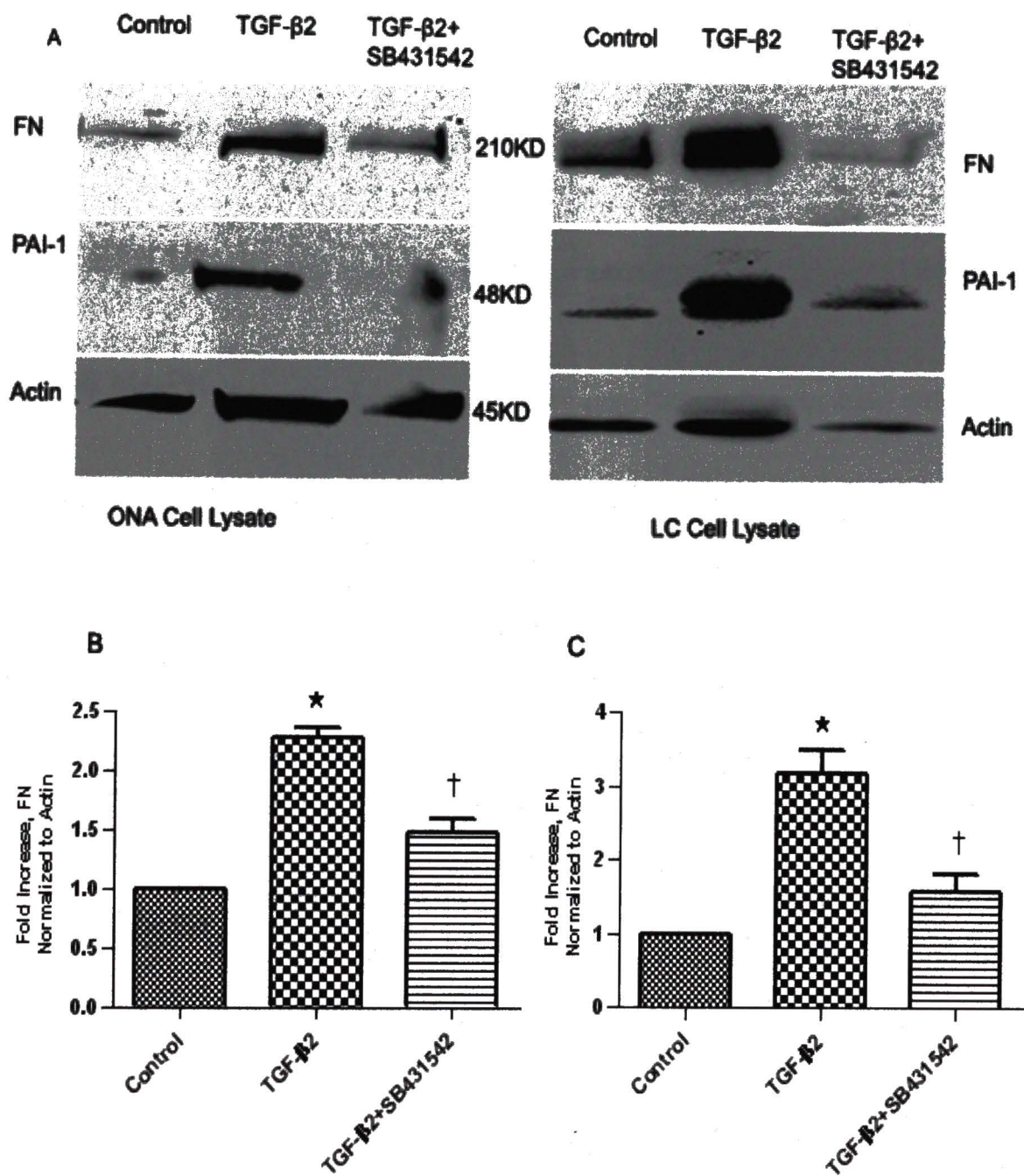


Figure 6

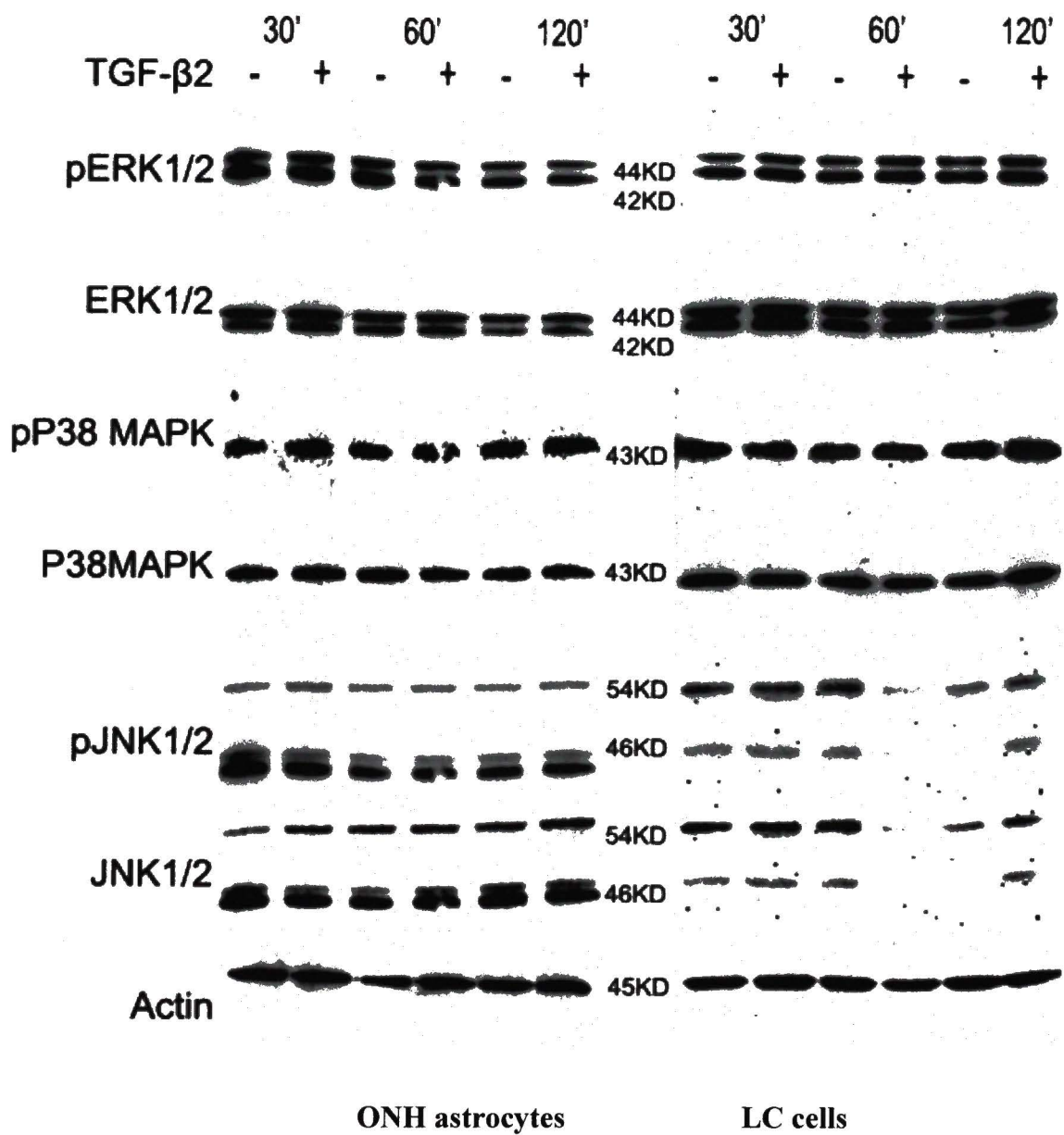


Figure7

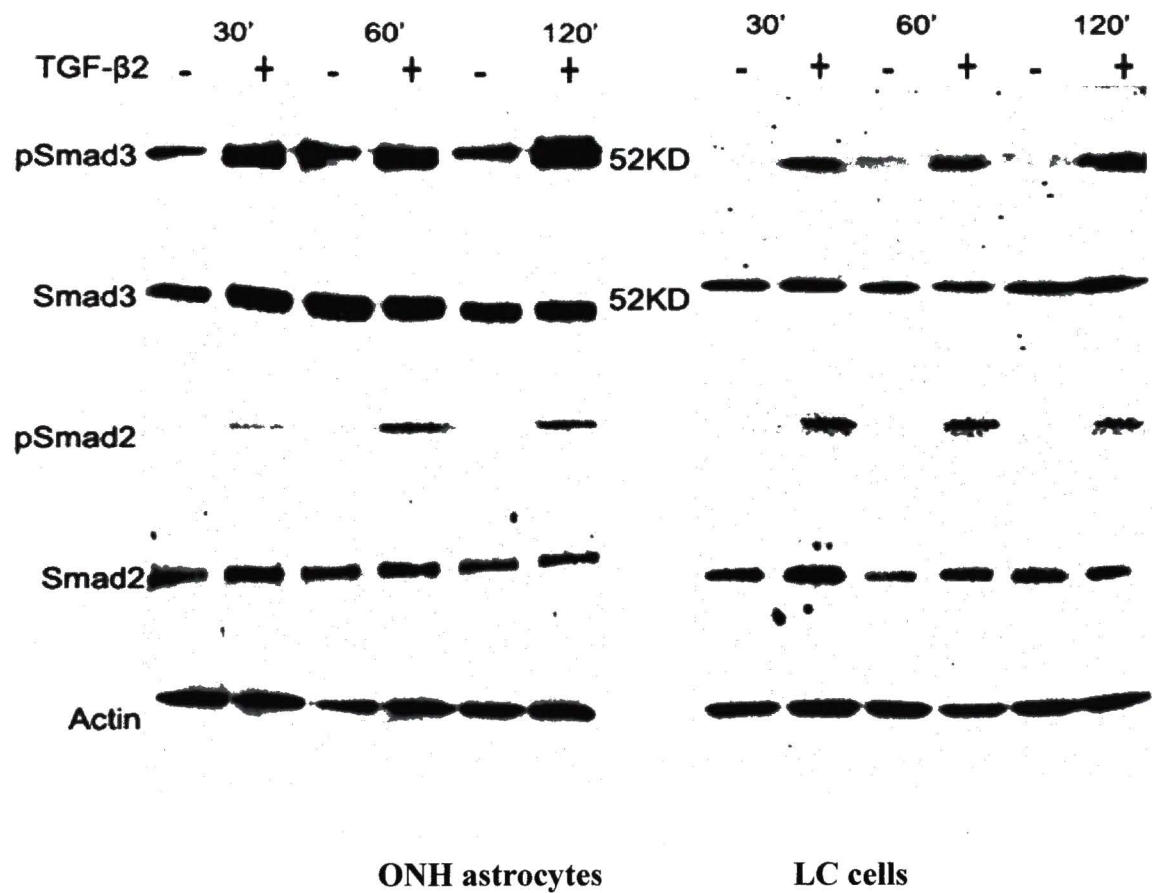


Figure 8

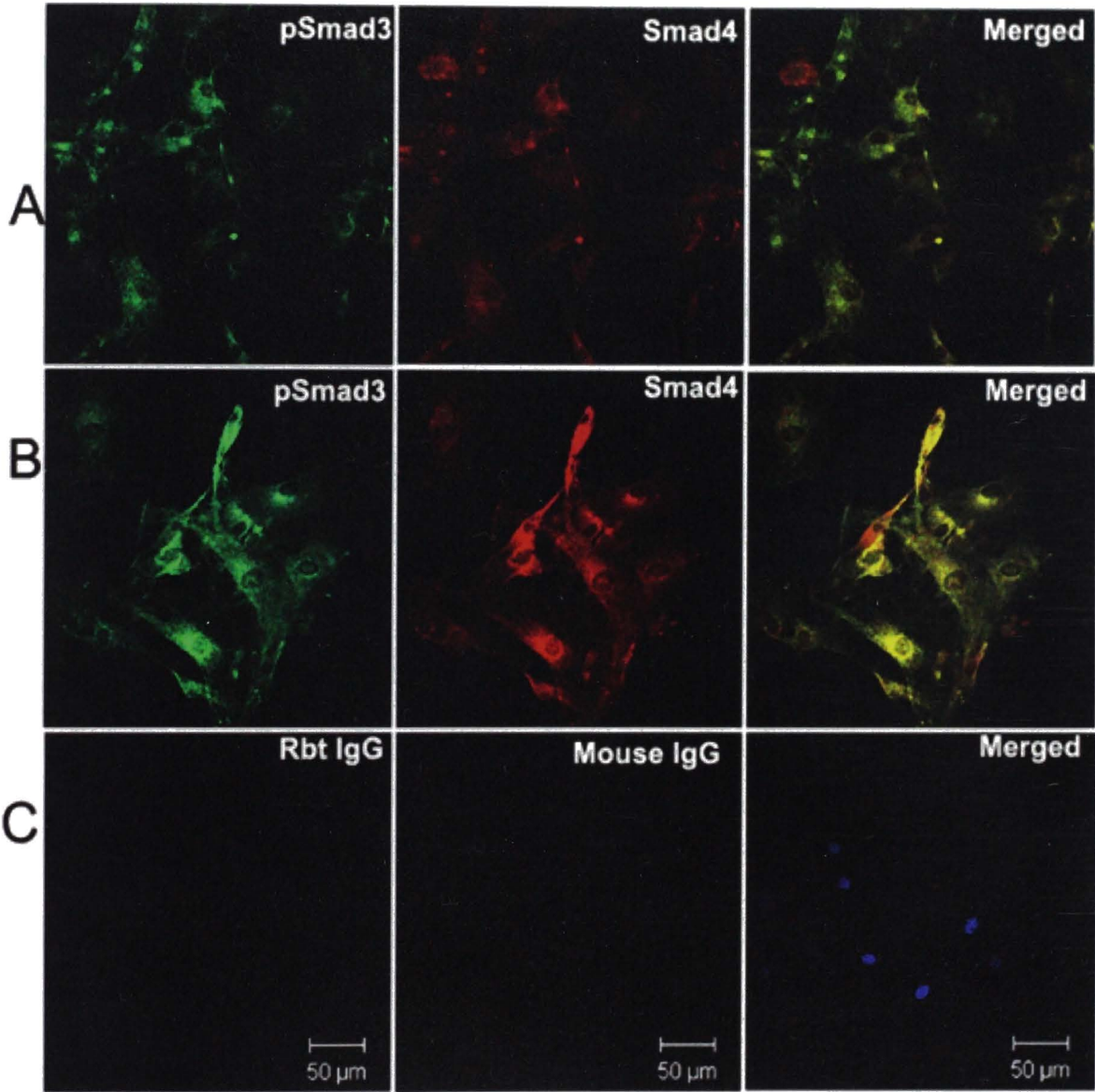


Figure 9

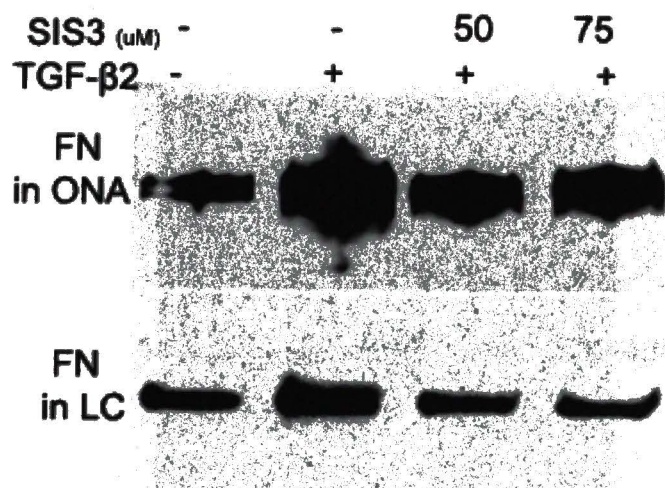
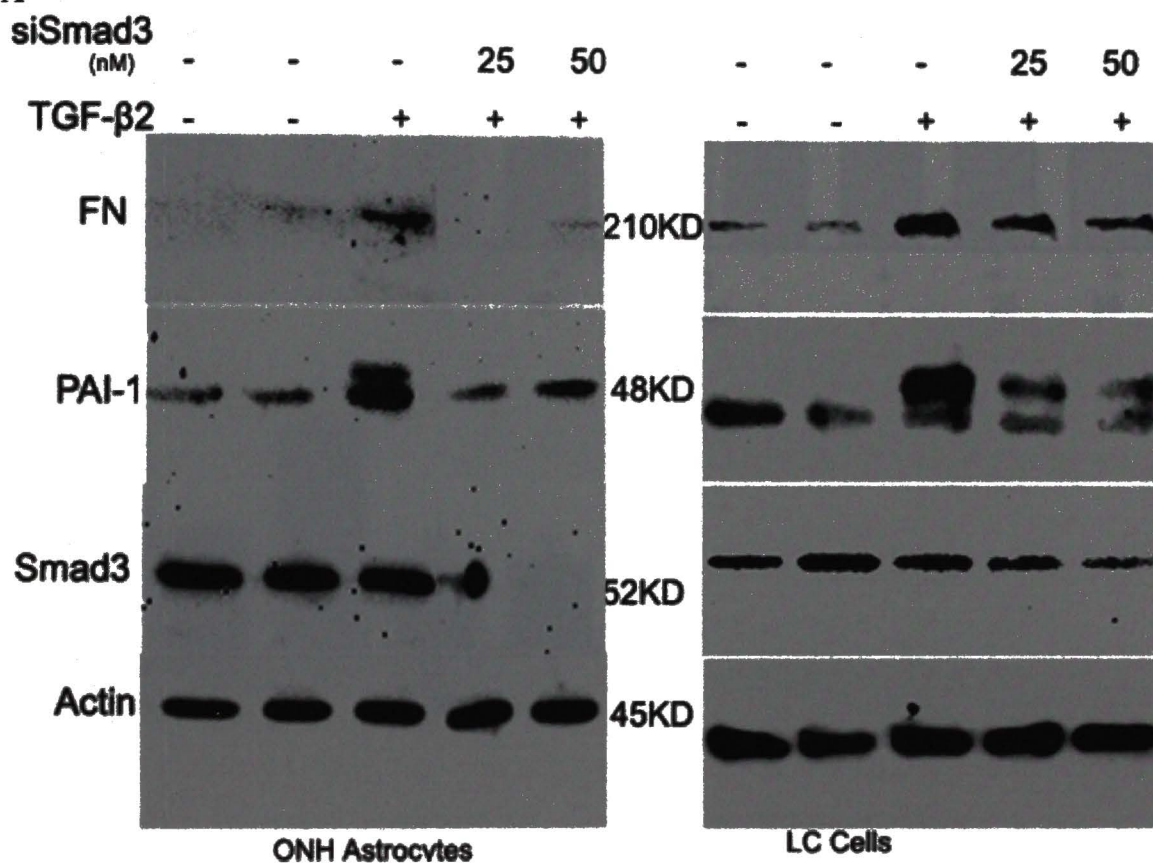


Figure 10

A



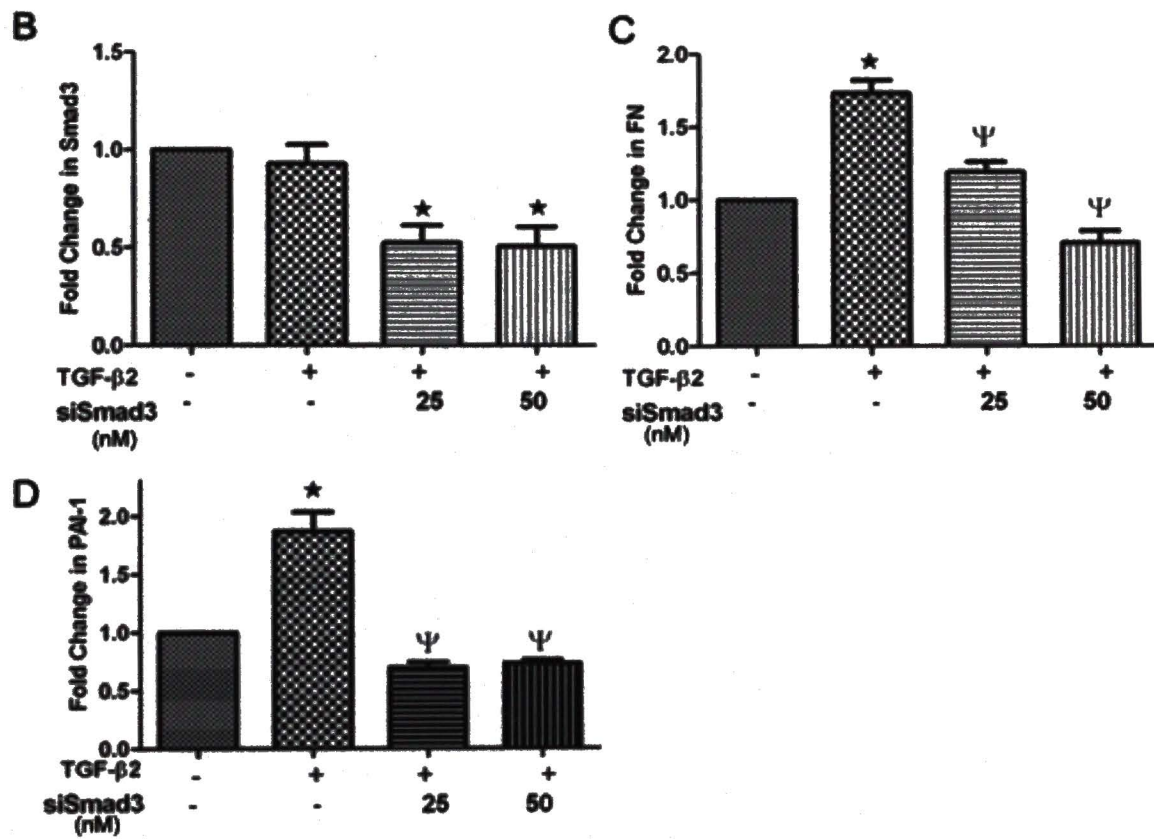
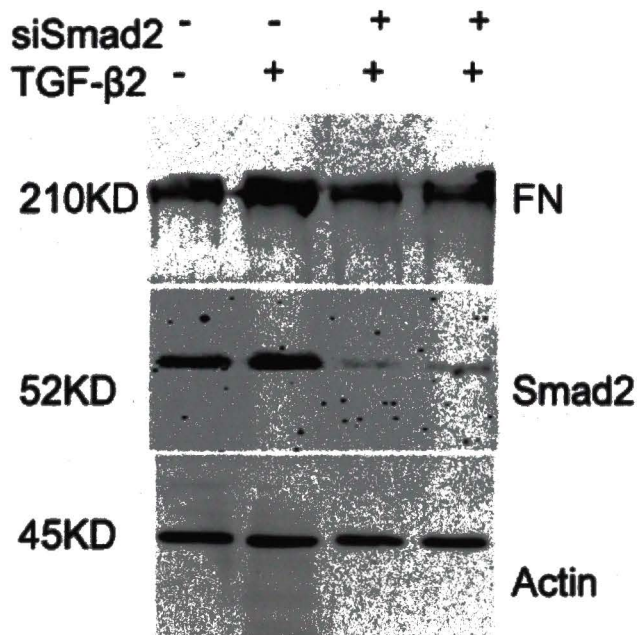
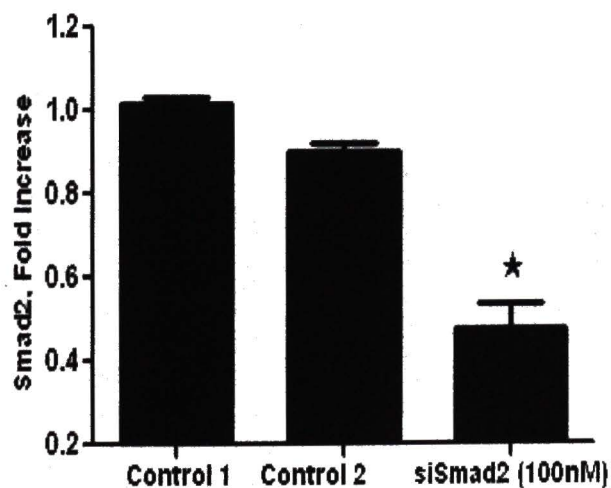


Figure 11

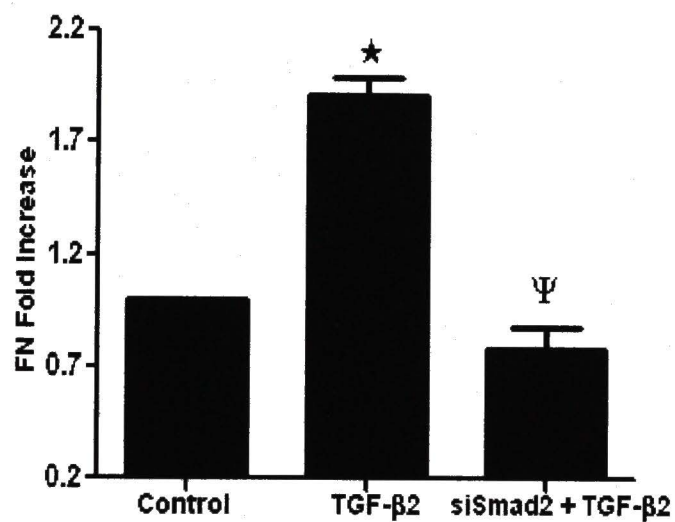
A



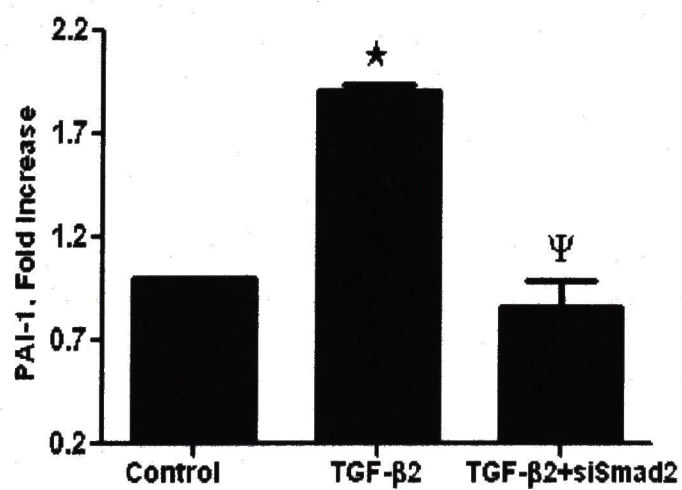
B



C



D



References

1. Quigley HA. Neuronal death in glaucoma. *Prog Retin Eye Res* 1999;18:39-57.
2. Quigley HA, Addicks EM. Chronic experimental glaucoma in primates. II. effect of extended intraocular pressure elevation on optic nerve head and axonal transport. *Invest Ophthalmol Vis Sci* 1980;19:137-52.
3. Lutjen-Drecoll E. Morphological changes in glaucomatous eyes and the role of TGFbeta2 for the pathogenesis of the disease. *Exp.Eye Res.* 2005;81:1-4.
4. Morrison JC, Dorman-Pease ME, Dunkelberger GR, Quigley HA. Optic nerve head extracellular matrix in primary optic atrophy and experimental glaucoma. *Arch Ophthalmol* 1990;108:1020-4.
5. Quigley HA, Addicks EM. Regional differences in the structure of the lamina cribrosa and their relation to glaucomatous optic nerve damage. *Arch Ophthalmol* 1981;99:137-43.
6. Quigley HA, Hohman RM, Addicks EM, Massof RW, Green WR. Morphologic changes in the lamina cribrosa correlated with neural loss in open-angle glaucoma. *Am J Ophthalmol* 1983;95:673-91.
7. Hernandez MR, Andrzejewska WM, Neufeld AH. Changes in the extracellular matrix of the human optic nerve head in primary open-angle glaucoma. *Am J Ophthalmol* 1990;109:180-8.

8. Hernandez MR. The optic nerve head in glaucoma: Role of astrocytes in tissue remodeling. *Prog Retin Eye Res* 2000;19:297-321.
9. Hernandez M GH. Extracellular matrix of the trabecular meshwork and optic nerve head. St. Louis: Mosby; 1996. 213-49 pp.
10. Hernandez MR, Pena JD. The optic nerve head in glaucomatous optic neuropathy. *Arch Ophthalmol* 1997;115:389-95.
11. Johnson EC, Morrison JC, Farrell S, Deppmeier L, Moore CG, McGinty MR. The effect of chronically elevated intraocular pressure on the rat optic nerve head extracellular matrix. *Exp Eye Res* 1996;62:663-74.
12. Anderson DR. Ultrastructure of human and monkey lamina cribrosa and optic nerve head. *Arch Ophthalmol* 1969;82:800-14.
13. Oyama T, Abe H, Ushiki T. The connective tissue and glial framework in the optic nerve head of the normal human eye: Light and scanning electron microscopic studies. *Arch.Histol.Cytol.* 2006;69:341-356.
14. Hernandez MR, Igoe F, Neufeld AH. Cell culture of the human lamina cribrosa. *Invest Ophthalmol Vis Sci* 1988;29:78-89.
15. Lambert W, Agarwal R, Howe W, Clark AF, Wordinger RJ. Neurotrophin and neurotrophin receptor expression by cells of the human lamina cribrosa. *Invest Ophthalmol Vis Sci* 2001;42:2315-23.

16. Roberts AB, Heine UI, Flanders KC, Sporn MB. Transforming growth factor-beta. major role in regulation of extracellular matrix. *Ann.N.Y.Acad.Sci.* 1990;580:225-232.
17. Roberts AB, Piek E, Bottinger EP, Ashcroft G, Mitchell JB, Flanders KC. Is Smad3 a major player in signal transduction pathways leading to fibrogenesis? *Chest* 2001;120:43S-47S.
18. Schnaper HW, Hayashida T, Hubchak SC, Poncelet AC. TGF-beta signal transduction and mesangial cell fibrogenesis. *Am.J.Physiol.Renal Physiol.* 2003;284:F243-52.
19. Tripathi RC, Li J, Chan WF, Tripathi BJ. Aqueous humor in glaucomatous eyes contains an increased level of TGF-beta 2. *Exp Eye Res* 1994;59:723-7.
20. Fleenor DL, Shepard AR, Hellberg PE, Jacobson N, Pang IH, Clark AF. TGFbeta2-induced changes in human trabecular meshwork: Implications for intraocular pressure. *Invest Ophthalmol Vis Sci* 2006;47:226-34.
21. Wordinger RJ, Fleenor DL, Hellberg PE, et al. Effects of TGF-beta2, BMP-4, and gremlin in the trabecular meshwork: Implications for glaucoma. *Invest.Ophthalmol.Vis.Sci.* 2007;48:1191-1200.
22. Pena JD, Taylor AW, Ricard CS, Vidal I, Hernandez MR. Transforming growth factor beta isoforms in human optic nerve heads. *Br J Ophthalmol* 1999;83:209-18.

23. Fuchshofer R, Birke M, Welge-Lussen U, Kook D, Lutjen-Drecoll E. Transforming growth factor-beta 2 modulated extracellular matrix component expression in cultured human optic nerve head astrocytes. *Invest.Ophthalmol.Vis.Sci.* 2005;46:568-578.
24. Attisano L, Tuen Lee-Hoeflich S. The smads. *Genome Biol* 2001;2:REVIEWS3010.
25. Balemans W, Van Hul W. Extracellular regulation of BMP signaling in vertebrates: A cocktail of modulators. *Dev Biol* 2002;250:231-50.
26. Hogan BL. Bone morphogenetic proteins: Multifunctional regulators of vertebrate development. *Genes Dev* 1996;10:1580-94.
27. Rahimi RA, Leof EB. TGF-beta signaling: A tale of two responses. *J.Cell.Biochem.* 2007;102:593-608.
28. Zhang M, Fraser D, Phillips A. ERK, p38, and smad signaling pathways differentially regulate transforming growth factor-beta1 autoinduction in proximal tubular epithelial cells. *Am.J.Pathol.* 2006;169:1282-1293.
29. Wang Z, Gao Z, Shi Y, et al. Inhibition of Smad3 expression decreases collagen synthesis in keloid disease fibroblasts. *J.Plast.Reconstr.Aesthet.Surg.* 2007;60:1193-1199.
30. Roberts AB, Russo A, Felici A, Flanders KC. Smad3: A key player in pathogenetic mechanisms dependent on TGF-beta. *Ann.N.Y.Acad.Sci.* 2003;995:1-10.

31. Kobayashi T, Liu X, Wen FQ, et al. Smad3 mediates TGF-beta1 induction of VEGF production in lung fibroblasts. *Biochem.Biophys.Res.Commun.* 2005;327:393-398.
32. Cheng HC, Ho TC, Chen SL, Lai HY, Hong KF, Tsao YP. Troglitazone suppresses transforming growth factor beta-mediated fibrogenesis in retinal pigment epithelial cells. *Mol.Vis.* 2008;14:95-104.
33. Zode GS, Clark AF, Wordinger RJ. Activation of the BMP canonical signaling pathway in human optic nerve head tissue and isolated optic nerve head astrocytes and lamina cribrosa cells. *Invest.Ophthalmol.Vis.Sci.* 2007;48:5058-5067.
34. Agapova OA, Ricard CS, Salvador-Silva M, Hernandez MR. Expression of matrix metalloproteinases and tissue inhibitors of metalloproteinases in human optic nerve head astrocytes. *Glia* 2001;33:205-16.
35. Chintala SK, Zhang X, Austin JS, Fini ME. Deficiency in matrix metalloproteinase gelatinase B (MMP-9) protects against retinal ganglion cell death after optic nerve ligation. *J Biol Chem* 2002;277:47461-8.
36. Vaillant C, Meissirel C, Mutin M, Belin MF, Lund LR, Thomasset N. MMP-9 deficiency affects axonal outgrowth, migration, and apoptosis in the developing cerebellum. *Mol Cell Neurosci* 2003;24:395-408.
37. Yamashita H, Ten Dijke P, Heldin CH, Miyazono K. Bone morphogenetic protein receptors. *Bone* 1996;19:569-74.

38. Verrecchia F, Mauviel A. Transforming growth factor-beta and fibrosis. *World J.Gastroenterol.* 2007;13:3056-3062.
39. Moustakas A, Heldin CH. Non-smad TGF-beta signals. *J.Cell.Sci.* 2005;118:3573-3584.
40. Nohe A, Keating E, Knaus P, Petersen NO. Signal transduction of bone morphogenetic protein receptors. *Cell.Signal.* 2004;16:291-299.
41. Pannu J, Nakerakanti S, Smith E, ten Dijke P, Trojanowska M. Transforming growth factor-beta receptor type I-dependent fibrogenic gene program is mediated via activation of Smad1 and ERK1/2 pathways. *J.Biol.Chem.* 2007;282:10405-10413.

Chapter IV

BONE MORPHOGENETIC PROTEIN 4 INHIBITS TGF-B2 STIMULATION OF EXTRACELLULAR MATRIX PROTEINS IN OPTIC NERVE HEAD CELLS: ROLE OF GREMLIN IN ECM MODULATION

Gulab S. Zode, Abbot F. Clark, and Robert J. Wordinger

Abstract:

The characteristic cupping of the optic nerve head (ONH) in glaucoma is associated with elevated TGF- β 2 and increased synthesis and deposition of extracellular matrix (ECM) proteins. In addition to TGF- β 2, the human ONH also expresses bone morphogenetic proteins (BMPs) and BMP receptors, which are members of the TGF- β superfamily. We examined the potential effects of BMP4 and the BMP antagonist gremlin on TGF- β 2 induction of ECM proteins in ONH cells. BMP-4 dose dependently inhibited TGF- β 2 induced fibronectin (FN) and PAI-1 expression in ONH astrocytes and lamina cribrosa (LC) cells ($P < 0.001$) and also reduced TGF- β 2 stimulation of collagen I, collagen VI, and elastin. Addition of gremlin blocked this BMP-4 response, increasing cellular and secreted FN as well as PAI-1 levels in both cell types. Gremlin was expressed in ONH tissues and ONH cells, and gremlin protein levels were significantly increased in the LC region of human glaucomatous ONH tissues. Interestingly, recombinant gremlin dose dependently increased ECM protein expression in cultured ONH astrocytes and LC cells. Gremlin stimulation of ECM required activation of TGF- β receptor and R-Smad3. TGF- β 2 increased gremlin mRNA expression and protein levels in ONH cells. Inhibition of either the type I TGF- β receptor or Smad3 phosphorylation blocked this TGF- β 2 induced gremlin expression. In conclusion, BMP4 blocked the TGF- β 2 induction of ECM proteins in ONH cells. The BMP antagonist gremlin reversed this inhibition, allowing TGF- β 2 stimulation of ECM synthesis. Increased expression of gremlin in the glaucomatous ONH may further exacerbate TGF- β 2 effects on ONH ECM metabolism.

by inhibiting BMP-4 antagonism of TGF- β 2 signaling. Modulation of the ECM via gremlin provides a novel therapeutic target for glaucoma.

Introduction

Primary open angle glaucoma (POAG) is a progressive optic neuropathy characterized by irreversible loss of retinal ganglion cells [RGC] (Quigley, 1999). The pathogenic factors responsible for POAG are still unknown. However, elevated intraocular pressure (IOP) is a major risk factor (Rohen, 1983; Rohen et al., 1993; Sommer et al., 1991). Elevated IOP is caused by impaired aqueous humor outflow and is associated with characteristic morphological and biochemical changes in the trabecular meshwork [TM] (Lutjen-Drecoll E, Rohen JW, 1996; Rohen et al., 1993). In glaucoma, elevated IOP can damage the optic nerve head [ONH] (Gottanka et al., 1997), which is detrimental to RGC axon viability. Glaucomatous ONH changes also include activation of astrocytes (Hernandez, 2000), altered growth factor synthesis (Pena et al., 1999), changes in ECM synthesis and composition (Hernandez M, 1996; Hernandez et al., 1990) as well as inhibition of retrograde transport of neurotrophins to RGC (Quigley et al., 2000).

Damage to the optic nerve is thought to occur in the lamina cribrosa (LC) region of the ONH (Quigley and Addicks, 1981; Quigley et al., 1983). The LC region is composed of characteristic sieve-like connective tissue cribriform plates through which RGC axons exit the eye (Oyama et al., 2006). The cupping of the optic disc and compression and excavation of the cribriform plates of the LC are characteristics of glaucomatous ONH remodeling (Quigley and Addicks, 1981; Quigley et al., 1983). Normally, the ECM in the ONH forms a framework and gives structural resiliency to the ONH (Oyama et al., 2006). In glaucoma, increased area and density of the basement membrane including

thickened collagen fibers (increased collagen I, and VI) and elastin fibers (disorganized distribution and deposition referred as elastosis) have been correlated to weakness of the LC (Hernandez M, 1996; Hernandez et al., 1990). Optic nerve head astrocytes and LC cells are two major cell types present in the ONH that support axons by synthesizing growth factors and ECM (Hernandez et al., 1988; Hernandez, 2000).

In the glaucomatous ONH, TGF- β 2 levels are increased (Pena et al., 1999) and appear to be involved in POAG pathogenesis (Gottanka et al., 2004; Lutjen-Drecoll, 2005; Tripathi et al., 1994). Fuchshofer and colleagues demonstrated that TGF β -2 treatment upregulates mRNA and protein expression of Col1 alpha 1, Col4 alpha 2, fibronectin (FN), connective tissue growth factor (CTGF), tissue transglutaminase (TGM2), and thrombospondin-1 (TSP-1) in cultured ONH astrocytes (Fuchshofer et al., 2005; Neumann et al., 2008). They suggested that TGF β -2 initiated ECM changes in the glaucomatous ONH. Taken together, elevated TGF- β 2 levels are associated with increased synthesis and deposition of ECM components and subsequent remodeling of the glaucomatous ONH.

However, within a given tissue, the actions of most growth factors are often counterbalanced by other growth factors (Fuchshofer et al., 2007; Wordinger and Clark, 2007; Wordinger et al., 2007). Bone morphogenetic proteins (BMP) were originally identified as osteoinductive cytokines that promote bone and cartilage formation but are now known to control multiple functions in a variety of cells (Balemans and Van Hul, 2002). Many studies indicate that BMPs antagonize TGF- β 2 signaling, thus maintaining

normal homeostasis with respect to ECM proteins. Recent reports have indicated that BMPs antagonize TGF- β signaling in fibrotic diseases of kidney (Zeisberg et al., 2003), lung (Izumi et al., 2006), and liver (Kinoshita et al., 2007). BMP antagonism of TGF- β signaling was also observed in mesangial cells (Wang and Hirschberg, 2004), pulmonary myofibroblasts (Izumi et al., 2006), cultured TM cells (Fuchshofer et al., 2007; Wordinger et al., 2007a), and epithelial-to-mesenchymal transition (EMT) in the kidney (Zeisberg et al., 2003). In kidney mesangial cells, BMP-7 inhibited TGF- β signaling by reducing the nuclear accumulation of R-Smad3 (Wang and Hirschberg, 2004).

Intracellular and extracellular antagonists tightly regulate the biological activity of BMPs (Nohe et al., 2004). Gremlin is an important extracellular BMP antagonist that acts by directly binding BMP-2, BMP-4 and BMP-7, thus preventing these BMPs from interacting with their high affinity receptor complex (Balemans and Van Hul, 2002). We have previously reported that gremlin blocked BMP-4 inhibition of TGF- β 2 induction of FN in cultured TM cells and elevated IOP in a perfused anterior eye segment model (Wordinger et al., 2007a). We have also reported that ONH astrocytes and LC cells express proteins for BMP (Zode et al., 2007), BMP receptors and BMP antagonists including gremlin (Wordinger et al., 2002). In addition, ONH astrocytes and LC cells are capable of responding to BMPs via the canonical Smad signaling pathway (Zode et al., 2007).

The purpose of the present study was to determine the effects of TGF- β 2, BMP4, and gremlin on ECM metabolism in cultured ONH cells and to examine gremlin expression in the normal and glaucomatous ONH.

Methods and Materials

Optic Nerve Head Dissection and Cell culture

Human ONH cells (ONH astrocytes and LC cells) were generated from dissected ONHs and characterized according to previous reports (Lambert et al., 2004). Briefly, human donor eyes from regional eye banks were obtained within 24 hours of death, and the LC region of the ONH was dissected from the remaining ocular tissue. Lamina cribrosa tissues were cut into three to four explants and placed in culture plates containing Dulbecco's modified Eagle's medium (DMEM, Hyclone Laboratories, Logan, Utah) containing L-glutamine (0.292 mg/ml, Gibco BRL Life Technologies, Grand Island, NY), penicillin (100 units/ml,)/streptomycin (0.1 mg/ml, Gibco BRL Life Technologies), amphotericin B (4 µg/ml, Gibco BRL Life Technologies), and 10% fetal bovine serum (Gibco BRL Life Technologies). Optic nerve head astrocytes and LC cells were isolated and characterized as previously reported (Hernandez et al., 1988; Lambert et al., 2001).

Treatment of ONH Astrocytes and LC Cells

ONH astrocytes and LC cells were grown in 12 well plates. Cells were allowed to become confluent, washed twice with sterile PBS, and kept in serum free medium for 24 hours. Fresh serum free medium was added to ONH astrocytes and LC cells, and then the cells were treated with recombinant TGF-β2, BMP-4, and/or gremlin (R&D system, Inc., Minneapolis, MN) for 48 hours. For the BMP-4 dose response study, ONH astrocytes and LC cells were incubated with increasing concentrations of BMP-4 (2.5, 5, 10, and 20ng/ml) alone or together with TGF-β2 (5ng/ml) for 48 hrs. Cell lysates and culture

medium were collected for further studies. To examine the effect of inhibiting the type I TGF- β receptor (Alk5) or inhibiting phosphorylation of Smad3, cells were preincubated with SB431542 (10uM, Pro. # S4317; Sigma-Aldrich, St. Louis, MO) or SIS3 (50uM, EMD Chemicals, Inc, San Diego, CA) respectively for 1 hr prior to growth factor treatment.

Immunostaining

Six human donor eyes (3 age-matched normal verses glaucomatous) were obtained from regional eye banks within 6 hours of death and fixed in 10% formalin. Fixed tissues were dehydrated, embedded in paraffin, and 8-um sections were obtained. Sections were deparaffinized, rehydrated and placed in 0.1% Triton, followed by 20 mM glycine for 15 minutes each. Sections were blocked in 10% normal serum. Slides were incubated overnight with primary antibody (Table 1) diluted 1:100 in 1.5% (v/v) normal serum, followed by 2 hour incubation in appropriate Alexa Fluor™ secondary antibodies (1:200, Invitrogen Corporation, CA). Sections were incubated with DAPI for 30 minutes to stain nuclei, washed, and then mounted. Images were captured using a Zeiss 410 confocal imaging system (Carl Zeiss, Thornwood, NY).

Images were captured from the lamina cribrosa region and the relative intensity of gremlin was analyzed using Image J software (NIH). Confocal images were analyzed by Image J software and relative intensity was measured. Statistical analysis of staining intensity was performed with an unpaired Student's t test using GraphPadPrism 5.

Protein Extraction and Western Blot Analysis

Cell Lysate: Total cellular protein was extracted from cultured ONH astrocytes and LC cells using Mammalian Protein Extraction Buffer (#78501, Pierce Biotech, Rockford, IL.) with Protease Inhibitor Cocktail (#78415, Pierce Biotech, Rockford, IL). Protein concentration was determined using the Bio-Rad Dc protein assay system (Bio-Rad Laboratories, Richmond, CA). The cellular protein was separated on denaturing polyacrylamide gels and then transferred to PVDF membranes by electrophoresis. Blots were blocked with SuperBlock Blocking Buffer (Prod# 37537 Pierce Biotech, Rockford, IL) for 1hrs. The blots were then incubated overnight with specific primary antibodies (Table 1). The membranes were washed with tris-buffered saline tween buffer (TBST) and processed with corresponding horseradish peroxidase-conjugated secondary antibody (Table 1). The proteins were then visualized in a Fluor ChemTM 8900 imager (Alpha Innotech corporation, San Leandro, CA 94577) using ECL detection reagents (SuperSignal West Femto Maximum Sensitivity Substrate, Pierce Biotechnology). To ensure equal protein loading, the same blot was incubated again with a β -actin monoclonal antibody and the blot was developed using a horseradish peroxidase-conjugated secondary antibody. To detect secreted proteins in conditioned medium, equal volumes of conditioned medium were evaluated by western blots and processed as described above.

ELISA Immunoassay for Fibronectin

Conditioned medium was obtained from ONH astrocytes and LC cells and centrifuged at 2000/rpm to remove cellular debris. A total 50 ul of conditioned medium was diluted to 150 ul with dilution buffer, and soluble fibronectin was quantified using a commercially available ELISA kit (cat # ECM 300; Chemicon International, Temecula, CA). Soluble fibronectin (ug/ml) was plotted for each treatment using GraphPadPrism 5.

RNA extraction and RT- PCR:

Total RNA was isolated using TRIzol reagent (Invitrogen Life Technologies, Carlsbad, CA). First strand cDNA synthesis and details of the PCR procedure used in our laboratory have been published previously. Primers for gremlin were designed using primer3 software: Gremlin5': GTCACACTCAACTGCCCTGA; Gremlin3': ATGCAAACGACACTGCTTCAC PCR and gel electrophoresis was done as reported previously (Wordinger et al., 2002).

Quantitative PCR:

Real time PCR was performed with a PCR master mix (SYBR Green; Strategene) using a Mx3000P Real-Time System (Strategene La Jolla, CA). Each reaction contained 12.5 ul of 2X master mix, 500nM of gremlin 5' and 3' primers, and 2.5 ng cDNA from ONH astrocytes and LC cells. PCR primers were designed with the Primer 3 design program: Gremlin5': GTCACACTCAACTGCCCTGA Gremlin3': ATGCAAACGACACTGCTTCAC and TBP 5': GAAACGCCGAATATAATCCA, TBP 3': GCTGGAAAACCCAACTTCTG. Cycle threshold values were normalized to TATA

binding protein (TBP) and were analyzed using Graph Pad Prism software. Results are expressed as means \pm SE. Statistical analysis was performed with One Way ANOVA combined with Bonferroni test using GraphPadPrism 5. ($P < 0.05$ was considered to be significant).

Small interfering RNA and transfection

siRNA for Smad3 and non-specific siRNA for control were purchased from Dharmacon (SMARTpool). Transfection of siRNA was performed as described previously (Kobayashi et al., 2005). Briefly, ONH astrocytes were plated in 12-well plates containing DMEM with 10% FBS. At 30-40% confluence, transfection of siRNA was performed. In one tube, 4 μ l of DharmaFECT 1 Transfection Reagent (T-2001-01 Dharmacon, Inc. IL) was mixed gently with 200 μ l of Opti-MEM medium (Invitrogen Corporation, CA) and incubated 5 min at room temperature. In separate tubes, various concentrations of siRNA were mixed gently with 200 μ l of Opti-MEM medium. These two tubes were combined, gently mixed, and incubated for 20 min at room temperature. After incubation, DMEM without FBS and antibiotics was added to obtain a final volume of 2 ml for each well (1nM, 10nM, and 100nM of Smad3 siRNA and 100nM of control siRNAs). Cells were washed with sterile PBS twice and incubated with siRNA transfection solution for 48 h at 37 °C. ONH cells were then washed with serum-free DMEM medium and treated with gremlin (1ng/ml) in serum-free DMEM medium for 24 hrs. The culture medium was analyzed for soluble FN and cell lysates were analyzed for Smad3, FN, and actin levels.

Results

BMP-4 dose dependently inhibits TGF- β 2 stimulated FN and PAI-1 protein expression in ONH astrocytes and LC cells

We sought to determine whether BMP-4 inhibits TGF- β 2 stimulation of ECM synthesis and secretion in ONH astrocytes and LC cells. We first performed a BMP-4 dose response study. Optic nerve head astrocytes and LC cells were treated with either a) TGF- β 2 (5ng/ml) alone, b) BMP-4 alone at various concentrations (e.g. 2.5, 5, 10, or 20 ng/ml), or c) TGF- β 2 (5 ng/ml) together with different concentrations of BMP-4 (2.5, 5, 10, or 20 ng/ml). Changes in ECM were measured by ELISA in ONH astrocytes (Figure 1A) and by western blot analysis in LC cells (Figure 1B). TGF- β 2 increased both cellular PAI-1 and secreted FN in ONH astrocytes (Figure 1A) and LC cells (Figure 1B). BMP-4 alone did not influence FN and PAI-1 protein levels. However, BMP-4 reduced the TGF- β 2 induction of FN and PAI-1 protein levels in a dose dependent manner ($P < 0.001$, $N=3$). Since a concentration of 10ng/ml BMP-4 effectively inhibited TGF- β 2 regulation of ECM proteins, we utilized this concentration in subsequent studies.

BMP-4 inhibits TGF- β 2 mediated ECM stimulation in ONH astrocytes and LC cells

We next sought to determine whether BMP-4 inhibits TGF- β 2 stimulation of other ECM proteins, including type I collagen, type VI collagen, and elastin. ONH astrocytes and LC cells were treated with a) TGF- β 2 (5ng/ml) alone, b) BMP-4 (10ng/ml) alone, or c) a combination of TGF- β 2 (5ng/ml) and BMP-4 (10ng/ml). Western blot analysis was used

to determine protein levels of cellular FN, PAI-1, collagen I, collagen VI, and elastin (Figure 2A). Our data indicated that TGF- β 2 increased cellular FN, PAI-1, collagen I, collagen VI, and elastin protein levels. BMP-4 alone did not have any effect on these ECM proteins. However, when BMP-4 was co-incubated with TGF- β 2, BMP-4 reduced cellular FN, PAI-1, collagen I, collagen VI, and elastin to control levels. These results indicate that BMP-4 inhibits TGF- β 2 regulation of ECM proteins in ONH astrocytes and LC cells. Cellular FN normalized to β -actin in ONH astrocytes (N=3) and LC cells (n=5) was analyzed by densitometry. Densitometric analysis indicated that TGF- β 2 treatment increased FN protein levels three fold in LC cells and two fold in ONH astrocytes (Figure 2B and 2C). BMP-4 alone did not have any effect on cellular FN but when coincubated with TGF- β 2, BMP-4 reduced FN levels to that of the vehicle control ($P<0.001$).

Gremlin Blocks BMP-4 Inhibition of TGF- β 2 Stimulated Cellular and Secreted FN and PAI-1 in ONH Astrocytes and LC Cells

Gremlin, a secreted extracellular BMP antagonist, binds to BMP-4 and inhibits BMP signaling. Therefore, we examined whether gremlin blocks the BMP-4 inhibition of TGF- β 2 stimulated cellular and secreted FN and PAI-1 in ONH astrocytes and LC cells. Gremlin blocked BMP-4 inhibition of TGF- β 2 stimulated cellular and secreted FN and PAI-1 (Figures 3A and 3B). Thus, protein levels of cellular and secreted FN and PAI-1 were similar to that following TGF- β 2 stimulation alone. Densitometric analysis for secreted FN revealed that TGF- β 2 significantly increased FN ($p<0.001$) and that BMP-4 significantly reduced secreted FN to vehicle control levels ($p<0.001$) in cultured ONH

astrocytes and LC cells (Figures 3C and 3D). These results verify that BMP-4 inhibits TGF- β 2 stimulated ECM synthesis and deposition in human ONH astrocytes and LC cells. In addition, we demonstrated that gremlin blocked BMP-4 inhibition of TGF- β 2 regulation of ECM proteins, leading to increased ECM expression ($P < 0.001$).

Gremlin is Increased in Human Glaucomatous ONH Tissues

Since the above results demonstrated that exogenous gremlin blocked the inhibitory role of BMP-4 with respect to TGF- β 2 signaling in ONH astrocytes and LC cells, we wanted to determine whether ONH cells expressed endogenous gremlin mRNA and protein. Amplification products of expected size for gremlin (126 bp) were uniformly expressed by both ONH astrocytes and LC cells (Figure 4A). There were no apparent differences in gremlin mRNA expression between ONH astrocytes and LC cells. Each of the cDNA samples from ONH astrocytes and LC cells exhibited actin PCR amplification products of the expected size (350 bp). During PCR amplification reactions, control reactions were negative for amplification products, demonstrating that the PCR method and reagents used yielded specific amplified products only when a cDNA source was included.

We next sought to determine whether gremlin protein was present in ONH astrocytes and LC cells. Cell lysates from both ONH astrocytes and LC cells contained gremlin protein at the correct molecular weight (21kD) (Figure 4B). We further determined that gremlin was secreted by ONH astrocytes and LC cells (Figure 4C). Two bands were observed at 21KD and 18KD in both ONH astrocytes and LC cells corresponding to previously

reported glycosylated and non-glycosylated forms (Topol et al., 2000), respectively. In addition, gremlin protein was found in ONH and retinal tissues (Figure 4D).

To verify the presence of gremlin protein in the human ONH tissues, we immunolocalized gremlin in paraffin embedded normal (n=3) and glaucomatous (n=3). ONH tissue samples (Figure 5). Figures 5a and 5b show orientation of lamina cribrosa region in H&E stained human ONH samples at low and high magnification, respectively. Figures 5c and 5d represent gremlin staining merged with nuclear stain DAPI in glaucomatous and normal ONH samples, respectively. Gremlin is localized in the lamina cribrosa region along the axon bundles. No staining was observed in controls that included IgG treatment or omission of primary antibody (Figures 5e and 5f). The relative intensity of gremlin measured by Image J software (NIH) indicated that gremlin protein was increased significantly in aged matched glaucomatous ONH tissues ($p < 0.05$, $n=3$) (Figure 5g).

Gremlin Increases ECM Proteins in ONH astrocytes and LC Cells

Our data suggested that gremlin may modulate ECM proteins via inhibiting BMP-4 antagonism of TGF- β 2 signaling, leading to unopposed TGF- β 2 mediated ECM stimulation. To examine whether increased levels of gremlin in glaucomatous ONH increase ECM proteins, we treated cultured ONH astrocytes and LC cells with increasing concentrations of recombinant gremlin (50, 100, 250, 500ng/ml and, 5, or 10ug/ml). ELISA analysis demonstrated that gremlin increased fibronectin secretion in a dose response fashion in ONH astrocytes (Figure 6A) and LC cells (Figure 6B). Gremlin

increased fibronectin approximately 20 fold (at 1ug/ml) to 60 fold (at 10ug/ml). Exogenous gremlin also increased secreted collagen I, collagen VI, and PAI-1 in ONH astrocytes and LC cells (Figure 6C).

Inhibition of the Type I TGF- β Receptor Activity or siRNA knockdown of R-Smad3 Blocks Gremlin Stimulation of FN and PAI-1 in ONH Cells

Our data suggest that gremlin stimulation of ECM may be mediated via inhibition of BMP-4 antagonism of TGF- β 2 signaling. This would result in unopposed TGF- β 2-driven stimulation of ECM proteins. Therefore, we examined whether inhibition of TGF- β 2 signaling pathway could block the gremlin effects on ECM. We pretreated ONH astrocytes with the type I TGF- β receptor inhibitor SB431542 followed by incubation with gremlin (1ug/ml). The gremlin induction of soluble fibronectin was significantly decreased to vehicle control levels by addition of type I TGF- β receptor inhibitor (Figure 7A).

R-Smad3 is a downstream signaling molecule essential for TGF- β 2 induction of fibronectin expression in ONH cells (Zode et al., unpublished). ONH astrocytes were treated with R-Smad3 siRNA or control siRNAs for 48 hrs. Smad3, FN, PAI-1, and actin protein levels were assessed by densitometric analysis of western immunoblots (Figure 7B-D). Transfection with Smad3-siRNA (1nM, 10nM, and 100nM) resulted in significant reduction of R-Smad3 protein levels compared to control siRNA in ONH astrocytes ($P<0.001$) (Figures 7B and 7C). Control siRNAs did not significantly alter Smad3 proteins levels compared to vehicle control indicating specific silencing by our target

siRNAs. ONH astrocytes were treated with gremlin in the presence or absence of R-Smad3 siRNA for 24 hrs. All three siRNA concentrations clearly inhibited R-Smad3 expression (Figures 7B and 7C), which blocked gremlin mediated stimulation of FN and PAI-1 (Figures 7B and 7D). The gremlin increased FN and PAI-1 was significantly reduced to vehicle control levels by inhibition of R-Smad3 ($P < 0.001$; $n=4$) (Figure 6D).

TGF- β 2 Increases Gremlin mRNA and Protein in ONH Astrocytes and LC Cells

Elevated TGF- β 2 levels in glaucomatous ONH may induce gremlin expression, increasing ECM. Therefore, we examined whether TGF- β 2 levels also stimulated gremlin expression in ONH cells. Optic nerve head astrocytes and LC cells were treated with recombinant TGF- β 2 (5ng/ml) and changes in gremlin mRNA and protein were analyzed by QPCR and western blot analysis. TGF- β 2 increased gremlin mRNA in LC cells, and this effect was blocked by addition of SIS3, a specific R-Smad3 inhibitor (Figure 8A). The TGF- β 2 stimulation of gremlin protein was also blocked by a type I TGF- β receptor inhibitor (Figure 8B). In addition, TGF- β 2 treatment for 24 and 48 hours increased the secretion of gremlin protein in cultured ONH astrocytes and LC cells (Figure 8C).

Discussion

In the present study, we examined the effect of BMP-4 and BMP antagonist gremlin on TGF- β 2 stimulated ECM expression in ONH astrocytes and LC cells. Recombinant TGF- β 2 increased cellular FN, PAI-1, collagen I, collagen VI, and elastin in these ONH astrocytes and LC cells. Recombinant BMP-4 reduced this TGF- β 2 stimulated soluble FN and PAI-1 in a dose dependant fashion. Furthermore, BMP-4 also blocked TGF- β 2 induction of collagen I, collagen VI, and elastin, indicating that BMP-4 is capable of reducing the fibrogenic actions of TGF- β 2 in ONH astrocytes and LC cells. Gremlin blocked BMP-4 inhibition of TGF- β 2, leading to increased levels of ECM proteins. Furthermore, ONH astrocytes and LC cells make and secrete gremlin protein. Gremlin protein is significantly increased in the LC region of glaucomatous ONH tissues. Interestingly, recombinant gremlin alone increased ECM proteins in dose dependant fashion in ONH astrocytes and LC cells. Inhibition of TGF- β receptor and siRNA knockdown of R-Smad3 reduced gremlin stimulation of ECM proteins. Exogenous TGF- β 2 increased cellular and secreted gremlin protein. Inhibition of TGF- β signaling via Smad3 or type I TGF- β receptor blocked the TGF- β 2 induction of gremlin. These results indicate that increased TGF- β 2 can induce gremlin expression, which may play a pivotal role in the glaucomatous ONH by inhibiting endogenous BMP antagonism of TGF- β 2 action. This would lead to increased ECM synthesis and deposition in the glaucomatous ONH. Therefore, inhibition of TGF- β 2 signaling (inhibition of TGF- β RI or reduction of Smad3) reduced gremlin stimulated ECM proteins.

Increased levels of TGF- β 2 in glaucomatous ONH are associated with increased ECM synthesis and deposition (Fuchshofer et al., 2005; Kirwan et al., 2005; Neumann et al., 2008). ONH astrocytes and LC cells are TGF- β 2 responsive, and their activation leads to ECM synthesis and deposition in the glaucomatous ONH. (Zode, unpublished). Other studies demonstrated that TGF- β 2 treatment increased collagen I, collagen VI, collagen IV, elastin, MMP-2, TIMP-1/-3, PAI-1, FN, CTGF, TGM 2, and TSP-1 expression in ONH astrocytes (Fuchshofer et al., 2005; Neumann et al., 2008). In the present study, we also demonstrated that TGF- β 2 increased FN, collagen I, collagen VI, and elastin in ONH astrocytes as well as LC cells. Elevated TGF- β 2 may promote fibrosis through an increase in PAI-1 synthesis. Active PAI-1 inhibits plasmin formation and MMP activation and thus inhibits fibrinolysis and ECM degradation, resulting in increased ECM deposition (McLennan et al., 2000). Thus, these findings support the hypothesis that TGF- β 2 could be major initiation factor for ECM modification and deposition in the glaucomatous ONH.

Another member of TGF- β superfamily that regulates TGF- β 2 signaling in various cells is BMPs. Knockout studies in mice indicate that BMP-4 and BMP-7 are essential in the early morphogenesis of the eye. A heterozygous deficiency of BMP-4 results in anterior segment dysgenesis and elevated IOP (Chang et al., 2001). We have previously demonstrated the presence of a variety of BMPs, BMP receptors and its canonical Smad signaling pathway in ONH tissues and in ONH astrocytes and LC cells (Wordinger et al.,

2002; Zode et al., 2007). In the present study, BMP-4 dose dependently reduced TGF- β 2 stimulation of FN and PAI-1 expression in ONH astrocytes and LC cells. In addition, BMP-4 also reduced TGF- β 2 stimulation of collagen I, VI and elastin. These results indicate that BMP-4 is capable of reducing TGF- β 2 mediated ECM remodeling within the ONH.

Inhibition of TGF- β signaling via BMPs may not be a unique feature of human ONH astrocytes and LC cells. BMPs have emerged as anti-fibrotic agents primarily by inhibiting the profibrotic actions of TGF- β s in various fibrotic diseases. Zeisberg and colleagues demonstrated that BMP-7 inhibits TGF- β induced epithelial-to-mesenchymal transition (Zeisberg et al., 2003). Izumi et al., 2006 reported that BMP-7 opposes TGF- β 1 mediated collagen induction in mouse pulmonary myofibroblasts (Izumi et al., 2006). Finally, in mesangial cells, BMP7 inhibits TGF β -driven fibrogenesis, primarily by reducing nuclear accumulation of R-Smad3 (Wang and Hirschberg, 2004).

We previously demonstrated that expression BMP-4 is not altered significantly in glaucomatous ONH (Zode et al., 2007). However, altered expression of endogenous antagonists can inhibit BMP functions in human ONH. One such antagonist is gremlin. Gremlin inhibits BMP-2, BMP-4 and BMP-7 via binding to form heterodimers. This binding prevents these BMPs from interacting with their receptors and leads to subsequent inhibition of downstream signaling (Balemans and Van Hul, 2002; Myllarniemi et al., 2008). Recently, gremlin has been implicated in fibrotic changes in kidney (Mezzano et al., 2007; Roxburgh et al., 2006), lung (Myllarniemi et al.,

2008), liver (Boers et al., 2006), and osteoarthritis (Tardif et al., 2004) via modulating ECM. Interestingly, we previously reported that gremlin blocked the BMP-4 inhibitory effect on TGF- β 2 in the human trabecular meshwork. More importantly, gremlin increased intraocular pressure in *ex vivo*-cultured eyes (Wordinger et al., 2007a; Wordinger et al., 2007b). Findings from the present study indicate that gremlin also blocks BMP-4 inhibition of TGF- β 2 stimulated ECM proteins, increasing ECM synthesis and deposition in cultured ONH cells.

We also found that ONH astrocytes and LC cells make and secrete gremlin protein. Additionally, increased levels of gremlin in the glaucomatous ONH suggested the role of gremlin in ECM remodeling of the ONH. The various findings from present and previous studies support that gremlin inhibits endogenous BMPs antagonism of TGF- β 2 signaling, increasing ECM proteins in the glaucomatous ONH. First, both ONH astrocytes and LC cells make and secrete TGF- β 2 and BMPs. These cells also exhibit the canonical BMP and TGF- β signaling pathways (Zode et al., 2007, Zode et al., unpublished). Second, we show that BMPs maintain the normal homeostasis of ECM via balancing TGF- β 2 effects on ECM and inhibition of BMP functions by gremlin resulted in increased ECM proteins. Third, exogenous gremlin increased FN, collagen I, collagen VI, and PAI-1 in ONH astrocytes and LC cells supporting the hypothesis that exogenous gremlin may block BMP inhibition of TGF- β 2 signaling. This would result in unopposed TGF- β 2 stimulated ECM proteins. Therefore, inhibition of type I TGF- β receptor or reduction of Smad3 via siRNA blocked gremlin stimulation of fibronectin and PAI-1. In addition to the ability of

gremlin to directly bind and inhibit BMP action, it has recently been reported that gremlin may exert direct effects on cell function via BMP-independent mechanisms (Stabile et al., 2007).

The recapitulation of gremlin expression in fibrotic diseases appears to be associated with increased TGF- β protein levels (Kane et al., 2005; McMahon et al., 2000; Roxburgh et al., 2006). TGF- β is involved in gremlin induction in mesangial cells (McMahon et al., 2000). Our findings demonstrated that TGF- β 2 induces gremlin mRNA and protein in NH cells. We confirmed these results by inhibiting TGF- β 2 signaling pathway. SIS3 selectively inhibits TGF- β dependant R-Smad3 phosphorylation (Jinnin et al., 2006). Recombinant TGF- β 2-driven gremlin induction required active type I TGF- β receptor and phosphorylation of R-Smad3 in ONH astrocytes and LC cells. In addition, TGF- β 2 increased gremlin secretion in ONH astrocytes and LC cells. These results indicate that exogenous TGF- β 2 induced gremlin expression via TGF- β 2 activated Smad signaling.

In summary, the present *in vitro* studies indicate that an intricate balance between BMP-4 and TGF- β 2 may maintain normal homeostasis of ECM synthesis and deposition in ONH astrocytes and LC cells. Elevated TGF- β 2 in glaucomatous ONH may directly increase ECM synthesis and deposition. In addition, TGF- β 2 forms an autocrine loop with gremlin in which elevated levels of TGF- β 2 induce gremlin expression that subsequently blocks BMP regulation of TGF- β 2 actions, leading to a further increase in ECM synthesis and deposition.

Acknowledgments

The authors thank John Fuller for providing ONH astrocytes. The authors also like to thank Anne-Marie-Brun and I-Fen Cheng for technical assistance.

Table #1

List of Antibodies:

Antibody (cat #)	Dilutions (in TBST)	Source
Fibronectin (sc-18827)	1:1000	Santa Cruz Biotechnology, Inc. Santa Cruz, CA.
PAI-1 (sc-5297)	1:1000	Santa Cruz Biotechnology, Inc. Santa Cruz, CA.
Gremlin (PAB-10580)	1:500	Orbigen Inc. San Diego, CA
Collagen I (sc-8783)	1:500	Santa Cruz Biotechnology, Inc. Santa Cruz, CA.
Collagen VI (AB-7821)	1:2000	Millipore Corporate, Billerica, MA
Elastin (MAB-2503)	1:1000	Millipore Corporate, Billerica, MA
β -actin (MAB-1501)	1:2000	Millipore Corporate, Billerica, MA
Goat Anti Mouse(sc-2055)	1:20000	Santa Cruz Biotechnology, Inc. Santa Cruz, CA.
Goat Anti Rabbit(sc-2054)	1: 20000	Santa Cruz Biotechnology, Inc. Santa Cruz, CA.

Figure Legends

Figure 1: BMP-4 Dose Dependently Inhibits TGF- β 2-Induced Stimulation of FN and PAI-1 Proteins in ONH Astrocytes and LC Cells

ONH astrocytes and LC cells were treated with either TGF- β 2 (5ng/ml) alone, BMP-4 alone at various concentrations (2.5, 5, 10, or 20 ng/ml), or TGF- β 2 (5 ng/ml) together with different concentrations of BMP-4 (2.5, 5, 10, or 20 ng/ml). The effect of BMP-4 and TGF- β 2 on ECM proteins was measured by ELISA in ONH astrocytes (A) and by western blot in LC cells (B). [* verses Control, $P<0.001$; † verses TGF- β 2, $P<0.001$; n=3]

Figure 2: BMP-4 Inhibits TGF- β 2 Mediated Stimulation of ECM Proteins in ONH Astrocytes and LC Cells

ONH astrocytes and LC cells were treated with TGF- β 2 (5ng/ml), BMP-4 (10ng/ml) alone, or a combination of TGF- β 2 (5 ng/ml) and BMP-4 (10ng/ml). Total cell lysate was subjected to western blot analysis of cellular FN, PAI-1, collagen I, collagen VI, and elastin in ONH astrocytes and LC cells (A). Soluble FN normalized to actin was measured by densitometry and analyzed using one way ANOVA in ONH astrocytes (B) and LC cells (C). Densitometric analysis demonstrated that TGF- β 2 significantly increased FN, which was reversed by BMP-4 to control levels (* verses Control, $P<0.001$; † verses TGF- β 2, $P<0.001$) in ONH astrocytes (n=3) and LC cells (n=5).

Figure 3: Gremlin Blocks BMP-4 Inhibition of TGF- β 2-Induced FN and PAI-1 in Human ONH Astrocytes and LC Cells

ONH astrocytes and LC cells were treated with either TGF- β 2 (5ng/ml) alone, BMP-4 (10ng/ml) alone, TGF- β 2 (5 ng/ml) and BMP-4 (10ng/ml), or TGF- β 2 (5 ng/ml), BMP-4 (10ng/ml), and gremlin (1ug/ml). Total cell lysate and culture medium was subjected to western immunoblot for cellular FN and PAI- 1 (A) as well as secreted FN and PAI-1 (B) in ONH astrocytes and LC cells. Secreted FN was assessed using densitometric analysis in ONH astrocytes (C) and LC cells (D). TGF- β 2 significantly increased soluble FN ($P<0.001$; *verses control), which was reversed by BMP-4($P<0.001$; † verses TGF- β 2). The addition of gremlin to this regime significantly increased FN ($P<0.001$; ‡ verses TGF- β 2+BMP-4) in ONH astrocytes (n=3) and LC cells (n=4).

Figure 4. Gremlin Expression in Human ONH Tissues, ONH Astrocytes and LC Cells

(A) Ethidium bromide stained gel of RT-PCR amplified products for gremlin and actin from cultured human ONH astrocytes and LC cells. (B) Western immunoblot of cellular gremlin protein in ONH astrocytes and LC cells. B-actin was used as loading control (Not shown). Mouse recombinant gremlin protein was used as positive control for antibody (C) Western blot analysis of gremlin secreted by human ONH astrocytes and LC cells. ONH astrocytes and LC cells were grown in serum-free DMEM medium for 24-48 hours. Medium was collected and concentrated 50 times prior to loading onto a gel. A recombinant protein for gremlin (100ng/ml) served as positive control. (D) Gremlin immunoblot of human ONH and retina tissues.

Figure5. Immunohistochemical Evaluation of Gremlin Expression in Normal and Glaucomatous ONH Tissues

Representative immunostaining for gremlin localization in three aged matched normal verses glaucomatous human ONH tissues. H & E stained ONH samples at lower magnification (a) and at higher magnification (b): ON = optic nerve, LC = lamina cribrosa, ONH = optic nerve head, RL = retinal layer. Gremlin merged with DAPI in glaucomatous ONH (c) and in normal ONH (d); Control IgG merged with DAPI (e) and control (no primary antibody) merged with DAPI (f) in normal ONH. (g) Relative intensity measurements of gremlin in three aged matched normal and glaucomatous ONH tissues. There was statistically significant higher staining for gremlin in glaucomatous ONH tissues compared to normal human ONH tissues, indicating gremlin is increased in glaucomatous ONH tissues (student t test). [$P < 0.05$; * verses normal human ONH tissues; $n=3$].

Figure 6: Effect of Gremlin on ECM Proteins in ONH astrocytes and LC cells

ONH astrocytes and LC cells were treated with varying concentrations recombinant gremlin. Soluble fibronectin was assessed by ELISA in (A) ONH astrocytes and (B) LC cells. Culture medium was subjected to western blot analysis of collagen I, collagen VI, and PAI-1 in ONH astrocytes and LC cells (C).

Figure 7: Inhibition of Type I TGF- β Receptor or siRNA Knockdown of R-Smad3 Blocks Gremlin Induced Stimulation of FN and PAI-1 in ONH Astrocytes

(A) Inhibition of type I TGF- β receptor significantly blocks gremlin effect on soluble FN. ONH astrocytes were preincubated with SB431542 (10 μ M, type I TGF- β receptor inhibitor) and then treated with gremlin (250ng/ml). Soluble FN was measured by ELISA ($P < 0.001$; * verses control; Ψ verses gremlin; N=4). (B) Downregulation of R-Smad3 blocked gremlin stimulation of FN and PAI-1 by in ONH astrocytes. ONH astrocytes (n=4) were treated with siRNA for Smad3 (1nM, 10nM, and 100nM) and control siRNA for 48 hrs and then treated with recombinant gremlin (1 μ g/ml) for 24 hrs. Cellular FN, PAI-1, total Smad3, and actin were assessed by western blot. (C) Specific silencing of R-Smad3. Relative densities of R-Smad3 and actin were measured using densitometric analysis. R-Smad3 was normalized to actin and fold change in R-Smad over vehicle control was plotted ($P < 0.001$; * verses control; n=4). (D) R-Smad3 knockdown reduced gremlin-induced stimulation of FN. Relative density of FN and actin was measured using densitometric analysis. FN was normalized to actin and fold change in FN over vehicle control was plotted ($P < 0.001$; * verses control; \dagger verses gremlin; n=4).

Figure 8: Effect of TGF- β 2 on Gremlin mRNA and Protein in ONH Astrocytes and LC Cells

ONH astrocytes and LC cells were preincubated with SIS3 (specific inhibitor of R-Smad3) or SB431542 (Type I TGF- β receptor inhibitor) 1 hr prior to treatment with TGF- β 2. Changes in gremlin expression were assessed using: (A) QPCR analysis of

gremlin mRNA expression in LC cells. LC cells preincubated with SIS3 (50uM) blocked the TGF- β 2 induction of gremlin. (B) Western blot for cellular gremlin in LC cells. Treatment with TGF- β 2 increased cellular gremlin, which was blocked by addition of TGF- β receptor inhibitor (SB431542, 10uM). (C) Western blot analysis for secreted gremlin in culture medium of ONH astrocytes and LC cells. Treatment with TGF- β 2 for 24 and 48 hrs increased gremlin secretion in ONH astrocytes and LC cells.

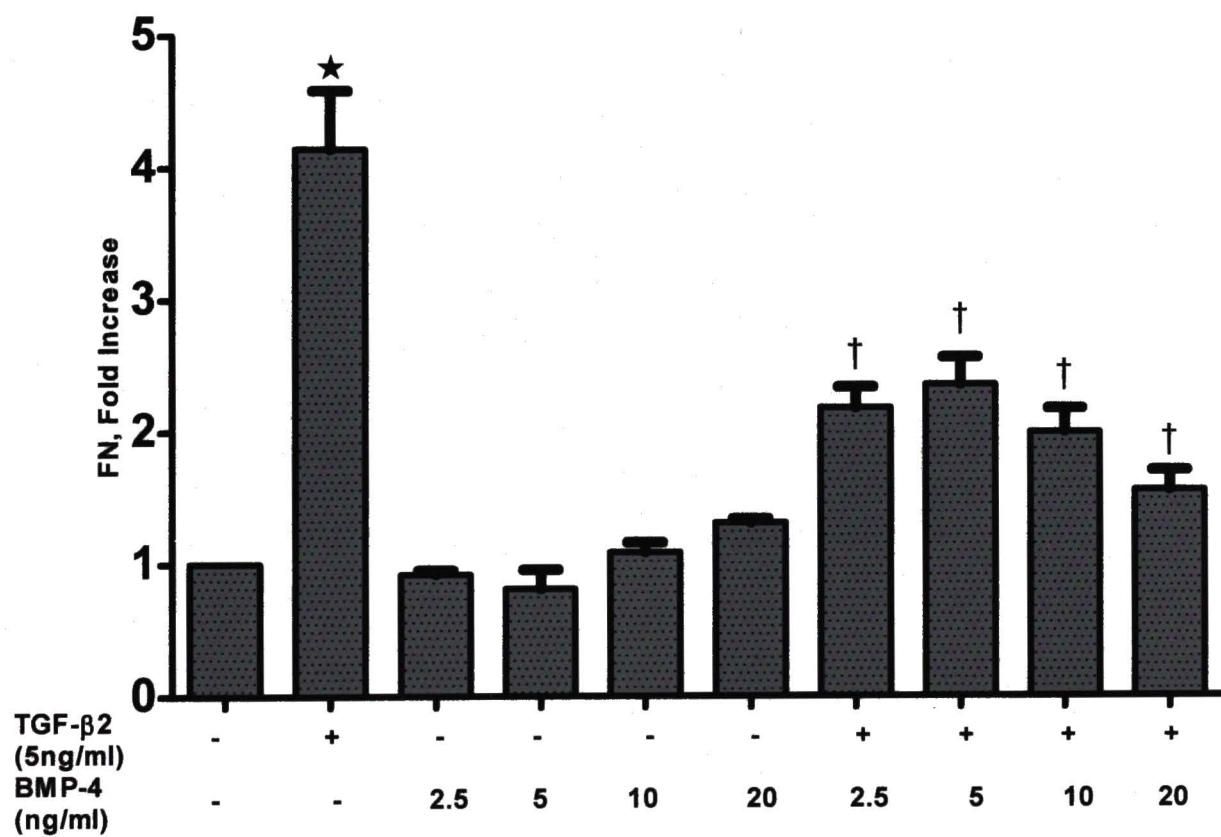
Figure 9. Interactions between gremlin, BMP-4, and TGF- β 2 that modulates ECM in the ONH

In glaucomatous ONH, elevated levels of TGF- β 2 increase ECM protein deposition, remodeling the ONH. Normally, BMP-4 antagonizes this TGF- β 2 signaling, thus maintaining normal ECM homeostasis. The increased TGF- β 2 in the glaucomatous ONH forms an autocrine loop with gremlin in which TGF- β 2 induces gremlin expression, blocking BMP-4 inhibition of TGF- β 2-driven stimulation of ECM proteins. This leads to unopposed TGF- β 2 actions on ECM and therefore, increased synthesis and deposition of ECM in the glaucomatous ONH.

Figures

Figure 1

A



B

BMP-4	-	-	2.5	5	10	2.5	5	10
TGFβ-2	-	5	-	-	-	5	5	5

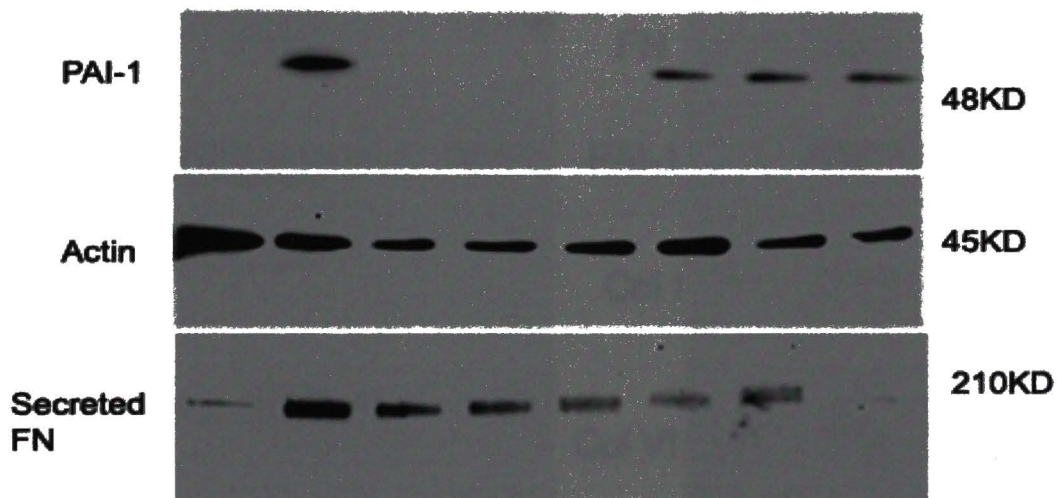
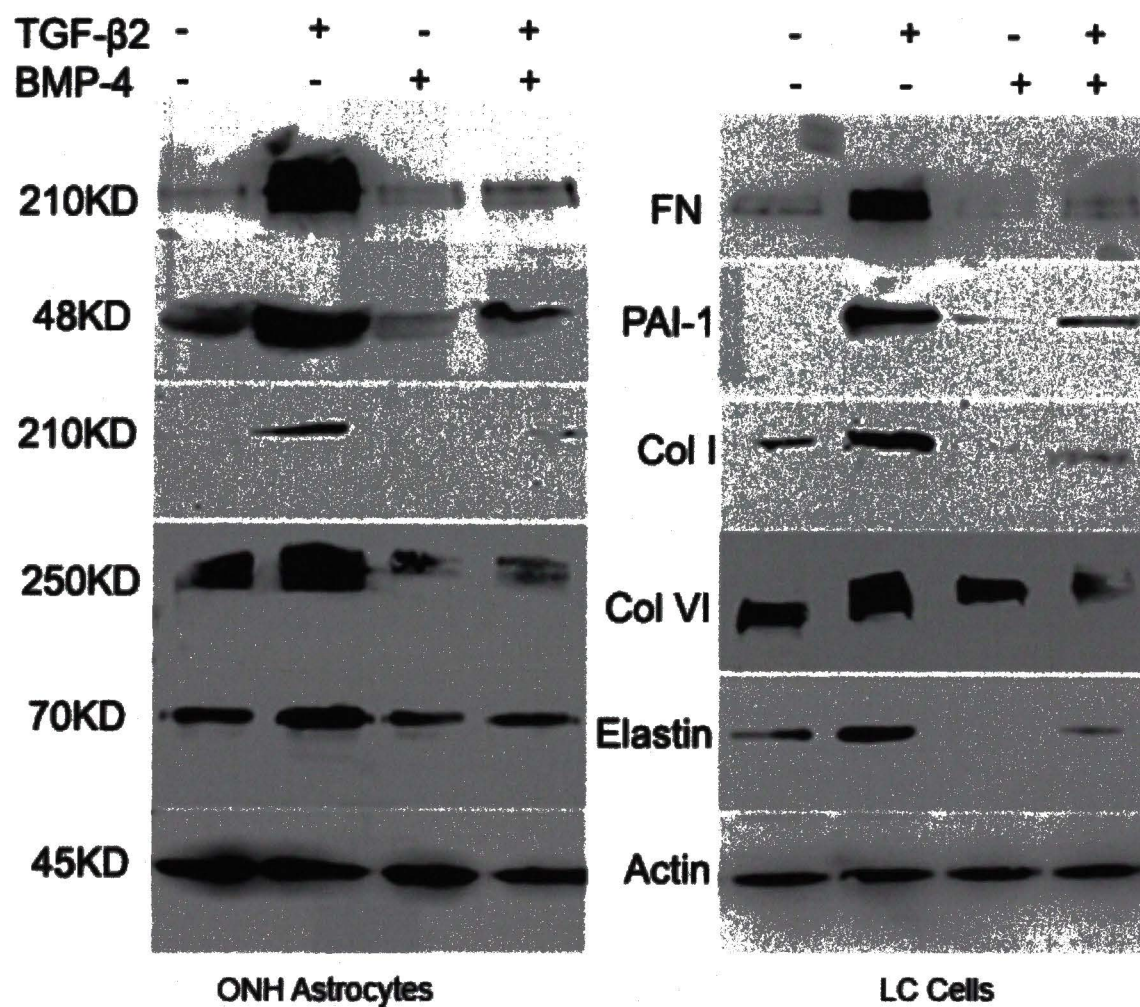
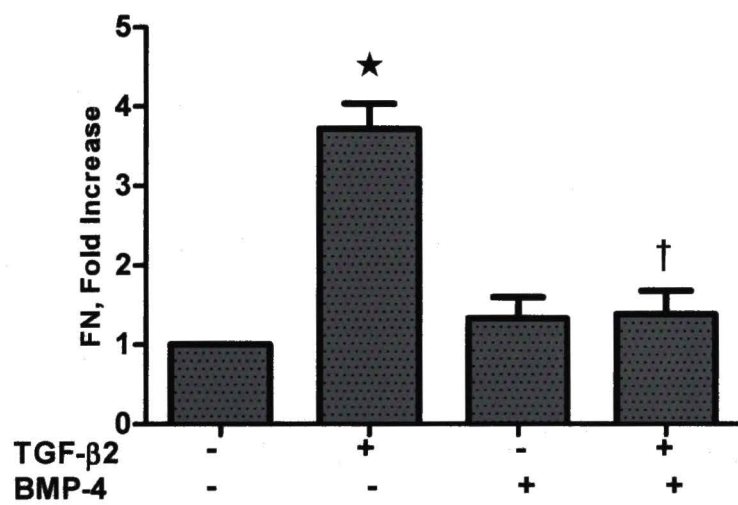


Figure 2

A



B



C

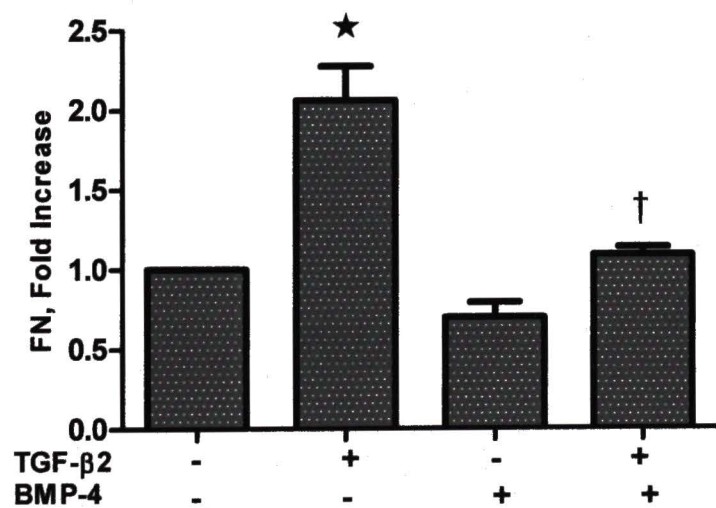
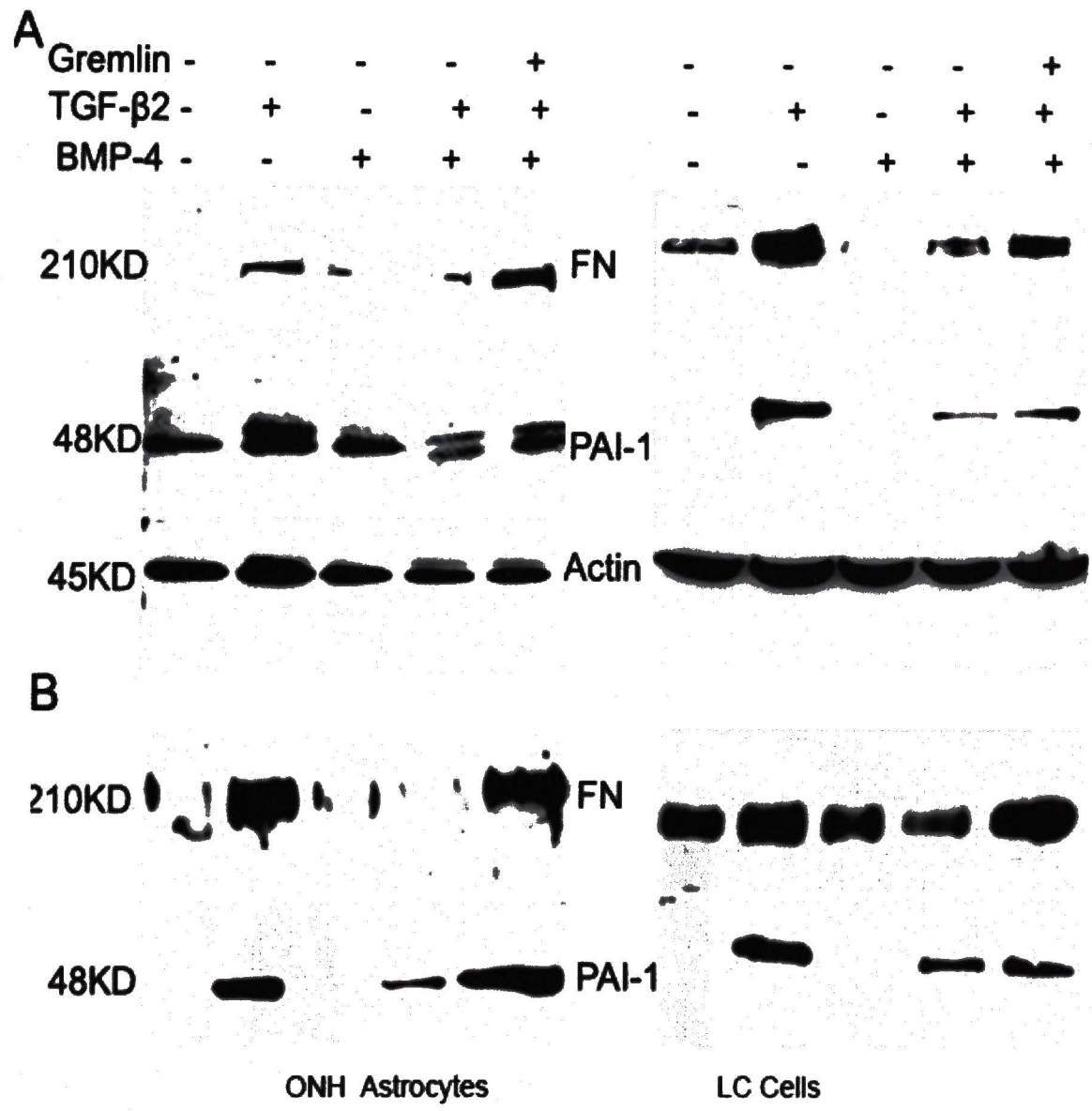
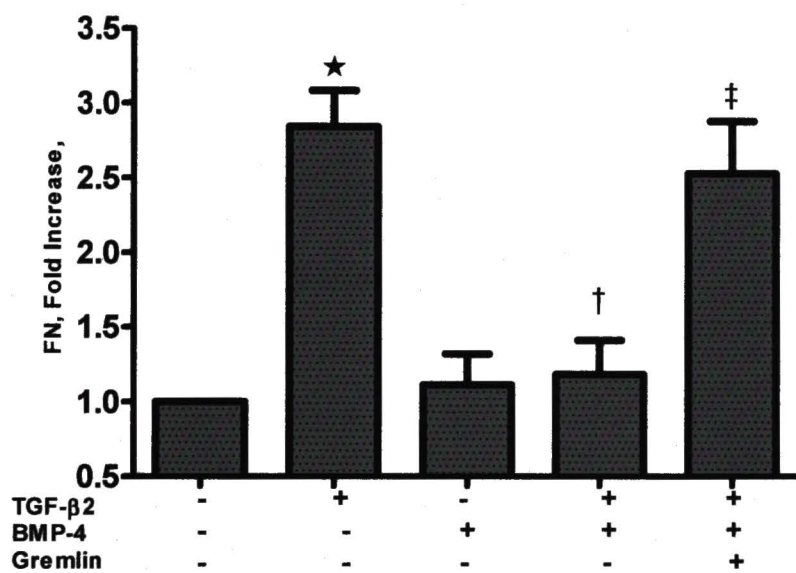


Figure 3



C



D

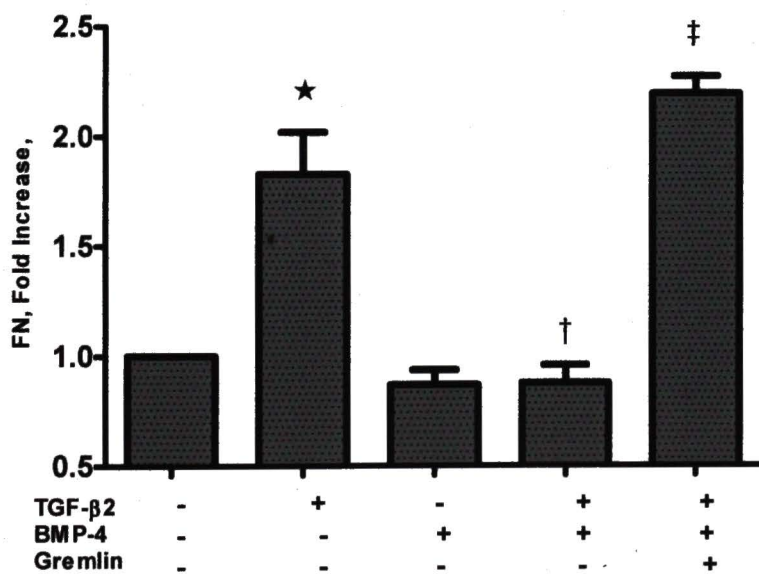


Figure 4

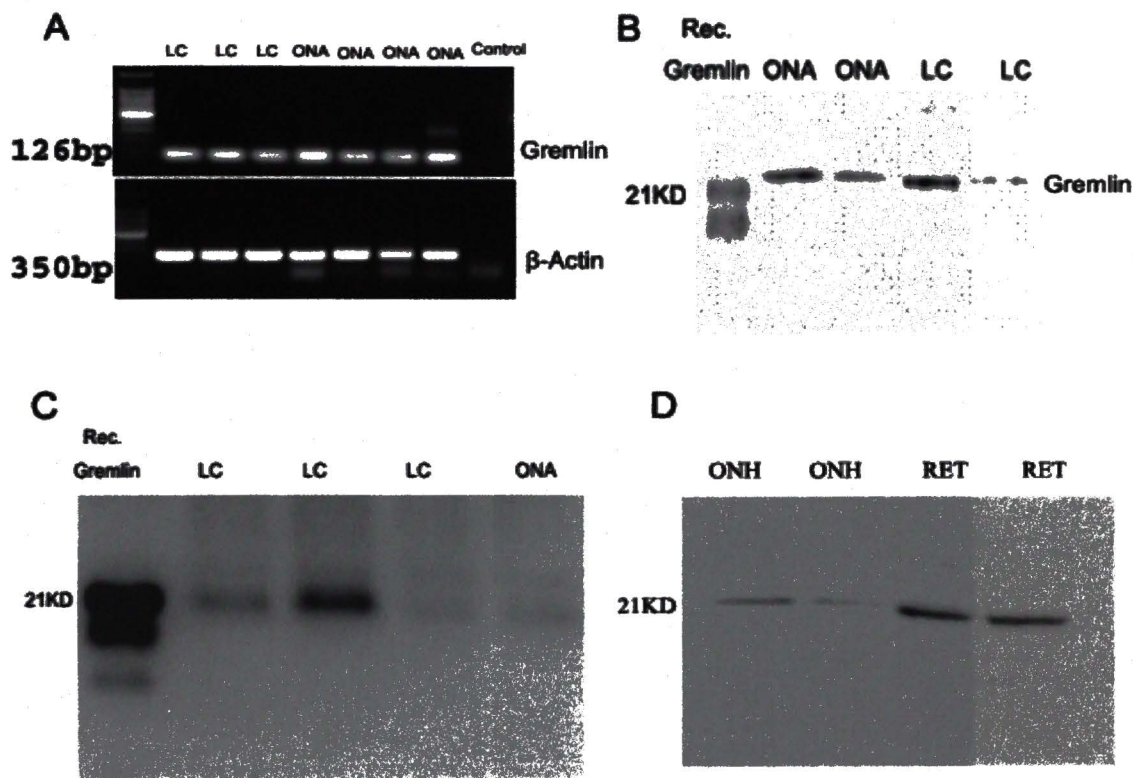


Figure 5

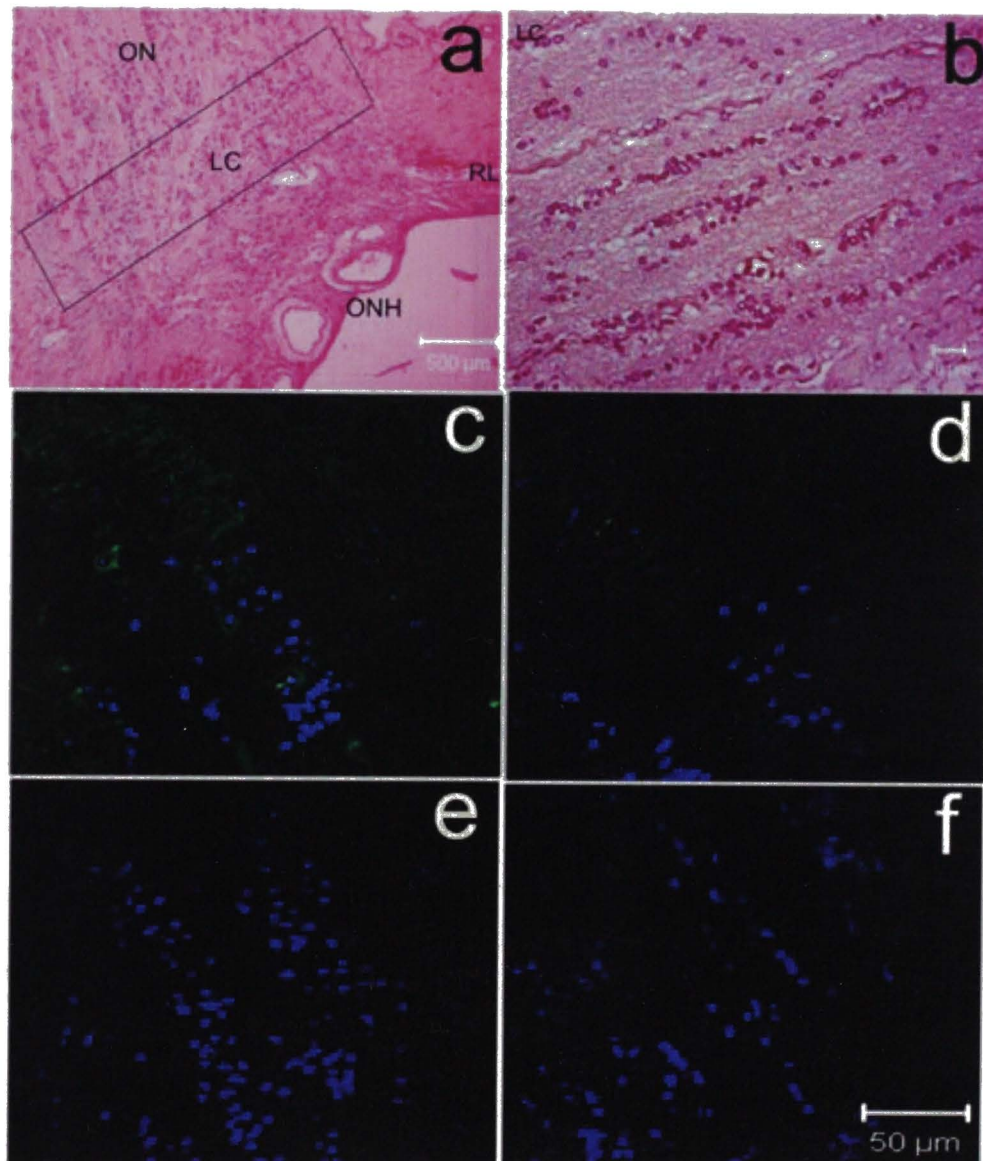


Figure 5g

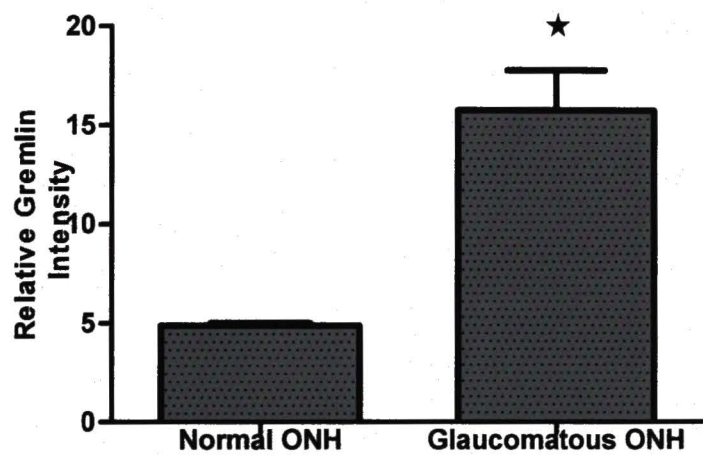


Figure 6

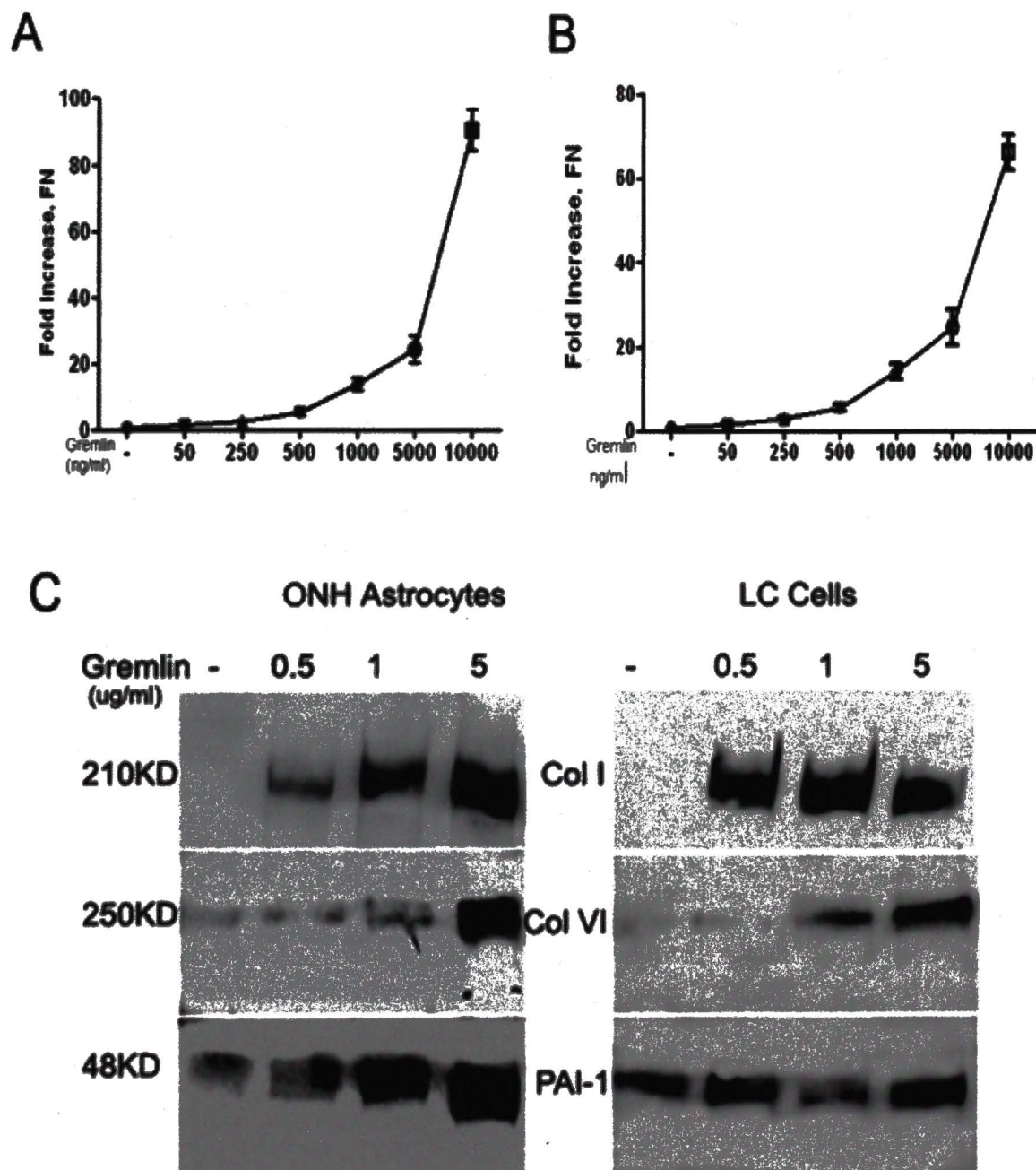
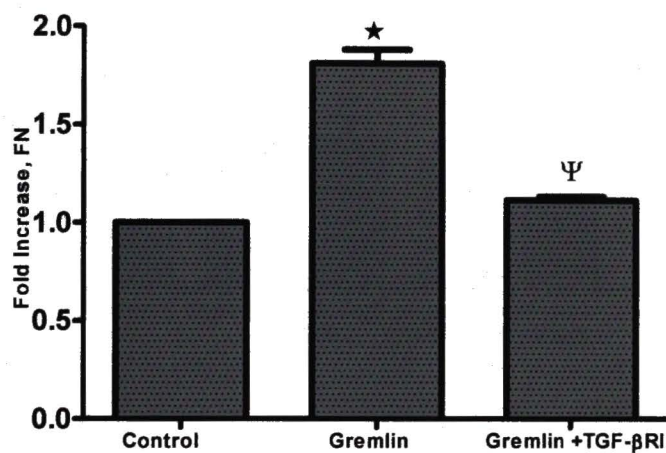
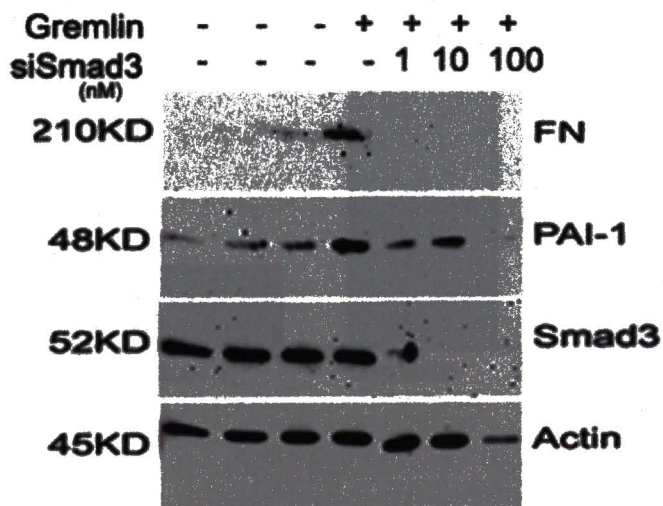


Figure7

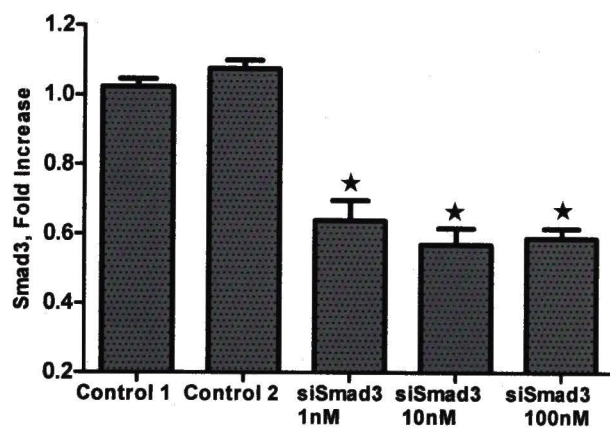
A



B



C



D

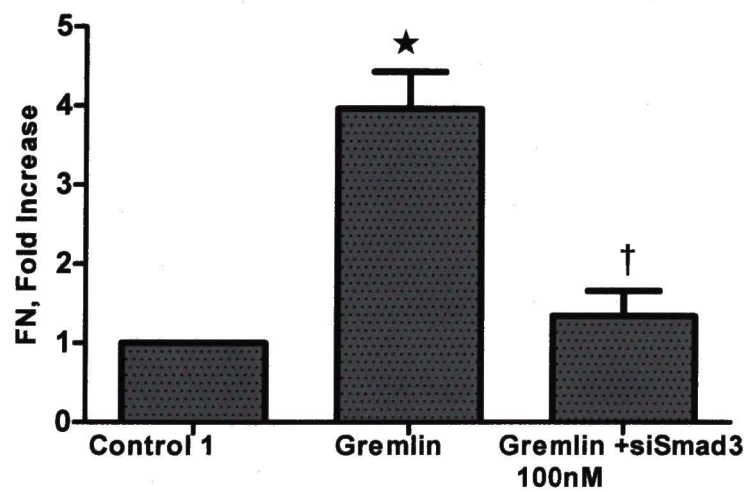


Figure 8

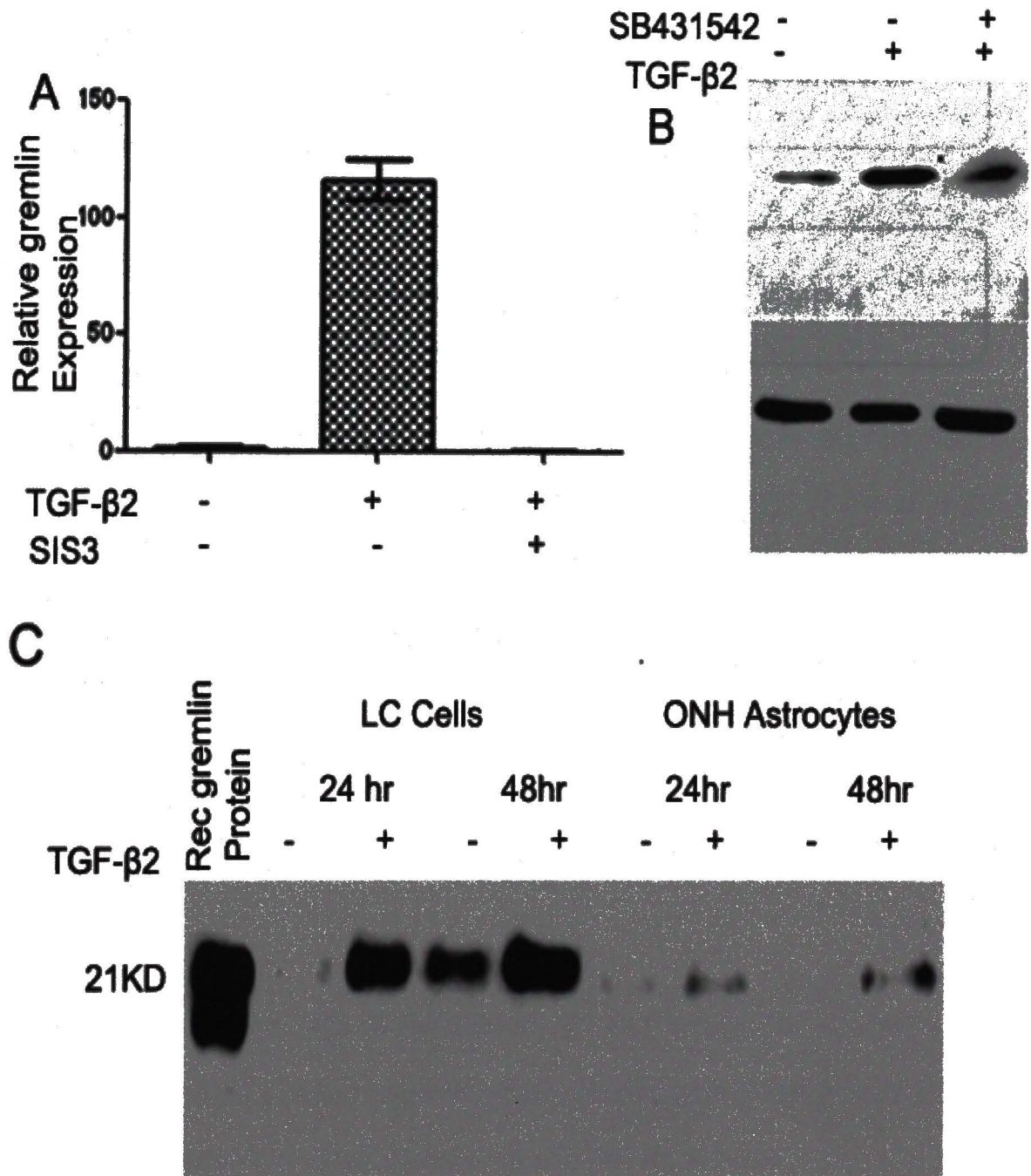
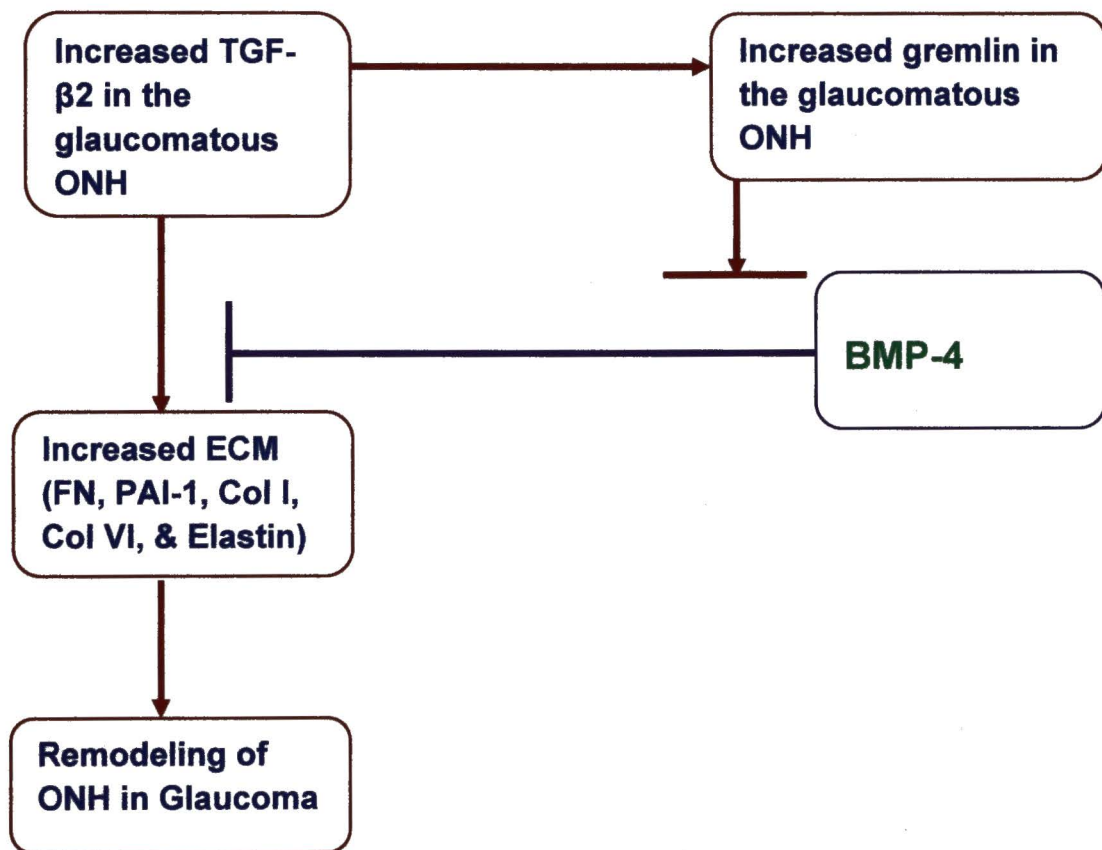


Figure 9



References

- Balemans, W. and Van Hul, W.** (2002). Extracellular regulation of BMP signaling in vertebrates: A cocktail of modulators. *Dev Biol* **250**, 231-50.
- Boers, W., Aarrass, S., Linthorst, C., Pinzani, M., Elferink, R. O. and Bosma, P.** (2006). Transcriptional profiling reveals novel markers of liver fibrogenesis: Gremlin and insulin-like growth factor-binding proteins. *J. Biol. Chem.* **281**, 16289-16295.
- Chang, B., Smith, R. S., Peters, M., Savinova, O. V., Hawes, N. L., Zabaleta, A., Nusinowitz, S., Martin, J. E., Davisson, M. L., Cepko, C. L. et al.** (2001). Haploinsufficient Bmp4 ocular phenotypes include anterior segment dysgenesis with elevated intraocular pressure. *BMC Genet* **2**, 18.
- Fuchshofer, R., Birke, M., Welge-Lussen, U., Kook, D. and Lutjen-Drecoll, E.** (2005). Transforming growth factor-beta 2 modulated extracellular matrix component expression in cultured human optic nerve head astrocytes. *Invest. Ophthalmol. Vis. Sci.* **46**, 568-578.
- Fuchshofer, R., Yu, A. H., Welge-Lussen, U. and Tamm, E. R.** (2007). Bone morphogenetic protein-7 is an antagonist of transforming growth factor-beta2 in human trabecular meshwork cells. *Invest. Ophthalmol. Vis. Sci.* **48**, 715-726.

- Gottanka, J., Chan, D., Eichhorn, M., Lutjen-Drecoll, E. and Ethier, C. R. (2004).** Effects of TGF-beta2 in perfused human eyes. *Invest. Ophthalmol. Vis. Sci.* **45**, 153-158.
- Gottanka, J., Johnson, D. H., Martus, P. and Lutjen-Drecoll, E. (1997).** Severity of optic nerve damage in eyes with POAG is correlated with changes in the trabecular meshwork. *J Glaucoma* **6**, 123-32.
- Hernandez M, G. H. (1996).** *Extracellular Matrix of the Trabecular Meshwork and Optic Nerve Head*, pp. 213-49. St. Louis: Mosby.
- Hernandez, M. R. (2000).** The optic nerve head in glaucoma: Role of astrocytes in tissue remodeling. *Prog Retin Eye Res* **19**, 297-321.
- Hernandez, M. R., Andrzejewska, W. M. and Neufeld, A. H. (1990).** Changes in the extracellular matrix of the human optic nerve head in primary open-angle glaucoma. *Am J Ophthalmol* **109**, 180-8.
- Hernandez, M. R., Igoe, F. and Neufeld, A. H. (1988).** Cell culture of the human lamina cribrosa. *Invest Ophthalmol Vis Sci* **29**, 78-89.
- Izumi, N., Mizuguchi, S., Inagaki, Y., Saika, S., Kawada, N., Nakajima, Y., Inoue, K., Suehiro, S., Friedman, S. L. and Ikeda, K. (2006).** BMP-7 opposes TGF-beta1-mediated collagen induction in mouse pulmonary myofibroblasts through Id2. *Am. J. Physiol. Lung Cell. Mol. Physiol.* **290**, L120-6.

Jinnin, M., Ihn, H. and Tamaki, K. (2006). Characterization of SIS3, a novel specific inhibitor of Smad3, and its effect on transforming growth factor-beta1-induced extracellular matrix expression. *Mol. Pharmacol.* **69**, 597-607.

Kane, R., Stevenson, L., Godson, C., Stitt, A. W. and O'Brien, C. (2005). Gremlin gene expression in bovine retinal pericytes exposed to elevated glucose. *Br. J. Ophthalmol.* **89**, 1638-1642.

Kinoshita, K., Iimuro, Y., Otagawa, K., Saika, S., Inagaki, Y., Nakajima, Y., Kawada, N., Fujimoto, J., Friedman, S. L. and Ikeda, K. (2007). Adenovirus-mediated expression of BMP-7 suppresses the development of liver fibrosis in rats. *Gut* **56**, 706-714.

Kirwan, R. P., Leonard, M. O., Murphy, M., Clark, A. F. and O'Brien, C. J. (2005). Transforming growth factor-beta-regulated gene transcription and protein expression in human GFAP-negative lamina cribrosa cells. *Glia* **52**, 309-324.

Kobayashi, T., Liu, X., Wen, F. Q., Fang, Q., Abe, S., Wang, X. Q., Hashimoto, M., Shen, L., Kawasaki, S., Kim, H. J. et al. (2005). Smad3 mediates TGF-beta1 induction of VEGF production in lung fibroblasts. *Biochem. Biophys. Res. Commun.* **327**, 393-398.

Lambert, W., Agarwal, R., Howe, W., Clark, A. F. and Wordinger, R. J. (2001). Neurotrophin and neurotrophin receptor expression by cells of the human lamina cribrosa. *Invest Ophthalmol Vis Sci* **42**, 2315-23.

Lambert, W. S., Clark, A. F. and Wordinger, R. J. (2004). Neurotrophin and trk expression by cells of the human lamina cribrosa following oxygen-glucose deprivation. *BMC Neurosci.* **5**, 51.

Lutjen-Drecoll E, Rohen JW. (1996). Morphology of aqueous outflow pathways in normal and glaucomatous eyes. In *The Glaucomas* (ed. Ritch R, Shields MB, Krupin T), pp. 89-123. Mosby: St. Louis.

Lutjen-Drecoll, E. (2005). Morphological changes in glaucomatous eyes and the role of TGFbeta2 for the pathogenesis of the disease. *Exp. Eye Res.* **81**, 1-4.

McLennan, S. V., Fisher, E., Martell, S. Y., Death, A. K., Williams, P. F., Lyons, J. G. and Yue, D. K. (2000). Effects of glucose on matrix metalloproteinase and plasmin activities in mesangial cells: Possible role in diabetic nephropathy. *Kidney Int. Suppl.* **77**, S81-7.

McMahon, R., Murphy, M., Clarkson, M., Taal, M., Mackenzie, H. S., Godson, C., Martin, F. and Brady, H. R. (2000). IHG-2, a mesangial cell gene induced by high glucose, is human gremlin. regulation by extracellular glucose concentration, cyclic mechanical strain, and transforming growth factor-beta1. *J Biol Chem* **275**, 9901-4.

Mezzano, S., Droguett, A., Burgos, M. E., Aros, C., Ardiles, L., Flores, C., Carpio, D., Carvajal, G., Ruiz-Ortega, M. and Egido, J. (2007). Expression of gremlin, a bone

morphogenetic protein antagonist, in glomerular crescents of pauci-immune glomerulonephritis. *Nephrol. Dial. Transplant.* **22**, 1882-1890.

Myllarniemi, M., Lindholm, P., Ryyanen, M. J., Kliment, C. R., Salmenkivi, K., Keski-Oja, J., Kinnula, V. L., Oury, T. D. and Koli, K. (2008). Gremlin-mediated decrease in bone morphogenetic protein signaling promotes pulmonary fibrosis. *Am. J. Respir. Crit. Care Med.* **177**, 321-329.

Neumann, C., Yu, A., Welge-Lussen, U., Lutjen-Drecoll, E. and Birke, M. (2008). The effect of TGF- β 2 on elastin, type VI collagen, and components of the proteolytic degradation system in human optic nerve astrocytes. *Invest. Ophthalmol. Vis. Sci.* **49**, 1464-1472.

Nohe, A., Keating, E., Knaus, P. and Petersen, N. O. (2004). Signal transduction of bone morphogenetic protein receptors. *Cell. Signal.* **16**, 291-299.

Oyama, T., Abe, H. and Ushiki, T. (2006). The connective tissue and glial framework in the optic nerve head of the normal human eye: Light and scanning electron microscopic studies. *Arch. Histol. Cytol.* **69**, 341-356.

Pena, J. D., Taylor, A. W., Ricard, C. S., Vidal, I. and Hernandez, M. R. (1999). Transforming growth factor beta isoforms in human optic nerve heads. *Br J Ophthalmol* **83**, 209-18.

Quigley, H. A. (1999). Neuronal death in glaucoma. *Prog Retin Eye Res* **18**, 39-57.

Quigley, H. A. and Addicks, E. M. (1981). Regional differences in the structure of the lamina cribrosa and their relation to glaucomatous optic nerve damage. *Arch Ophthalmol* **99**, 137-43.

Quigley, H. A., Hohman, R. M., Addicks, E. M., Massof, R. W. and Green, W. R. (1983). Morphologic changes in the lamina cribrosa correlated with neural loss in open-angle glaucoma. *Am J Ophthalmol* **95**, 673-91.

Quigley, H. A., McKinnon, S. J., Zack, D. J., Pease, M. E., Kerrigan-Baumrind, L. A., Kerrigan, D. F. and Mitchell, R. S. (2000). Retrograde axonal transport of BDNF in retinal ganglion cells is blocked by acute IOP elevation in rats. *Invest Ophthalmol Vis Sci* **41**, 3460-6.

Rohen, J. W. (1983). Why is intraocular pressure elevated in chronic simple glaucoma? anatomical considerations. *Ophthalmology* **90**, 758-65.

Rohen, J. W., Lutjen-Drecoll, E., Flugel, C., Meyer, M. and Grierson, I. (1993). Ultrastructure of the trabecular meshwork in untreated cases of primary open-angle glaucoma (POAG). *Exp Eye Res* **56**, 683-92.

Roxburgh, S. A., Murphy, M., Pollock, C. A. and Brazil, D. P. (2006). Recapitulation of embryological programmes in renal fibrosis--the importance of epithelial cell plasticity and developmental genes. *Nephron Physiol.* **103**, p139-48.

Sommer, A., Tielsch, J. M., Katz, J., Quigley, H. A., Gottsch, J. D., Javitt, J. and Singh, K. (1991). Relationship between intraocular pressure and primary open angle glaucoma among white and black americans. the baltimore eye survey. *Arch Ophthalmol* **109**, 1090-5.

Stabile, H., Mitola, S., Moroni, E., Belleri, M., Nicoli, S., Coltrini, D., Peri, F., Pessi, A., Orsatti, L., Talamo, F. et al. (2007). Bone morphogenic protein antagonist Drm/gremlin is a novel proangiogenic factor. *Blood* **109**, 1834-1840.

Tardif, G., Hum, D., Pelletier, J. P., Boileau, C., Ranger, P. and Martel-Pelletier, J. (2004). Differential gene expression and regulation of the bone morphogenetic protein antagonists follistatin and gremlin in normal and osteoarthritic human chondrocytes and synovial fibroblasts. *Arthritis Rheum.* **50**, 2521-2530.

Topol, L.Z.; Bardot,B.; Zhang,Q.; Resau,J.; Huillard,E.; Marx,M.; Calothy,G.; Blair,D.G. Biosynthesis, post-translation modification, and functional characterization of Drm/Gremlin. *J.Biol.Chem.*, 2000, 275, 12, 8785-8793

Tripathi, R. C., Li, J., Chan, W. F. and Tripathi, B. J. (1994). Aqueous humor in glaucomatous eyes contains an increased level of TGF-beta 2. *Exp Eye Res* **59**, 723-7.

Wang, S. and Hirschberg, R. (2004). Bone morphogenetic protein-7 signals opposing transforming growth factor beta in mesangial cells. *J Biol Chem* **279**, 23200-6.

Wordinger, R. J., Agarwal, R., Talati, M., Fuller, J., Lambert, W. and Clark, A. F. (2002). Expression of bone morphogenetic proteins (BMP), BMP receptors, and BMP associated proteins in human trabecular meshwork and optic nerve head cells and tissues. *Mol Vis* **8**, 241-50.

Wordinger, R. J. and Clark, A. F. (2007). Bone morphogenetic proteins and their receptors in the eye. *Exp. Biol. Med. (Maywood)* **232**, 979-992.

Wordinger, R. J., Fleenor, D. L., Hellberg, P. E., Pang, I. H., Tovar, T. O., Zode, G. S., Fuller, J. A. and Clark, A. F. (2007a). Effects of TGF-beta2, BMP-4, and gremlin in the trabecular meshwork: Implications for glaucoma. *Invest. Ophthalmol. Vis. Sci.* **48**, 1191-1200.

Wordinger, R. J., Zode, G. and Clark, A. F. (2007b). Focus on molecules: Gremlin. *Exp. Eye Res.*

Zeisberg, M., Hanai, J., Sugimoto, H., Mammoto, T., Charytan, D., Strutz, F. and Kalluri, R. (2003). BMP-7 counteracts TGF-beta1-induced epithelial-to-mesenchymal transition and reverses chronic renal injury. *Nat. Med.* **9**, 964-968.

Zode, G. S., Clark, A. F. and Wordinger, R. J. (2007). Activation of the BMP canonical signaling pathway in human optic nerve head tissue and isolated optic nerve head astrocytes and lamina cribrosa cells. *Invest. Ophthalmol. Vis. Sci.* **48**, 5058-5067.

Chapter V

Conclusions

The results from the present study support the concept that TGF- β 2 is elevated in the LC region of glaucomatous ONH and is involved in increasing ECM proteins by ONH astrocytes and LC cells. Importantly, BMP-4 inhibits TGF- β 2 mediated stimulation of ECM proteins levels in ONH astrocytes and LC cells. Elevated TGF- β 2 induces gremlin expression that subsequently blocks BMP-4 inhibition of TGF- β 2 signaling. This inhibition results in unopposed TGF- β 2 signaling, thus increasing ECM proteins in the glaucomatous ONH.

The first investigation examined whether human ONH tissues and ONH cells express the canonical BMP signaling pathway (figure1). Results demonstrated that BMP-4 and Smad signaling proteins were present in human ONH tissues, isolated ONH astrocytes, and LC cells. In addition, exogenous BMP-4 treatment of ONH astrocytes and LC cells resulted in increased phosphorylation of R-Smad1/5/8 and enhanced interaction of pSmad1 with Co-Smad4 indicating activation of downstream signaling through the canonical Smad pathway. Thus, cells within the human ONH can respond to locally released BMPs via paracrine or autocrine mechanisms.

The second series of experiments examined the signaling pathways utilized by TGF- β 2 to stimulate synthesis and secretion of ECM proteins by ONH astrocytes and LC cells (Figure1). Results from this investigation support that TGF- β 2 increases ECM proteins

via activation of the Smad signaling pathway. TGF- β 2 increased ECM protein levels in ONH astrocytes and LC cells. Interestingly, recombinant TGF- β 2 activated R-Smad2/3 phosphorylation but did not alter phosphorylation of ERK1/2, p38, or JNK1/2. TGF- β 2 increased the co-localization of pSmad3 with Co-Smad4 in the nucleus of LC cells. In addition, inhibition of the TGF- β I receptor activity or inhibition of the phosphorylation of R-Smad3 reduced TGF- β 2 stimulated FN production in ONH astrocytes and LC cells. Knockdown of R-Smad2 or R-Smad3 via siRNA also reduced TGF- β 2 stimulated production of ECM proteins by ONH cells. Thus, TGF- β 2 activates TGF- β receptor and downstream R-Smad2/3 to increase ECM proteins in ONH astrocytes and LC cells (figure1).

The third investigation tested the effect of BMP-4, gremlin and TGF- β 2 on ECM protein production in ONH astrocytes and LC cells. These experiments demonstrated that (1) BMP-4 inhibits TGF- β 2 stimulation of ECM proteins in ONH astrocytes and LC cells, (2) gremlin blocks BMP-4 inhibition of TGF- β 2 stimulated ECM protein production in ONH astrocytes and LC cells, (3) gremlin is increased in the LC region of the glaucomatous ONH, (4) ONH astrocytes and LC cells make and secrete gremlin protein, (5) gremlin increases ECM proteins in ONH astrocytes and LC cells, (6) gremlin stimulation of ECM proteins requires an active TGF- β I receptor and R-Smad3, (7) TGF- β 2 increases gremlin proteins in ONH astrocytes and LC cells, and (8) TGF- β 2 induced gremlin requires active TGF- β signaling pathway including TGF- β receptor I activity and phosphorylated Smad3 (figure1).

Significantly, these observations confirm that TGF- β 2 is increased in glaucomatous ONH and plays an important role in pathogenesis of glaucoma. Elevated TGF- β 2 levels in glaucoma induce ECM remodeling that may be detrimental to axonal survival (figure 1). However, ONH tissues express BMPs that maintains normal homeostasis of ECM in ONH via counterbalancing TGF- β signaling. However, TGF- β 2 induces gremlin expression, which blocks BMP-4 inhibition of TGF- β 2 signaling. This leads to unopposed TGF- β 2 stimulated ECM proteins, remodeling ONH (figure 1). These experiments suggest the role of gremlin in pathogenesis of glaucoma. Our studies also indicate of Smad2/3 is an important downstream mediator for TGF- β 2 and gremlin induced ECM remodeling (figure 1). Thus, modulation Smad2/3 provides a novel therapeutic target to prevent the ECM remodeling in glaucoma

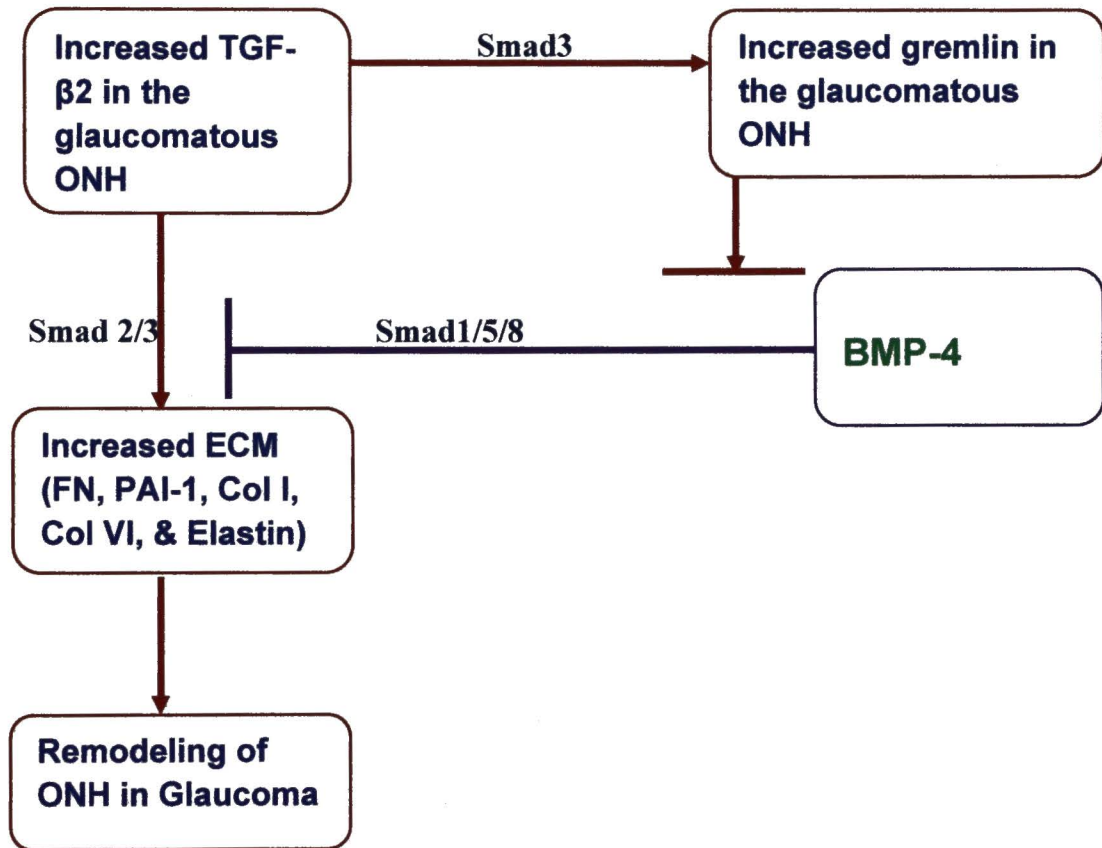


Figure 1: Gremlin Inhibition of BMP-4 Antagonism of TGF-β2 Increases ECM Proteins in the Glaucomatous ONH

Chapter VI

Future Directions

1. *In-vivo* examination of the effects of BMP-4 and BMP antagonist gremlin on TGF- β 2 stimulated ECM.
 - . Effect of TGF- β 2 will be examined by intravitreal injection of adenoviral TGF- β 2. ECM changes will be examined using western blot analysis of ONH. Furthermore, Smad3 knockout mice will be utilized to examine whether TGF- β 2 utilizes Smad3 to stimulate ECM.
 - Next, recombinant BMP-4 will be intravitreally injected in TGF- β 2 treated mice. ECM changes in ONH tissues will be examined.
 - Finally, gremlin effects on ECM remodeling of ONH will examined by intravitreal administration of gremlin adenovirus.
 - We will also examine whether inhibition Smad3 reduces gremlin induced ECM remodeling in the ONH tissues. Gremlin adenovirus will be administered intravitreally in the Smad3 knockout mice. ECM changes will be examined by western blot analysis of ONH tissues.

2. To study signaling pathway utilized by BMP-4 to inhibit TGF- β 2 signaling.
 - Our data suggested that TGF- β 2 increases ECM via Smad2/3. Wang et al. 2006 demonstrated that BMP-7 utilizes Smad5 to antagonize TGF- β 2 signaling in mesangial cells. Therefore, we hypothesize that BMP-4 antagonize TGF- β 2 signaling in ONH cells via BMP activated Smad signaling.
 - We will examine whether BMP-4 inhibit TGF- β 2 signaling in Smad5 knockdown ONH cells. ECM changes will be measured.
 - However, role of BMP activated non-Smad signaling pathways including ERK1/2, p38, and JNK1/2 is also possible. We will examine the role of these pathways by using pharmacological inhibitors and siRNA knockout studies.
3. To investigate the mechanism for gremlin induced ECM stimulation in ONH cells.
 - We will overexpress gremlin protein tagged with GFP protein and examine the localization of gremlin in ONH cells.
 - Next, we will conduct immunoprecipitation of gremlin and examine the interacting molecules by mass spectrometry.

